POSITION ENCODERLESS SELF SYNCHRONISATION OF VARIABLE RELUCTANCE STEPPING MOTORS.

A thesis

submitted in fulfilment

of the requirements for the Degree

of

Master of Engineering

in the

University of Canterbury,

Christchurch, New Zealand.

by

J. D. Marvelly.

1987

ABSTRACT.

The principal application of stepping motors to date is in low power open loop positioning systems. It is widely known that self synchronisation offers a significant improvement in dynamic performance in addition to step integrity. The necessary positional feedback is traditionally provided by a position encoder. However the fitting of such a device is usually expensive and inconvenient.

Previous analyses of stator current waveforms of motors driven from the conventional L/R drive have revealed rotor position dependant characteristics which can be used to provide self positional feedback. A variety of different schemes using both on and off phases have been proposed in the literature. Successful self synchronisation utilising some of these characteristics has been reported for multiple stack variable reluctance stepping motors.

When the active suppression drive is used, the variable reluctance stepping motor offers high specific output and efficiency making it a contender in controlled speed drive applications as well. Lower manufacturing cost makes the single stack motor additionally attractive.

A single stack stepping motor driven under self synchronised control from self positional feedback and using active suppression drives is potentially an efficient cost effective drive offering precision speed and position control. The single stack motor has significant mutual inductances between phases. This coupling considerably complicates the task of obtaining self positional feedback, especially when active suppression drives are used.

This research investigates the suitability of the single stack variable reluctance stepping motor to position encoderless self synchronisation when driven by an active suppression drive and chopper current limiting.

An algorithm for obtaining the necessary self positional feedback has been developed and the equipment necessary to implement it has been designed and constructed. Certain characteristics which restrict the performance of the algorithm have been observed during operation. These characteristics have been explained in terms of the significant mutual inductances between phases inherent in the single stack motor.

A linear model of the on and de-energising phase currents has been developed and implemented numerically. The results have been used to generate theoretical torque vs speed plots. These plots show good agreement with the measured performance.

A linear model of the self positional feedback algorithm has been developed to further the analytical understanding of the advances made experimentally. The numerical solutions identify the cause of the performance restrictions and simulate the nature of the observed self positional feedback characteristics closely.

A suggestion is made for continuing research which is believed likely to yield significant results.

TABLE OF CONTENTS.

ACKNOWLEDGEMENTS.

I wish to acknowledge my supervisor Dr. G.R. Dunlop for his guidance during this research.

This opportunity is also taken to acknowledge Electropar ltd., the New Zealand University Grants Committee and the Canterbury University Grants Committee for their contributions towards the funding of the project. Electropar ltd. also supplied the motor used in this research and a commercial controller. IBM, Digital Equipment Corporation and the New Zealand Electricity Department are also acknowledged for the supply and funding of computing equipment which has been utilised in this research.

Personal financial assistance was gratefully received through the Todd Motors Research Scholarship (1986) and the Mercer Memorial Scholarship (1986).

Finally, I wish to thank my parents. This research is not only the culmination of my own efforts but also of their selfless support throughout my education.

CHAPTER 1.

A REVIEW OF STEPPING MOTOR CONTROL.

1.1 Introduction.

The stepping motor is the most widely used motor in the field of low power precision position control. This is largely due to its incremental motion upon commutation from one phase to the next. The number of commutations or steps necessary to reach a specified target is easily determined and then executed without positional feedback. This positioning is accomplished by driving the motor synchronously from a commutation pulse train generated by the controller. This feature enables precision positional control from a simple control system and hence the widespread use of the step motor in this field.

While such a simple system is capable of precision positioning, its dynamic performance is limited. The limited performance is a result of the stepping motor being driven under open loop control. A major problem is mechanical resonance of the load inertia, as an under damped resonant system usually results. The resonant frequency is set by the inertia of the rotor and load and the restoring torque acting towards the position detents. As the stepping rate approaches the resonant frequency or a sub harmonic of it, the rotor and load will oscillate about the detent positions with increasing amplitude. If the amplitude becomes sufficiently large, the rotor will overshoot to the next detent position and step integrity will be lost. Mechanical damping can be applied, but this restricts the slewing performance of the motor. Electronic and control based damping schemes have been devised which do not restrict the slewing performance of the motor as

much. However like mechanical damping they generally lower the efficiency of the drive.

A second restriction on performance inherent in open loop control is the lack of control over the rotor position relative to the detent positions upon commutation. The rotor teeth must be in advance of their next detent position at all times if the motor is to continuously produce positive torque. The performance of the stepping motor is very dependant on the size of this angle of advance or lead. The angle in advance of the detent position at the instant of commutation has been termed the Lead Angle and is a key variable in analysing stepping motor performance. To maximise the torque output, it is necessary to find the optimum lead angle.

The optimum lead angle is speed dependant as well as being influenced by the individual characteristics of the motor. In open loop control the required lead angle is determined by the motor speed, acceleration, stator current and load. It is usually not possible to have any control over the lead angle as the only controlled variable is the motor speed. The lead angle is set by the operating conditions defined by the above variables and usually at some non optimal value.

The optimum lead angle can only practicably be maintained by obtaining positional feedback and implementing closed loop control. Positional feedback can be used solely as confirmation of stepping, indicating when synchronisation has been lost. This simple usage of feedback while often termed closed loop control, does not directly improve the dynamic performance of an otherwise open loop control system. Such a system makes no attempt to control the lead angle, so the motor's torque output cannot be maximised. Any performance improvement will stem from greater confidence in operating near the

point of poling or where synchronisation is lost.

The most advantageous use of positional feedback is in self synchronised control of commutation. Self synchronisation is the implementation of closed loop control where commutation is triggered in response to an attained rotor position. Such a system controls the lead angle. In an advanced form it is capable of maintaining the lead angle at the optimum value and therefore maximising the dynamic performance as well as ensuring step integrity.

Considerable literature on the broad subject of maximising stepping motor performance has been published in recent years. The various aspects of stepping motor performance this literature addresses can be categorised into three main areas.

1. Applications.

2. Design, measurement and modelling.

3. Methods of control.

1.2 Applications.

This small area of the literature is primarily concerned with applying stepping motor drives to particular applications. The publications usually address specific applications where stepping motors have not previously been used, and have traditionally been the domain of other types of motor. Typically the current practice and unique requirements of the specified application are discussed, and

experimental results supporting the use of stepping motors are presented. The implementation of small hybrid stepping motor drives is now a popular area of research in the field of stepping motor application. For example Ferris et al. (1981) describe the application of a standard four phase hybrid stepping motor to a high performance closed loop incremental motion control system suitable for paper feeding in line printers. The benefits of using D.C. servo motors in this application are discussed also. The results presented show that for the intended application the stepping motor equals the performance of D.C. servo motors, and is more efficient and cost effective.

1.3 Design, Measurement and Modelling.

In addition to researching new applications for stepping motors, research into the design parameters which affect the performance has been undertaken. This research has produced literature on motor performance measurement and on the development of measurement apparatus. Vallon and Jufer discuss (1981) a microprocessor based system which analyses the performance of a motor by minimising the time needed to reach a specified rotor displacement from zero speed. A high resolution encoder is used to implement closed loop control over a range of different lead angles. The lead angle profile necessary to maximise the acceleration over the speed range is recorded.

Computer simulation has been used in an attempt to overcome the problems of analytical modelling. With this approach the effects of non linearities can be included in an analysis. These appear as major terms in the governing equations and have been shown to have a

significant effect on performance. The results of programs which simulate stepping motor dynamic performance can be found in the literature.

1.4 Methods of Control.

Most literature is either partly or wholly devoted to the control of stepping motor performance. In recent years the performance offered by stepping motors has increased significantly. This is largely because they can be controlled efficiently by a microcomputer with minimal ancillary equipment. Improvements in the performance of micro computers and the reduction in their cost has made sophisticated dynamic control of stepping motors readily achievable and moderately inexpensive. Another contributing factor is the advances made in the performance of semiconductor switching devices. Power devices with high voltage ratings and high switching speeds are continually becoming a smaller portion of the total cost of the drive circuits. As a result much research is being done in the area of control methods. Most of the related literature is primarily concerned with point to point slew time minimisation. This end result has prompted work on two main fronts; firstly the development of alternative energisation methods, and secondly the formulation of new control algorithms and their assessment.

The most significant development in stepping motor energisation methods is the active suppression drive (cf. A. Cassat 1977). This drive features non dissipative suppression of the phase current during de-energisation by returning the stored field energy to the power

supply. The active suppression drive also features non dissipative chopper current limiting during energisation by switching the phase inductance between the energising current path and a low resistance "freewheeling" current path. These functions offer several motoring performance advantages in addition to increased drive efficiency.

Most of the control algorithm work has been aimed at improving performance in the open loop control mode. Phase plane related techniques as used by Hammad and Mathur (1977), Taft and Gauthier (1975) , Taft et al. (1981) and Kille and Klein (1980) are a popular method of predicting the maximum acceleration and deceleration for a given combination of drive circuitry and motor. Theoretically optimal velocity profiles can be generated and then executed by a microcomputer which are claimed to rival self synchronised control for slewing performance below resonant speed, and without the risk of dynamic instability in the target area. In addition the problems of resonance can be partially overcome by software controlled microstepping. However it is generally acknowledged in the literature that to maximise the step motors performance for a given frame size and to guarantee step integrity, self synchronisation is required. The improvements in step motor performance can be summarised by a comparison of the torque vs speed plots for a given motor for the two modes of control. Typically synchronisation brings about greater torque for a given speed and extends the useful speed range.

The positional feedback necessary to implement synchronisation is usually provided by a position encoder fitted to the motor. Position encoders sense discrete rotor positions which are fixed relative to phase detent positions. To commutate phases at rotor positions which do not coincide with these discrete positions requires

a controller capable of interpolating between adjacent sensed positions. The demands placed upon such a controller can be reduced if the encoder has a resolution somewhat greater than the step resolution of the motor. This means that the encoder is capable of detecting a number of discrete rotor positions per step. If such an encoder is used, a degree of inter step interpolation is automatically accomplished by the encoder. However for any motor with other than coarse steps an encoder of comparatively high resolution and accuracy is required. To achieve high resolution and accuracy a high level of overall precision is required. But such a device is expensive to manufacture, difficult to install and align accurately. Also it is usually required to operate without regular maintenance in an environment where dirt, heat and vibration may all be problems.

The disadvantage of using a position encoder to achieve self synchronised control could be largely overcome if some electrical characteristic of the motor could be used to provide positional feedback. It is in this area that this research effort is directed. The aim is to investigate the suitability of the single stack variable reluctance stepping motor to self synchronisation when driven by active suppression drives with chopper current limiting. Conclusive results will reveal whether a given method could resolve the necessary lead angles to maximise the torque output of the motor.

To this end, a method of obtaining self positional feedback has been developed. It is described in detail and performance measurements and a mathematical analysis are presented.

CHAPTER 2.

THEORY

2.1 Introduction.

The first chapter identifies the advantages of closed loop control of stepping motors and in particular when using self positional feedback. A system based on a single stack variable reluctance motor driven by an active suppression drive and chopper current limiting is proposed.

This chapter presents an analytical discussion of the system components which are used to produce such a system. A linear model for the phase currents of an active suppression driven motor is developed. The existing self positional feedback algorithms are analysed and a new algorithm is introduced and its theoretical performance is analysed.

2.2 The Variable Reluctance Motor.

The variable reluctance stepping motor is characterised by having a soft iron multiple pole rotor. In producing torque it relies on the principle of variation in the flux path reluctance between the stator and rotor poles as the rotor rotates. The poles are identified electrically as regions of minimum path reluctance and they are identified mechanically as "teeth" on the stator and rotor. The torque exerted on the rotor can be shown to act in the direction of decreasing path reluctance. The net effect is magnetic attraction

between the stator and rotor poles. The attraction leads to alignment of the poles.

There are two main types of variable reluctance (VR) motor, the multiple stack and the single stack motor.

2.2.1 The Multiple Stack VR Motor.

The multiple stack construction is so named because each phase has its own stator section which is magnetically independent from all the others. The motor is constructed through the axial "stacking" of all the phases. Each stack usually has its own section of rotor, the teeth of which do not continue into the next stack. The relationship between the teeth in different stacks of a typical three phase multiple stack motor is shown in figure 2.1. The stator and rotor characteristically have the same number of teeth. The rotor teeth in each stack are shown to be angularly misaligned with respect to the stator teeth in all the other stacks. Alternatively, the stator teeth may be equivalently misaligned between phases. Whether the misalignment is between the stator or rotor teeth, the misalignment between phases is equal to the tooth pitch divided by the number of phases. Only one phase has its stator and rotor teeth aligned at a time. The rotor positions where the rotor and stator teeth are aligned are termed the detent positions. The phases detent sequentially as the rotor is rotated. In this way one electrical cycle of the motor moves the rotor one tooth pitch.

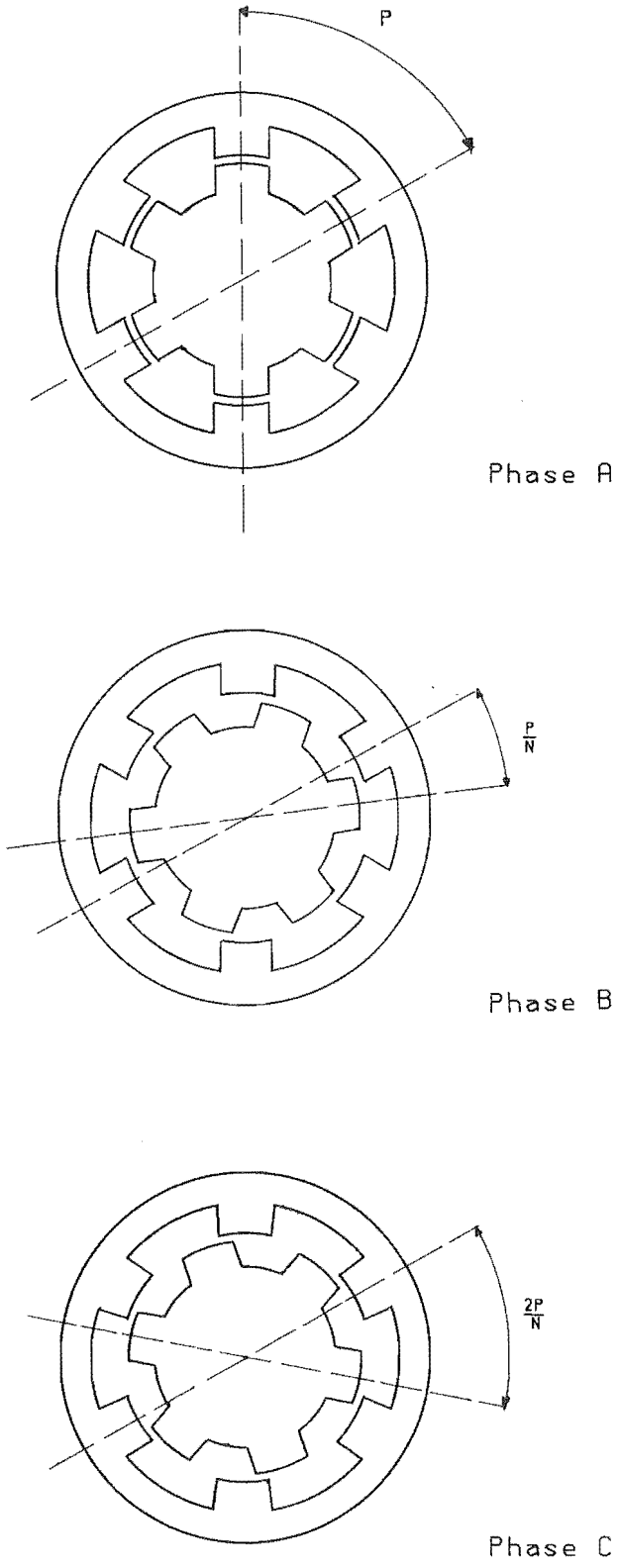

Fig 2.1

The inter stack relationship between stator and rotor teeth for a typical three phase multiple stack motor.

2.2.2 The Single Stack VR Motor.

In the past most VR motors have been of the multiple stack construction but over the last decade the single stack motor has become increasingly more popular. The main reason for this is the high cost of manufacturing the multiple stack motor together with increasing demand for low cost motors. The single stack motor differs principally in that all of the phase windings are incorporated in one stator section. Unlike in the multiple stack motor the stator and rotor require a different number of teeth. The difference is usually by the number of stator teeth per phase. With this arrangement, like the multiple stack motor, one electrical cycle moves the rotor one tooth pitch. Figure 2.2 is a schematic diagram of the teeth arrangements of a single stack four phase motor. Commutation in the phase sequence A,B,C,D causes detenting in that sequence. However the rotor rotates in the opposite sense to that of the field path unlike in the multiple stack motor where the location of the field moves axially amongst the stacks. Because an electrical cycle moves the rotor one tooth pitch, the electrical angular velocity is greater than the mechanical angular velocity by a factor of the number of rotor teeth.

2.3 The Phase Inductances.

The variation in flux path reluctance within the motor results in the variation in phase inductances. Consequently knowledge of how the inductances vary enable inferences on the potential performance of

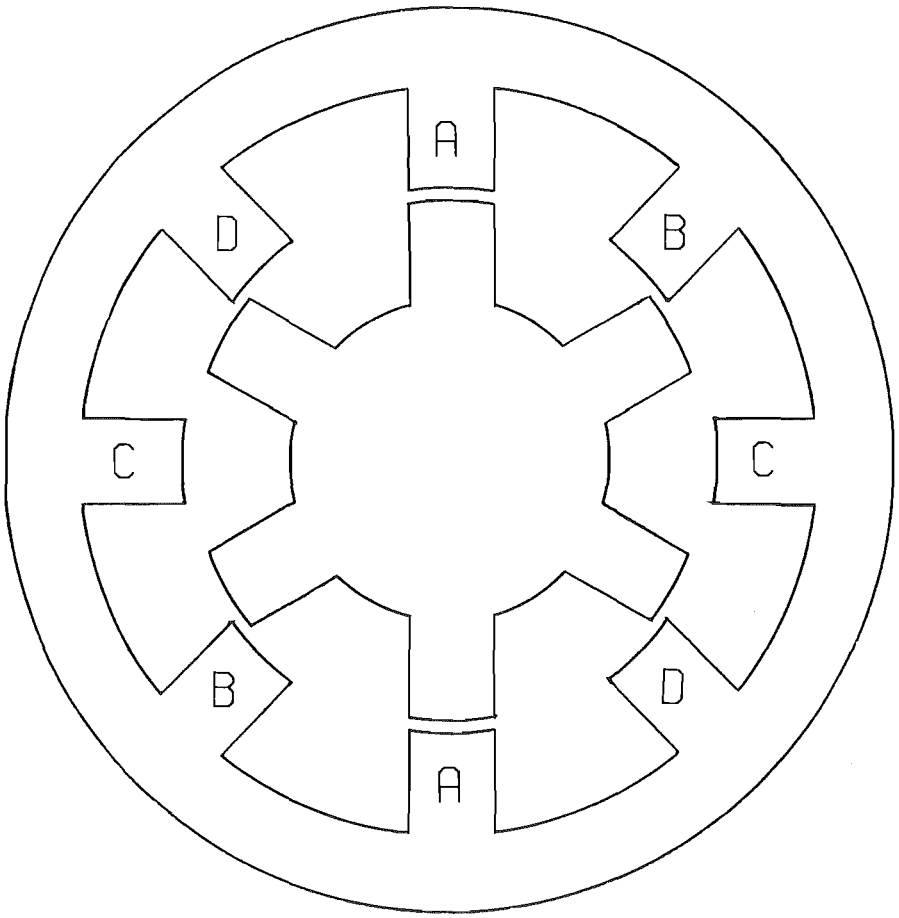

Fig 2.2 A single stack four phase motor.

the motor to be made. A theoretical plot of the phase inductances as functions of position within the electrical cycle is shown in figure 2.3. The phase inductances are represented sinusoidally. In practical motors the inductance variation is not exactly sinusoidal because of saliency in the pole configuration. However over much of a motor's electrical cycle the inductance variation is almost sinusoidal.

Figure 2.3 shows the ninety degree shift in electrical position between adjacent phase inductances inherent in the four phase motor. The detent positions are located as the points of maximum inductance and are labelled according to phase. The points of minimum phase inductance represent the rotor positions of maximum misalignment between the stator and rotor poles for a given phase. The two step separation between minimum and maximum inductance of a given phase can be seen.

2.4 Performance Criteria.

The performance of a variable reluctance stepping motor is a function of a number of variables. However the cumulative effect these variables have on performance can be expressed in terms of the resulting phase current and its time gradient as functions of rotor position.

The voltage across a phase winding during operation generally opposes the power supply voltage. This phase voltage therefore limits the current flowing in the phase. An analysis of the phase voltage enables calculations of the phase current and its gradient. An analysis of a phase voltage can therefore be used in modelling the performance of the motor for a particular set of operating conditions.

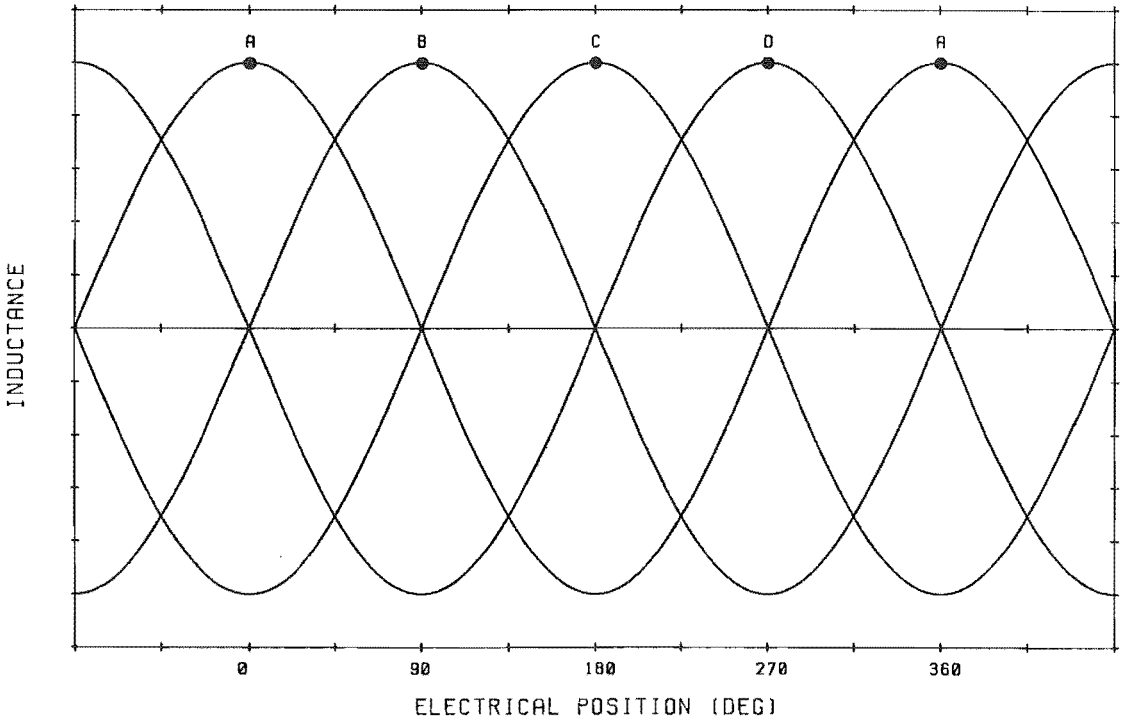

Fig 2.3 Theoretical phase inductances.

A general and complete expression for the voltage across a phase as a function of time can be written (cf. Kuo 1979). The expression is derived from consideration of the time rate of magnetic flux linkage change within the phase inductance. The total flux linkage can be expressed by the sum of a number of terms involving the product of inductance and current. The expression is derived rigorously by Kuo (1979) so the derivation is not reproduced here.

The general expression for the voltage across phase k of an n phase motor is,

$$V_k = R_k i_k + \sum_{j=1}^{n} \frac{d(L_{kj} i_j)}{dt} \qquad (2.1).$$

When expressed in terms of the transformational, motional and saturational components, this expression becomes,

$$V_k = R_k i_k + \sum_{j=1}^{n} L_{kj}\left(\frac{di_j}{dt}\right) + \left(\frac{\partial L_{kj}}{\partial \theta}\right)\left(\frac{d\theta}{dt}\right) i_j + \left(\frac{\partial L_{kj}}{\partial i}\right)\left(\frac{di_j}{dt}\right) i_j \qquad (2.2).$$

The transformational voltage is,

$$\sum_{j=1}^{n} L_{kj}\left(\frac{di_j}{dt}\right) \qquad (2.3).$$

This component is the summation of voltages induced in phase k through current change in the self and mutual inductances. The motion induced voltage is,

$$\sum_{j=1}^{n} \left(\frac{\partial L_{kj}}{\partial \theta}\right)\left(\frac{d\theta}{dt}\right) i_j \qquad (2.4).$$

This component is the summation of voltages induced in phase k through

change in the self and mutual inductances with rotor position. The saturation induced voltage is,

$$\sum_{j=1}^{n} \left(\frac{\partial L_{kj}}{\partial i_j}\right)\left(\frac{di_j}{dt}\right) i_j \qquad (2.5).$$

This component is the summation of voltages induced in phase k through change in the self and mutual inductances with current. Saturation imposes a current dependency on the phase inductance, causing a reduction in inductance with increasing saturation. A current dependant inductance at a given value of current is termed the incremental inductance at that current, and it is this value of inductance which must be used for exact calculations at significant portions of the rated current. In practical stepping motors, the rotor and stator teeth are subjected to the greatest flux density and are typically saturated when operating at high currents. This saturation is known to affect the performance of the motor. The inclusion of saturation terms renders equation 2.1 nonlinear and subsequent torque equations without closed form solution. Linear models which omit the saturation terms in equation 2.1 can be solved. While not exact these models are still useful as they illustrate how certain variables affect performance.

The torque output can be calculated by applying the principle of virtual work and considering the field energy decrease with respect to rotor position. A rigorous derivation of the torque output with rotor position expected by the linear model is also presented by Kuo (1979) and is not reproduced here. The torque expression for phase k from the linear magnetic model solution of,

$$T = \frac{1}{2} \sum_{k=1}^{n} \sum_{j=1}^{n} \left(\frac{\partial L_{kj}}{\partial \theta}\right) i_k i_j \qquad (2.6).$$

This expression includes both the self and mutual torques. It can be seen that the self torque produced is proportional to the current in that phase squared and the rate of inductance change with rotor position. In practical motors operating near rated current, saturation effects reduce the rate of inductance change with rotor position. This in turn reduces the torque output below that predicted by the linear model.

2.5 Drive Circuits.

The type of drive circuit used with a stepping motor governs the rates of current rise and suppression (decay) in the phase windings and hence the performance. The current which can be achieved during running is limited by the electrical time constant of the phase winding and drive circuit, the asymptotic current value and the motional voltage term of equation 2.1. This is particularly so at high speed where the time constant may be a significant portion of a phase's excitation period and the motional voltage term increases to a significant portion of the supply voltage. The motional voltage is in opposition to the power supply voltage and in effect reduces the asymptotic current. To obtain high torque output at high speed it is therefore necessary to have an energising circuit with a high asymptotic current and either a small electrical time constant or a high supply voltage. At low speed however where the time constant will

be a small portion of a phase excitation period, the current will approach the asymptotic value. This is likely to be many times the rated value if good high speed performance is to be achieved, potentially resulting in damage to the stator windings. Some means of low speed current limiting within the drive circuit which does not significantly decrease the current rise time is therefore necessary.

2.5.1 The L/R Drive.

The usual method of meeting the drive circuit requirements is the L/R type drive, shown in schematic form in figure 2.4.

The resistor R1 limits the current to a safe maximum value when the motor is running at low speed or at rest. When the phase is turned off, the magnetic flux decays producing a reverse voltage across the inductance. The associated current forward biases the suppression diode D and "freewheels" or circulates in the circuit formed by it and the suppression resistor R2. The rate at which the flux is dissipated is set by the value of R2 and expressed in terms of the time constant of this circuit. This flux must be dissipated rapidly in order to minimise the negative torque at the end of each step which the freewheeling current could produce. To achieve this a relatively large resistance must be used in the freewheeling path. The voltage across the switching device will reach a value of the supply voltage plus the voltage drop across R2, which for rapid field decay can be greater than twice the supply voltage. The requirements for good high speed performance can be met by making R1/L and R2/L large and using a high supply voltage. However when taken to an extreme the

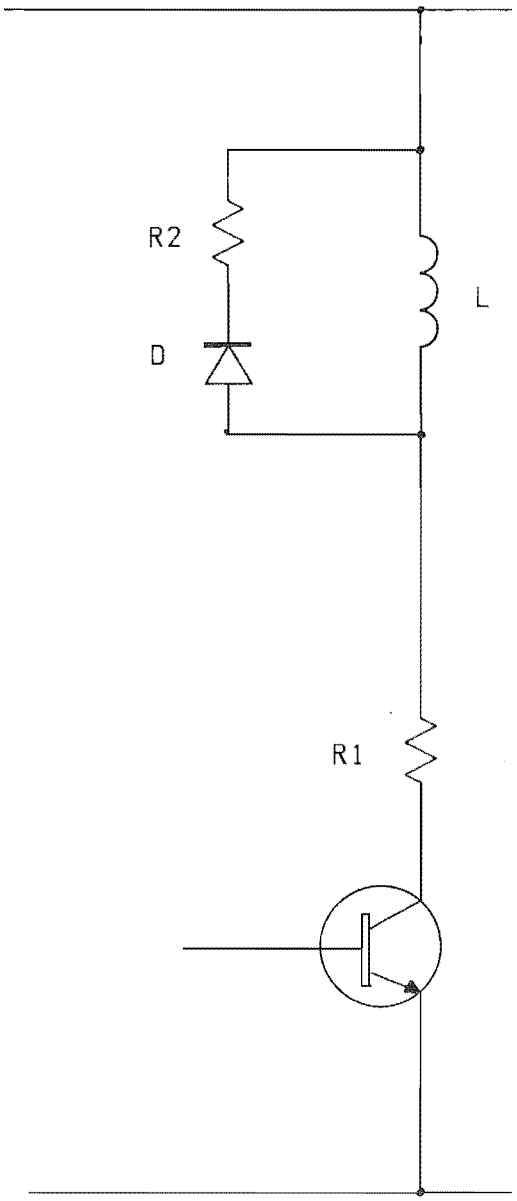

Fig 2.4 The conventional L/R drive.

dissipation in the current limiting and suppression resistors becomes excessive, so there is a practical limit to the performance this type of drive can offer. This is particularly so for large step motors where stator currents can be in excess of 10 amps.

2.5.2 The Active Suppression Drive.

A drive system which overcomes the dissipative problem is the Active Suppression Drive (cf. A. Cassat 1977). This drive differs from the L/R drive principally in that it is configured to return the field energy of a de-energising phase to the power supply. In this way the de-energising current is not dissipated at the end of the step but used for excitation of the consecutive phase. In addition to de-energising current salvaging, this type of drive usually incorporates non dissipative current limiting through chopping of the energising current. The schematic form the drive circuitry takes is shown in figure 2.5 and the characteristic current waveform during one whole cycle is shown in figure 2.6.

The current waveform exhibits three distinct regions. Each region characterises one of the three different functions which the drive performs. These functions can be termed as follows.

1. Energisation (current rise)
2. Freewheeling (large time constant current decay)
3. De-energisation. (field energy retrieval and suppression)

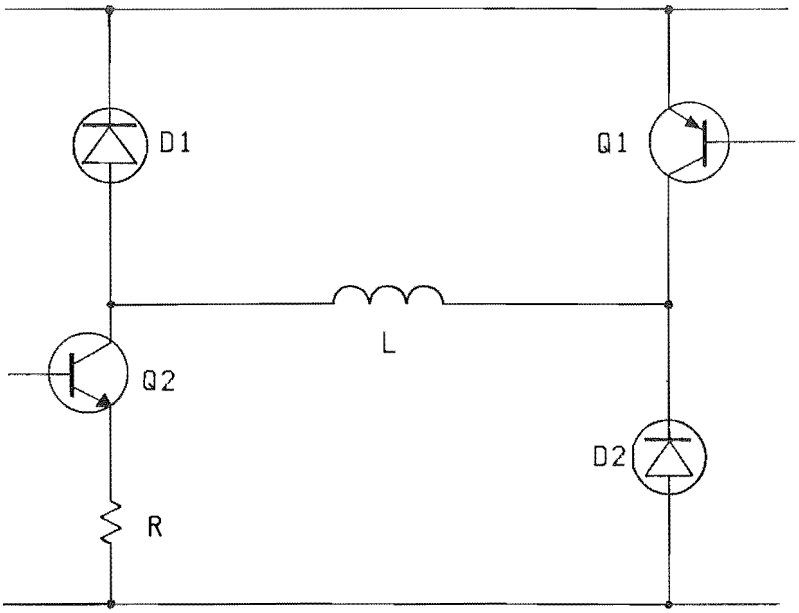

Fig 2.5 The active suppression drive.

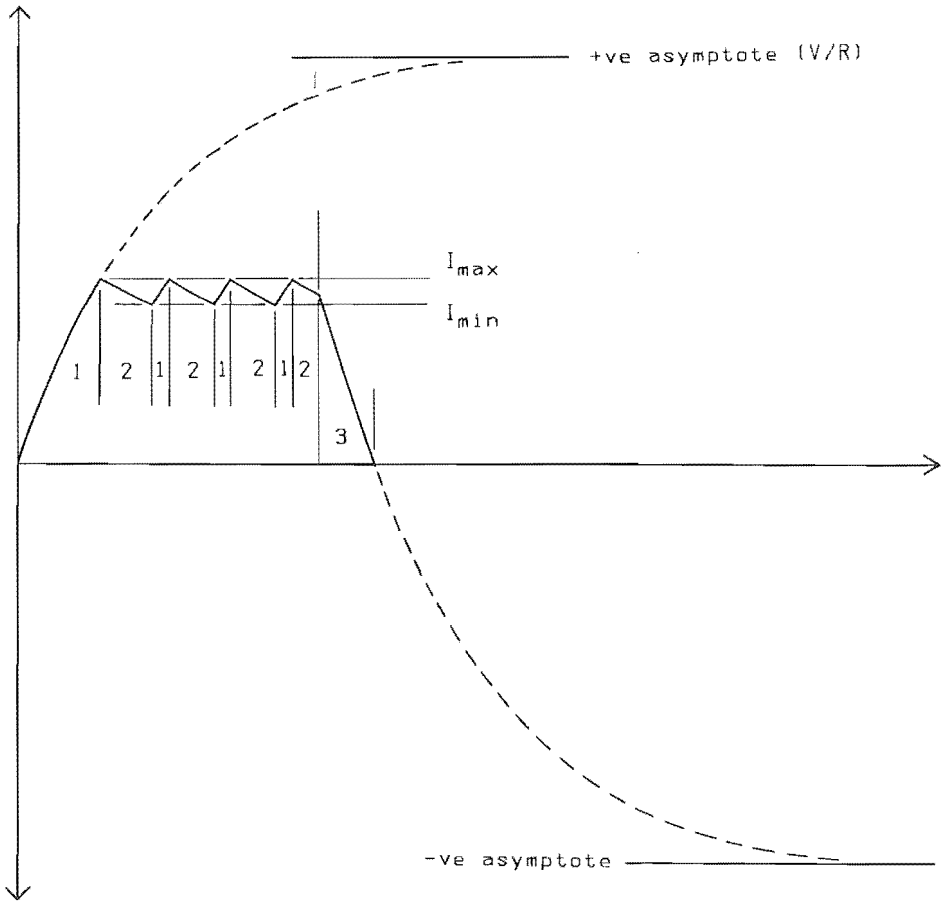

Fig. 2.6 The current waveform.

Energisation is commenced by simultaneously turning on the two switching devices Q1 and Q2 of figure 2.5. The energising current then passes through the current sensing resistor R and is allowed to rise until it reaches a preset level I_{max}. Current I_{max} is detected when the voltage across R exceeds the prescribed level. At this point switching device Q1 is turned off and the current is allowed to "freewheel". The freewheeling current circulates in the circuit formed by diode D2, the switching device Q2 and the current sensing resistor R. The time constant for this circuit is large so the freewheeling current decays slowly, however during chopping, the large time constant is advantageous as the rotor is mid-step and a positive torque is produced by the freewheeling current. When the current has decayed to the minimum level I_{min}, Q1 is once again turned on. This reverse biases D2 and the current in the phase rises until I_{max} is reached and the cycle repeats, maintaining a controlled mean current. Owing to the lack of current limiting resistor, the asymptotic current is very high, albeit with a large time constant. However a very high asymptotic current ensures moderately rapid current rise.

This type of drive also places tighter control on the freewheeling voltages, these being restricted to the diode forward bias voltage drops above and below the supply rails. Further the tight control over the freewheeling voltage allows a higher supply voltage to be used for a given voltage rating of the semiconductor switching devices, and hence yields reduced current rise time.

2.6 An Active Suppression Drive Circuit Linear Model.

A linear model of the active suppression drive has been developed in the course of the research and is described as follows.

The generalised form of the energising current path can be represented as shown below in figure 2.7. The current in this circuit is the solution of,

$$L(\theta)\left(\frac{di}{dt}\right) + i\left(R + \left(\frac{dL(\theta)}{dt}\right) \right) = V \qquad (2.7)$$

where the terms are, the supply voltage, the resistive voltage drop, the self induced voltage and the motional voltage. The rate of current rise is,

$$\left(\frac{di}{dt}\right) = \frac{V - i\left(R + \left(\frac{dL(\theta)}{dt}\right) \right)}{L(\theta)} \qquad (2.8).$$

The de-energising circuit can be represented in a generalised form as shown in figure 2.8. The current in this circuit is the solution of,

$$- L(\theta)\left(\frac{di}{dt}\right) - i\left(R + \left(\frac{dL(\theta)}{dt}\right) \right) = V \qquad (2.9).$$

When expressed in terms of the current gradient, the absolute rate of current decay is,

$$\left|\frac{di}{dt}\right| = \frac{V + i\left(R + \left(\frac{dL(\theta)}{dt}\right) \right)}{L(\theta)} \qquad (2.10).$$

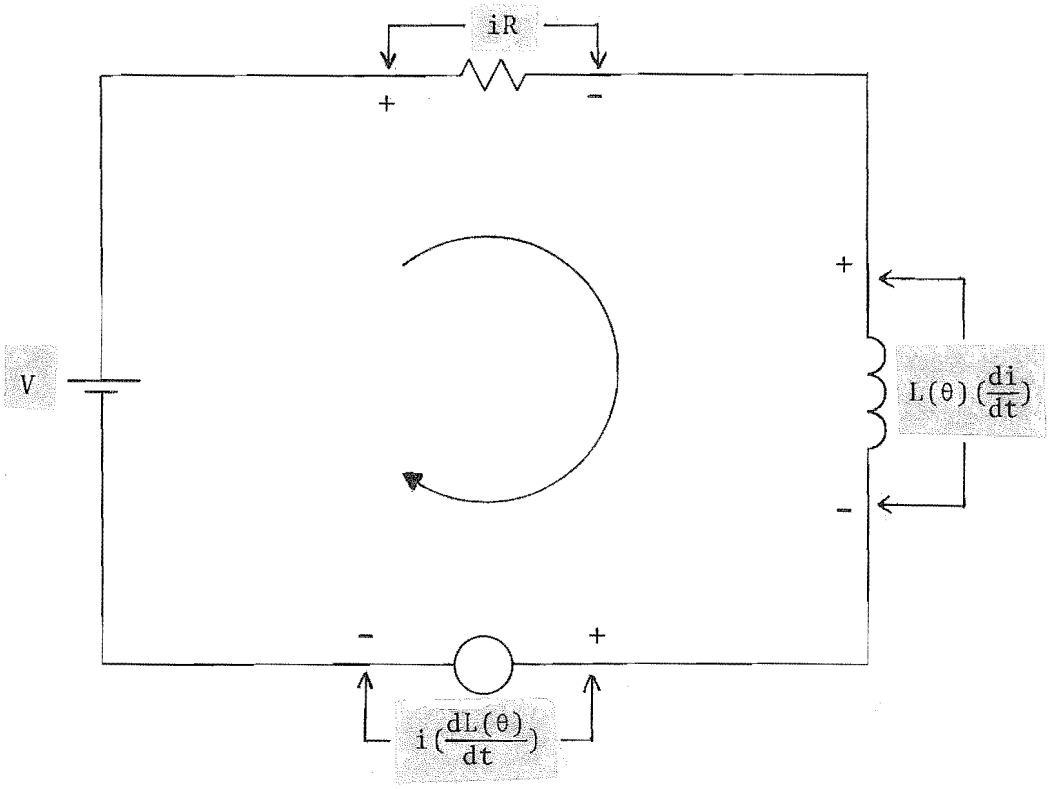

Fig. 2.7 The energising current path.

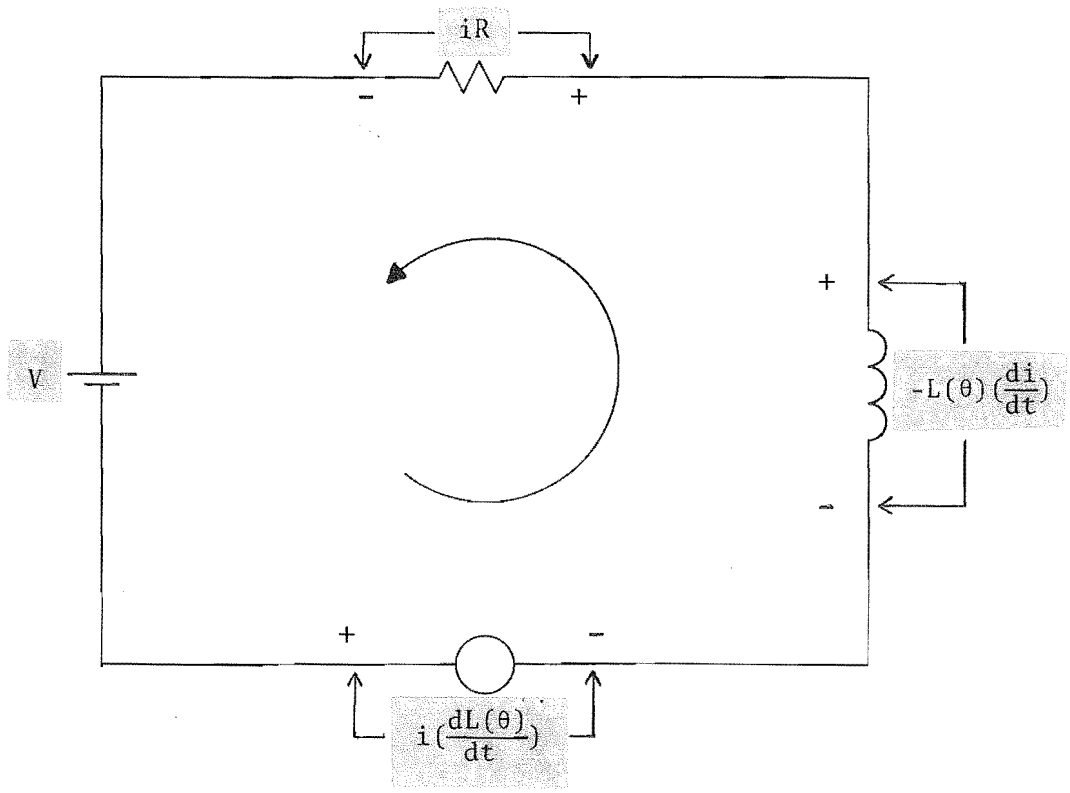

Fig. 2.8 The de-energising current path.

The freewheeling circuit can be represented in a generalised form as shown in figure 2.9. The current in this circuit is the solution of,

$$- L(\theta)\left(\frac{di}{dt}\right) - i\left(R + \left(\frac{dL(\theta)}{dt}\right) \right) = 0 \qquad (2.11).$$

The absolute rate of current decay is,

$$\left|\frac{di}{dt}\right| = \frac{i\left(R + \left(\frac{dL(\theta)}{dt}\right) \right)}{L(\theta)} \qquad (2.12).$$

It can be seen in the energising circuit representation of figure 2.7 that the motional voltage opposes the power supply voltage and reduces the rate of current rise. For a four phase motor, this is so for the two steps prior to detent, where the phase inductance increases as the rotor approaches the detent positions. Beyond this region where the phase inductance decreases as the rotor approaches detent, the motional voltage term adds to the power supply voltage and the current gradient will be increased. However energisation in this region only occurs at high speed and even then begins near the end of the region. The phase currents will therefore be low and the motional voltage term will hence be small in magnitude. Therefore practicably, the motional voltage only serves to decrease the rate of current rise.

In the de-energising circuit representation of figure 2.8, the motional voltage adds to the power supply voltage and increases the rate of current decay. This is the case when de-energisation occurs during either of the two steps immediately prior to the detent position, where the phase inductance increases as the rotor approaches the detent positions. Should de-energisation occur outside this two

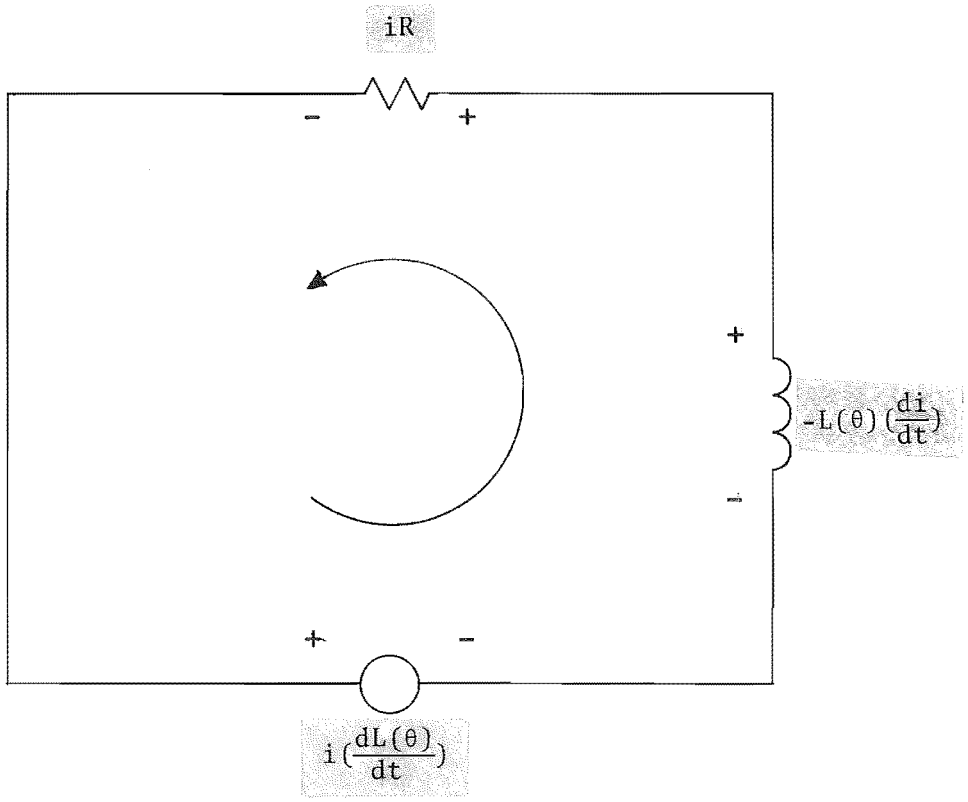

Fig. 2.9 The freewheeling current path.

step range, the motional voltage opposes the power supply voltage, and the rate of current decay is reduced. In practice this does not happen to any significant extent because at high speed where the motional voltage is significant, de-energisation occurs well within the two step range of increasing phase inductance.

The freewheeling circuit is represented in figure 2.9. This circuit is related to the de-energising circuit. The difference lies in the absence of the power supply voltage. This absence allows the current to decay naturally in accordance with the circuit time constant. Consequently the current decay is considerably slower than in the de-energising circuit. The slow current decay during freewheeling is desirable. The rate of freewheeling current decay plays a role in the low speed efficiency of the drive but has no influence on the high speed performance.

It can be concluded that the rate of current decay during de-energisation is generally increased by the motional voltage, whereas during energisation the rate of current rise is generally decreased. As the rate of current decay is typically faster than the rate of current rise, the de-energising current has usually reached zero in less than one step at high speed. At low speed the de-energising current reaches zero in a very small portion of one step. For most operating conditions this means the de-energising current will be dissipated before detent of the phase and no negative torque will result from it.

2.7 Lead Angle.

The position of the rotor teeth relative to the stator teeth of a phase as it is energised, has a significant effect on the torque output of the motor. This angular displacement of the rotor teeth in advance of the detent position of the phase when it is first energised is termed the "lead angle", and is illustrated by the theoretical static torque plots for a four phase motor in figure 2.10.

Static torque plots are plots of holding torque variation with rotor position and are generated by measuring the torque necessary to hold the rotor stationary over a range of rotor positions. In theoretical plots a sinusoidal torque variation with rotor position is usually assumed. The detent positions coincide with the points of zero torque output, from where a rotor displacement in either direction produces a torque acting in the opposite direction, i.e. a restoring torque. The restoring torque results from an increase in the flux path reluctance as rotor is moved away from the detent position. The other points of zero torque are meta-stable positions only and a displacement in either direction from one of these positions will cause the rotor to come to rest at an adjacent detent position. The detent positions are labelled according to phase, points A on the rotor position axis being the detents of phase A and the meta-stable points of phase C etc.

The lead angle for energisation of phase A is measured with respect to and in advance of the detent positions for phase A. The optimum lead angle varies as a function of speed, at low speed it is close to the value which gives maximum static torque output. The maximum positive and negative static torque outputs possible are

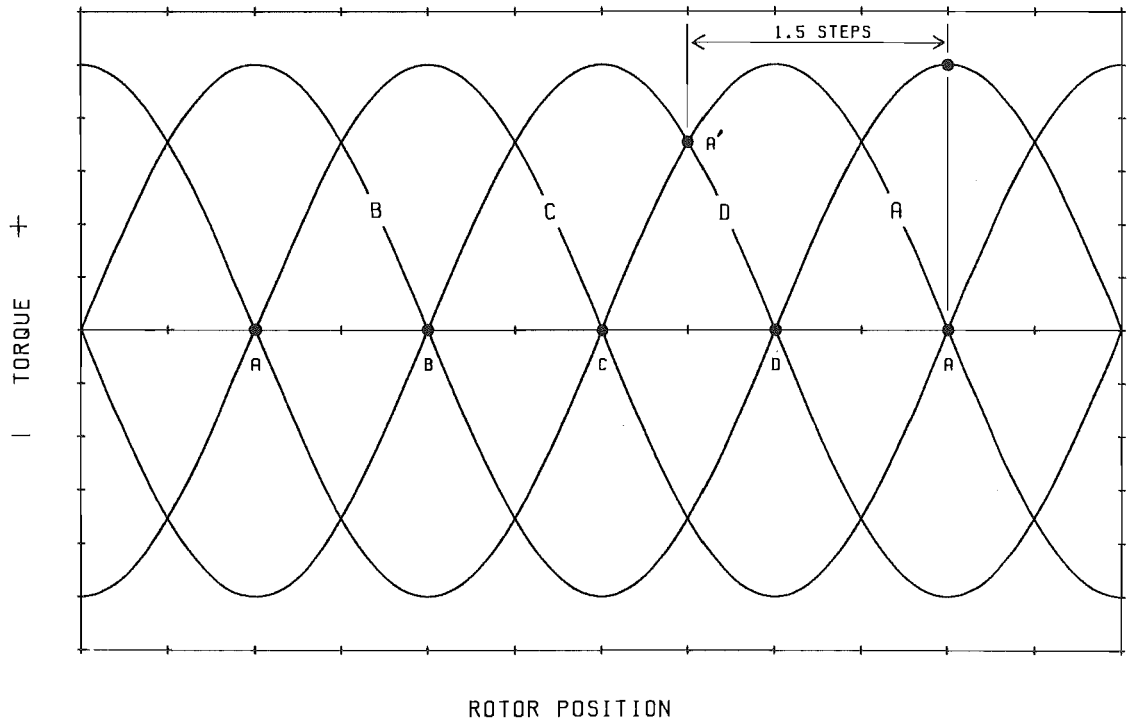

Fig. 2.10 Theoretical static torque plots.

illustrated by the envelope which contains the torque plots of all the phases. For the theoretical plots shown, this lead angle is 1.5 steps. The point A' shows where Phase A is energised to produce a 1.5 step lead angle for positive rotation. At greater speed however energisation must occur in advance of this position. This corresponds to a greater lead angle. The advance is necessitated by the finite rise time of the energising current. To achieve high current in rotor positions where it can produce high torque output, it is necessary to start energisation of the phase earlier. This requirement is compounded by the current limiting effect of the motional voltage which increases with speed.

Analytical derivations of the optimum lead angle for an L/R driven motor as a function of speed have been performed by Acarnley and Gibbons (1982), Rahman and Bell (1984) and Tal (1982). These derivations lead to the same final result. Acarnley and Gibbons (1982) express the result as an angular advance on the static torque lead angle, termed the switching angle. Their analysis yields,

$$\theta_s = \left(\frac{1}{p}\right) \tan^{-1}\left(\frac{\omega L}{R}\right) \qquad (2.13)$$

where p is the number of rotor teeth, L is the mean phase inductance, R is the total phase resistance and w is the electrical angular velocity.

This result is obtained through consideration of only the D.C. and fundamental components of voltage and current, and neglects saturation effects. This simplification is made as the second harmonic of current produces no nett torque during a step and higher harmonics will be heavily attenuated by the proportionately greater reactance at

the higher frequencies. A sinusoidal variation in phase inductance with rotor position is also assumed. Generally, in a practical motor this is only true for a portion of the phase inductance versus rotor position plot. However the phase inductance also varies periodically and as with the voltages and currents, only the fundamental component of the variation is considered in the derivation. With respect to the accuracy of the other assumptions made, the variation of phase inductance with rotor position may also be considered wholly sinusoidal. Saturation effects are neglected so that the nonlinear equations are avoided and an analytical solution can be obtained. This approach is supported by the fact that at high speed where the result is of greatest interest, the currents obtainable are lower and the extent of saturation is much reduced. Within the simplifying assumptions made equation 2.13 predicts the variation in lead angle with speed necessary to maximise the torque output. Calculated results yield values of optimum lead angle which are in reasonably good agreement with experimental results (Acarnley and Gibbons 1979).

The result is also applicable to the active suppression driven motor but only at very high speed when the phase current is not chopped.

2.8 Positional Feedback.

To operate a step motor at or near the optimum lead angle over a wide range of speeds and loads requires closed loop control through self synchronisation, and therefore positional feedback. The positional feedback is traditionally provided by an ancillary device

termed a position encoder. Position encoders are fitted to the frame of the motor and sense the relative position between the stator and parts with relative motion. The most widely used of these techniques are optical and Hall effect proximity detection.

A simplified optical encoder assembly is shown in figure 2.11. The rotating component is a disc with uniformly spaced slots. As the disc rotates with the rotor, the light beam between a source and a sensor is periodically interrupted. If one sensor is used, the resolution of the encoder is equal to the number of slots. If two sensors are used in quadrature, the resolution is doubled and direction detection is also possible. The resolution of the encoder can be increased further by adding extra sensors to the encoder. However the task of decoding the outputs from all the sensors into a contiguous pulse train and detecting rotation direction becomes increasingly more complex.

True positional feedback requires either continuous monitoring or the ability to interpolate between discreetly sensed rotor positions. Position encoders usually only sense one or two discrete positions per step, necessitating interpolation. Usually interpolation is achieved by starting an electronically implemented time delay when the sensed rotor position immediately in advance of the desired commutation point is signalled by the encoder. The commutation point and hence the lead angle is changed by varying the length of this delay. To produce a given lead angle requires knowledge of motor speed at any instant. At high speed a small change in the delay period brings about a significant change in the lead angle. This necessitates a very stable delay period if consistent performance is to be achieved. At low speed if the same position is to be used to trigger

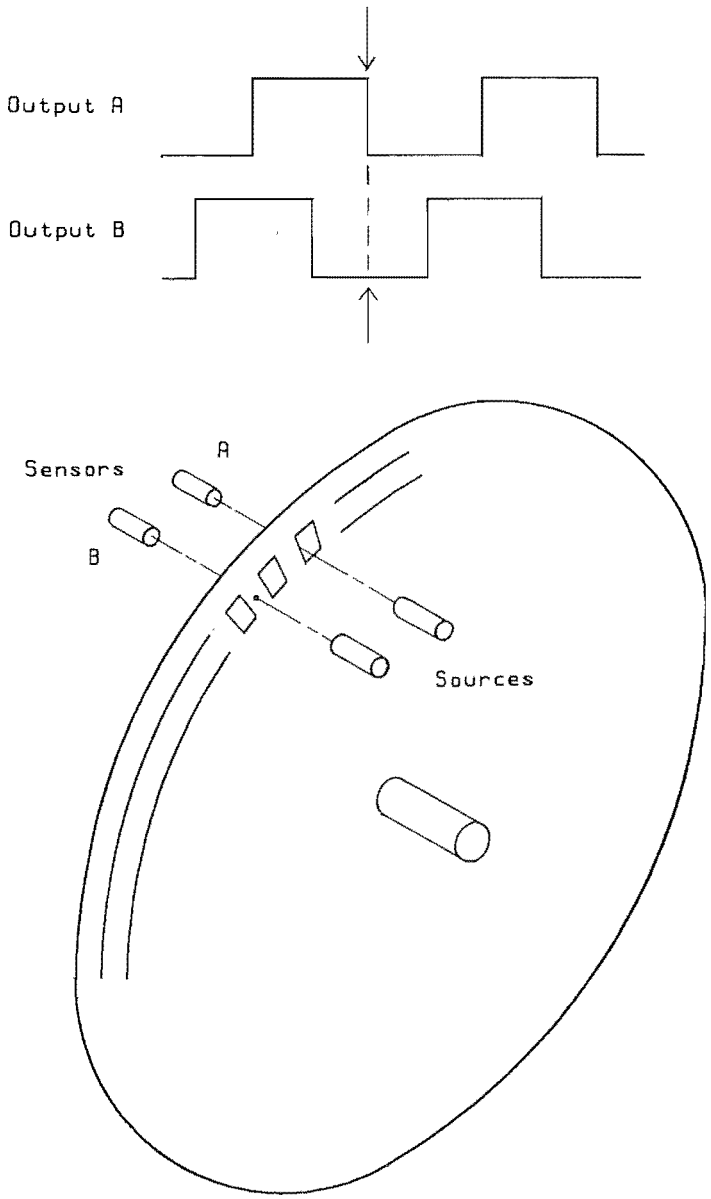

Fig. 2.11 Optical encoder assembly showing two sensors in quadrature.

the delay period, a much larger delay is required to produce the same lead angle. If the motor is to operate over a wide speed range, a delay which can be varied over a wide range with high accuracy, repeatability and in accordance with speed is required.

2.9 Self Positional Feedback.

The variation of the phase inductances with rotor position is the fundamental criterion which self positional feedback and hence encoderless self synchronisation is based on. Successful encoderless self synchronisation of motors under the L/R drive has been reported (cf. Kuo 1979, Jufer 1981 and Jufer and Campiche 1981) however for motors driven by the active suppression scheme it has only been discussed (cf. Acarnley et al. 1985).

2.9.1 Self Positional Feedback With The L/R Drive.

The techniques used with the L/R drive are well documented in the literature. These methods have been developed as a result of the unquestioned use of the L/R drive over a long period. Principally these techniques rely on detecting current extrema in either the on or off phases. Typical current waveforms are presented and analysed by Kuo (1979). The general phase voltage equation 2.1 can be analysed qualitatively to indicate what the criteria are for current extrema.

In on phase monitoring, the criteria for extrema can be analysed by setting the current gradient terms equal to zero. When

neglecting mutual and saturational terms as well, equation 2.1 reduces to,

$$V_k(t) = i_k(t)\left(R_k + \omega\left(\frac{\partial L_k(\theta)}{\partial \theta}\right) \right) \qquad (2.14).$$

It can be seen that the conditions for obtaining extrema in the on phase current depend on applied voltage, current limiting resistance and motor speed in addition to phase inductance variation with rotor position. If extrema are to be obtained, equation 2.14 must hold at some point during the step. This requires that R be matched to the motional voltage term and the current. At high speed it is necessary that R be kept small whereas at low speed, a higher value of R is required.

It is clearly inconvenient to vary the value of a resistor which is required to carry high current and dissipate appreciable power. Also, the value of R required to set the operating conditions and that required for monitoring may be in conflict. To produce the desired lead angle at a given speed, the value of R must be chosen to satisfy equation 2.14 at the correct point so as to provide an extrema. This value of R may produce lead angles at other speeds which are not only far from optimal, but which may not permit synchronisation of the motor. Typically the on phase current displays only one extrema, this being a local maximum, although at low speeds current waveforms exhibiting a maximum followed by a minimum have been reported. Typically only one detected rotor position per step is possible with on phase monitoring.

In off phase monitoring, the criteria for extrema can be assessed by setting the supply voltage equal to zero also. The

resulting equation is,

$$i_k(t)\left(R_k + \omega\left(\frac{\partial L_k(\theta)}{\partial \theta}\right) \right) = 0 \qquad (2.15).$$

The non trivial solution of which is,

$$R_k + \omega\left(\frac{\partial L_k(\theta)}{\partial \theta}\right) = 0 \qquad (2.16).$$

The major advantage of off phase monitoring is the availability of more than one phase for position monitoring. Extrema occur at different rotor positions in different phases, giving a range of different detectable lead angles. The requirements for extrema in the off phases are similar to those of the on phase. The value of the suppression resistor plays a governing role in the occurrence and position of extrema. As with on phase monitoring, the value of resistance in the current path required for monitoring may be in conflict with the value required to set the operating conditions of the motor. At high speed the de-energising current must be dissipated quickly in order to prevent the production of negative torque. This may require a value of suppression resistor too high to produce detectable extrema. Starting can also be a problem with off phase monitoring, as it relies on the freewheeling current of a previously energised phase. One phase must be spontaneously energised and the freewheeling current observed. However the motional voltage will be very low and the high starting current may cause saturation of the iron. This will lower the incremental inductance and give a reduced change in phase inductance with rotor position, making monitoring unreliable. Some of these problems can be overcome by monitoring

different phases at different times. For example on phase monitoring can be used during starting, and as the speed increases, monitoring can be changed to the off phases.

The performance of all extrema detecting methods is subject to the motional voltage characteristic of the motor. This individual characteristic may in many instances preclude self synchronisation. Also, the added complexity of the drive circuit modifications necessary to achieve effective self synchronisation over a wide speed range may make the scheme unattractive when compared with fitting a position encoder. Further, the sensitivity of extrema detecting methods is a function of the curvature or second derivative of the current waveforms thus making them very susceptible to noise generated by switching transients.

In conclusion, success with this type of positional feedback scheme is not assured.

2.9.2 Self Positional Feedback and Active Suppression.

The principle publication in the field of obtaining self positional feedback from motors driven by the active suppression drive is titled "Detection of rotor position in stepping and switched motors by monitoring of current waveforms" (P.P. Acarnley et al. 1985). This publication has served as the starting point for the advances made in this research.

In this publication two possible techniques of achieving self positional feedback over a wide speed range while using the active suppression drive have been proposed. The first monitors the current

rise time of the energised phase at aligned and misaligned rotor-stator tooth positions. In these positions, the change in phase inductance with rotor position is zero and hence the instantaneous motional voltage is also zero. This implies current rise times which are speed independent. It is suggested that the current rise times which correspond to the zero motional voltage rotor positions can be detected. However the current rise time is still subject to the effects of saturation, and it is not assured that a given rise time corresponds to a unique rotor position over the large current range typically encountered over a whole step. Furthermore, zero motional voltages do not occur at useful rotor positions for self synchronisation of the four phase motor used in this research. Aligned positions occur at detent and misaligned positions which are two steps in advance. Such positions will yield lead angles in the consecutive phase of one and three steps respectively. A one step lead is non optimal at any speed, being less than the lead angle for maximum static torque. A three step lead angle is extreme, and the motor may not produce sufficient torque in the positive direction to sustain synchronisation at any speed.

The second technique proposed monitors the current rise time during low level current chopping in a normally off phase. The current level is set to a small fraction of the current level in the on phase. In this way, the current rise time in the off phase can be observed without subtracting from the torque developed by the on phase. As the currents are very low, the off phase voltage can be considered free of the motional and the saturation induced voltages and hence, so can the current rise time. If the chopping rate is high enough compared with the motor speed, a large number of observations per step will be made,

approximating the ideal of continuous position monitoring. As with the on phase, the current in the off or "monitoring" phase is measured by observing the corresponding voltage across a current sensing resistor in the energising current path.

Acarnley et al. (1985) do not consider the effects of the mutual inductance between the on and monitoring phases. Only in a multiple stack motor implementation of this scheme is the flux leakage from the on phase into the monitoring phase negligible.

Using the active suppression drive linear model, the energising current in the monitoring phase may also be described by equation 2.7. The ratio of monitoring phase current to on phase current is small. Therefore to obtain signal voltage amplitudes in both on and monitoring phases which can easily be analysed, it is necessary that the value of the current sensing resistor in the monitoring phase be appropriately increased. The effect this has on equation 2.7 is to make the resistive voltage term swamp the motional voltage term to the extent where the motional voltage term can be disregarded, so equation 2.7 reduces to,

$$L\left(\frac{di}{dt}\right) + iR = V \qquad (2.17)$$

which has the solution,

$$i = \frac{V}{R}\left(1 - e^{-\left(\frac{R}{L}\right)t}\right) \qquad (2.18).$$

This is the familiar i(t) expression for rising current in a linear R/L circuit.

The time constant of the freewheeling current path during

chopping is large and unless steps are taken to increase the rate of current decay, the frequency of chopping and hence monitoring is limited. The chopping rate can be increased by reducing the width of the hysteresis band between the current limits I_{max} and I_{min}. But in the interests of good noise immunity, it is desirable to chop between broadly spaced current limits and to force the phase current to decay rapidly.

The inherently rapid current decay of active suppression can be employed at the end of each rise time measurement, rather than allowing the current to circulate in the freewheeling circuit. The advantage of using active suppression during the monitoring cycle is illustrated in figure 2.12. The amplitude of the monitoring current can be made larger for the same length of monitoring period. The enforced current decay in the monitoring phase can also be described by equation 2.9 because the de-energising current path of the monitoring phase is identical to that of the on phase. The resistance in the de-energising current path is therefore very much lower than that in the energising current path. As the resistive voltage drop and the motional voltage in the monitoring phase during de-energisation are both very small compared with the transformational voltage, they can be neglected and equation 2.9 reduces to,

$$-L\left(\frac{di}{dt}\right) = V \qquad (2.19).$$

As required, current decay is rapid.

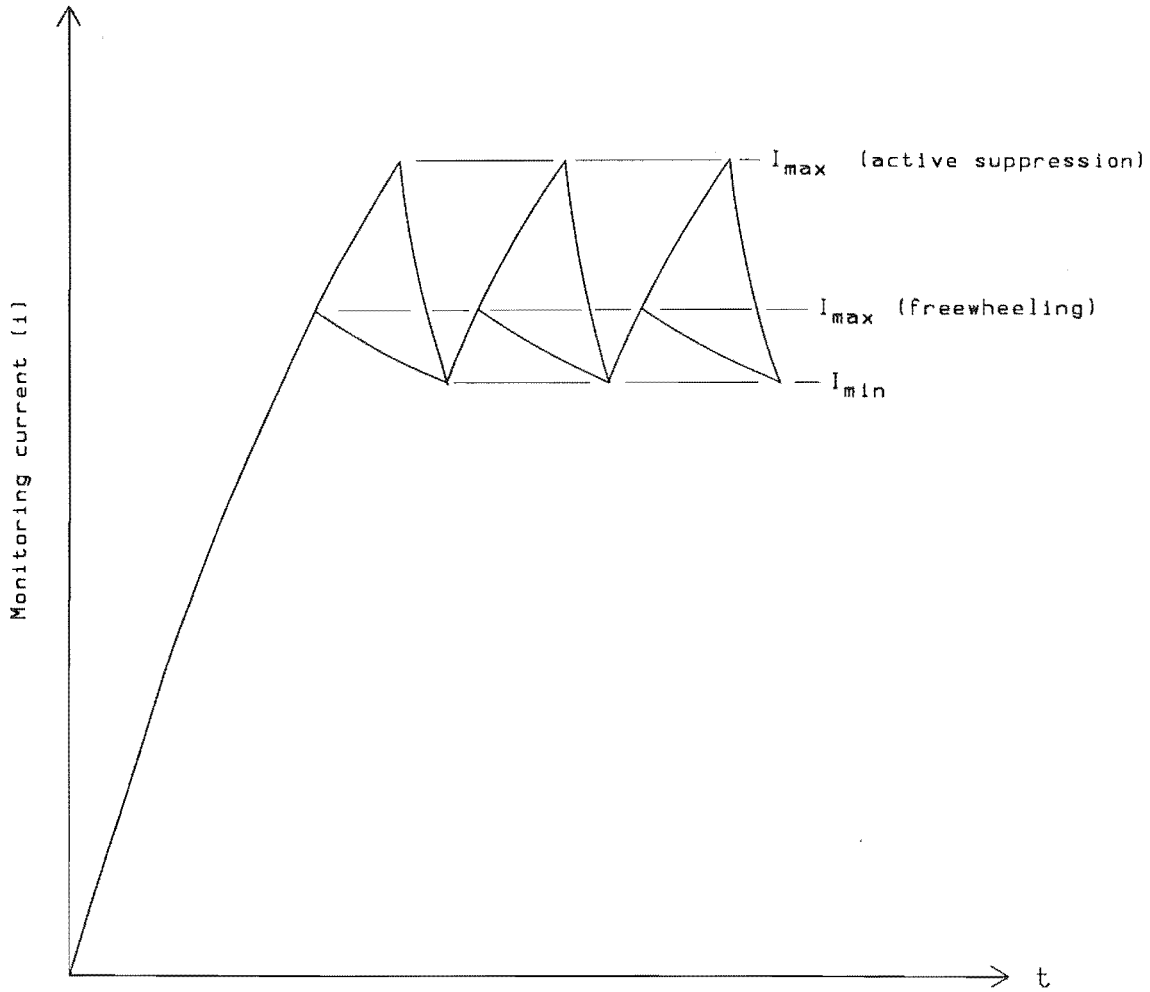

Fig. 2.12 Monitoring current chopping:
active suppression vs freewheeling.

2.10 The Position Monitoring Algorithm.

An algorithm was devised in the course of the research which is derived from the second method described by Acarnley et al. (1985). It has the advantage of being simpler to implement in terms of circuitry. The algorithm is to repeatedly energise the monitoring phase for a fixed period T and then measure the peak current reached at the end of this period rather than measure the time taken for a rise to a set level. The rotor position can then be derived from a voltage measurement rather than a time measurement.

The algorithm is illustrated in terms of the monitoring phase current in figure 2.13. The peak current during each monitoring cycle is observed as the maximum voltage across the current sensing resistor. This voltage is then compared with a reference voltage. If the first cycle shown is that obtained at maximum phase inductance, the increase in the peak current of subsequent cycles results from the decrease in the phase inductance with rotor motion. Monitoring of this phase continues until the reference voltage has been exceeded. Then a new phase is monitored with an equivalent starting position. If the two consecutive phases are electrically identical and the motor speed is constant, an exact repetition of the monitoring history of the first phase will result. Through decreasing the reference voltage, earlier cycles will exceed the reference voltage then the point of commutation will be advanced. The commutation advance means an increased lead angle. Increasing the reference voltage will have the opposite effect of a reduction in the lead angle.

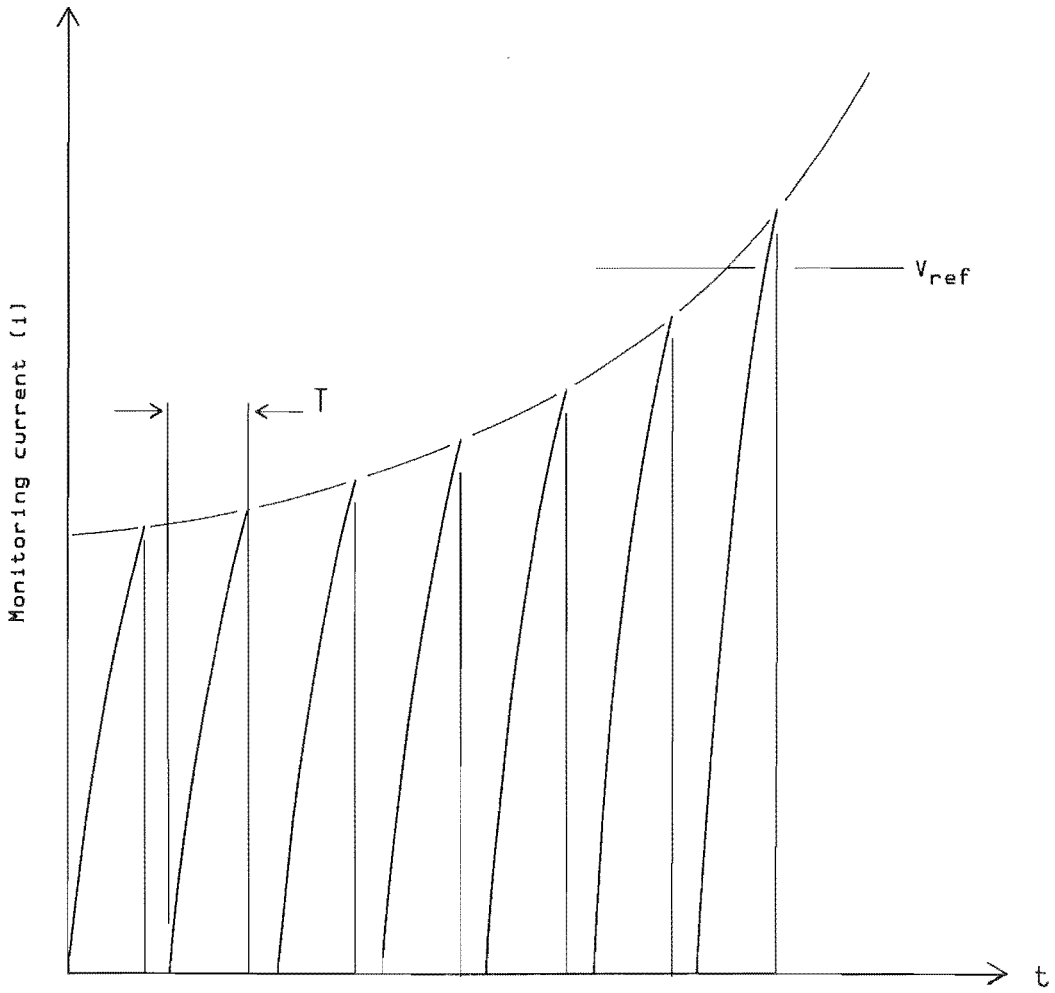

Fig. 2.13

The theoretical monitoring phase current waveform.

2.10.1 Spatial Requirements of the Monitoring Phase Inductance.

In the four phase motor under single phase excitation there are always three off phases, but only two are at zero current during the whole of a given step. Only these two phases are available for position monitoring. These phases are the first leading and orthogonal (second leading) phases. The first and most fundamental requirement of the monitoring phase is that the inductance at the point of commutation must only occur once per step otherwise premature commutation will occur. Premature commutation in one phase may have a compounding effect leading to further erroneous commutations and the subsequent loss of synchronisation.

The phase inductance plots reproduced in figure 2.14 show the theoretical rotor positions beyond which this first requirement is not met. The rotor positions where the inductance of a phase is the same at the beginning and end of a step bound the region where the first requirement is met. It is not necessary for the inductance to decrease monotonically for the entire step. However for reliable position detection, it is preferable that the decrease in monitoring phase inductance with rotor position is monotonic for most of a step. For these reasons the most suitable off phase to use is the orthogonal phase. This phase detents two steps in advance of the on phase detent position and as can be seen in the phase inductance plots has a monotonic decrease in inductance for the whole of this two step range.

Referring to figure 2.14, let phase A be the on phase with points A its detent positions, and its orthogonal phase C be the monitoring phase with point C its detent position. The position of any step where the inductance of phase C is the same at the beginning and

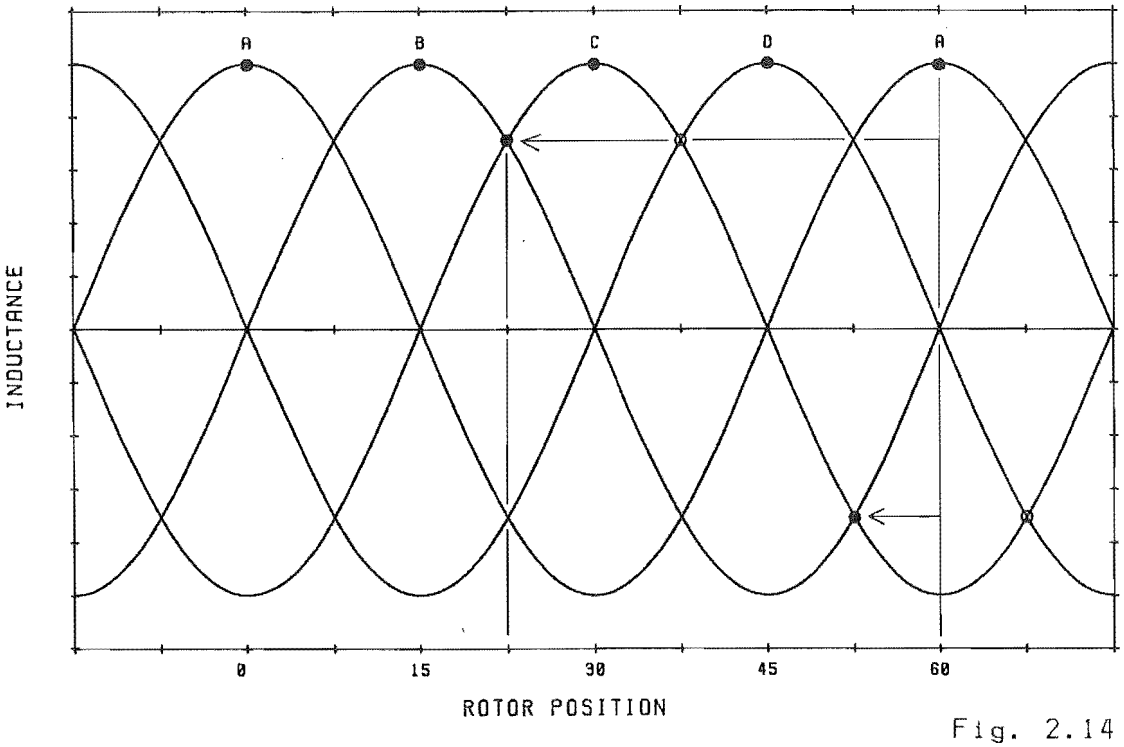

Fig. 2.14

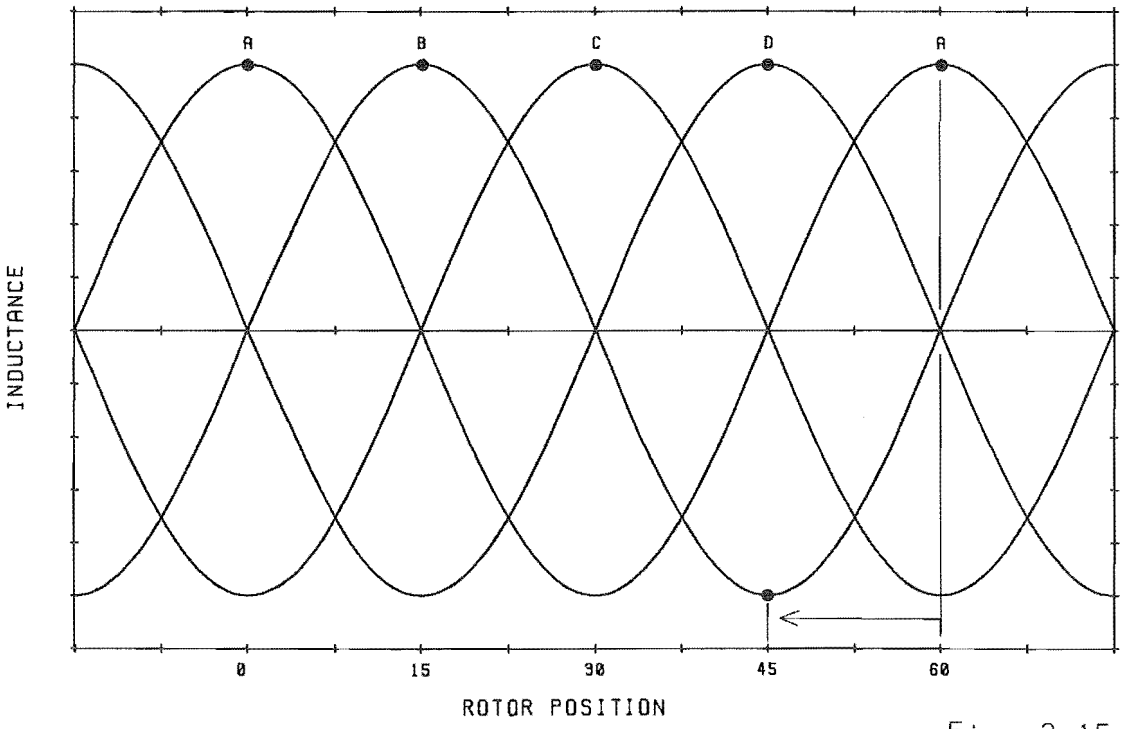

Fig. 2.15

end of the step is between the intersections with phases B and D. Therefore the step over which phase C is monitored must begin between the two points where phase C intersects with phase B. This defines two points in advance of the phase A detent position. These points correspond to lead angles of 2.5 and 0.5 steps with respect to the on phase, A. This implies that the lead angle must be less than 2.5 steps (37.5 degrees) and greater than 0.5 steps (7.5 degrees).

A second requirement of the monitoring algorithm is that the inductance of the consecutive monitoring phase is greater than the inductance of the present monitoring phase. If this criterion is not met, the monitoring voltage of the consecutive phase will exceed the reference voltage during the first monitoring cycle. An erroneous commutation will then result and synchronisation may be lost.

Inherent in the ninety degree shift between the inductances of the four phase motor are regions where this second criterion is not met. The regions where it is met are bounded by the rotor positions where adjacent phases have equal inductance. The phase inductance plots of figure 2.14 show these rotor positions. Let phase A again be the on phase and phase C the monitoring phase. Commutation from phase D to phase A had to occur between the points where phase B and C have equal inductance. From figure 2.14 these positions are 2.5 and 0.5 steps ahead of the detent position for phase A. As a result only lead angles less than 2.5 steps and greater than 0.5 steps can be produced. This is the lead angle range imposed by both monitoring phase inductance requirements.

Another restriction on the lead range results from the position of the minimum of the monitoring phase inductance in relation to the detent position of the next on phase. The algorithm compares only a

rising peak voltage to the reference voltage and can therefore only be applied in regions of decreasing monitoring phase inductance. The limitation can be seen in figure 2.15. where now phase D is the on phase and phase B the monitoring phase. Commutation to phase A as the on phase cannot occur closer to the phase A detent position than the minimum inductance position of phase B. This characteristic imposes a one step or 15 degree minimum lead angle.

2.11 Summary.

The position monitoring algorithm applied to a four phase variable reluctance stepping motor can theoretically generate lead angles in the range of 1 step to 2.5 steps. As is shown in the computer simulation of the drive system (chapter 5) 2.5 steps is an extreme lead angle and is only required at very high speeds. The minimum required lead angle is 1.5 steps, this being the lead angle which develops the maximum static torque output.

Theoretically an implementation of this position monitoring algorithm in conjunction with chopper current limiting and active suppression will produce an efficient variable speed drive capable of operating over a wide range of speeds and loads.

CHAPTER 3.

EXPERIMENTAL RESEARCH.

3.1 Introduction.

A number of stages of development in the experimental equipment were necessary in constructing the closed loop control system analysed in the previous chapter. This chapter details the most major developments.

3.2 The Motor.

The motor used was an Oulton type PLD112 rated at 4kW continuous output at 1500 rpm. This is one of a range of four motors covering a maximum continuous output range of 4kW to 22kW.

The PLD112 like the other motors is a single stack four phase variable reluctance motor. The stator has one pair of poles per phase and therefore has eight teeth. The rotor has six teeth which have a 5 degree skew over their length. The motor is designed for two phase energisation and is supplied with two phases pairs wired in series within the motor. Only the six terminations are brought out to the terminal box. To enable single phase operation and to have the phases electrically independent it was necessary to modify the motor. Independent flying leads were used for each of the eight stator windings and the necessary winding connections were made externally. The phase configuration for single phase excitation (as viewed from the non drive end of the motor) is illustrated in figure 3.1. This

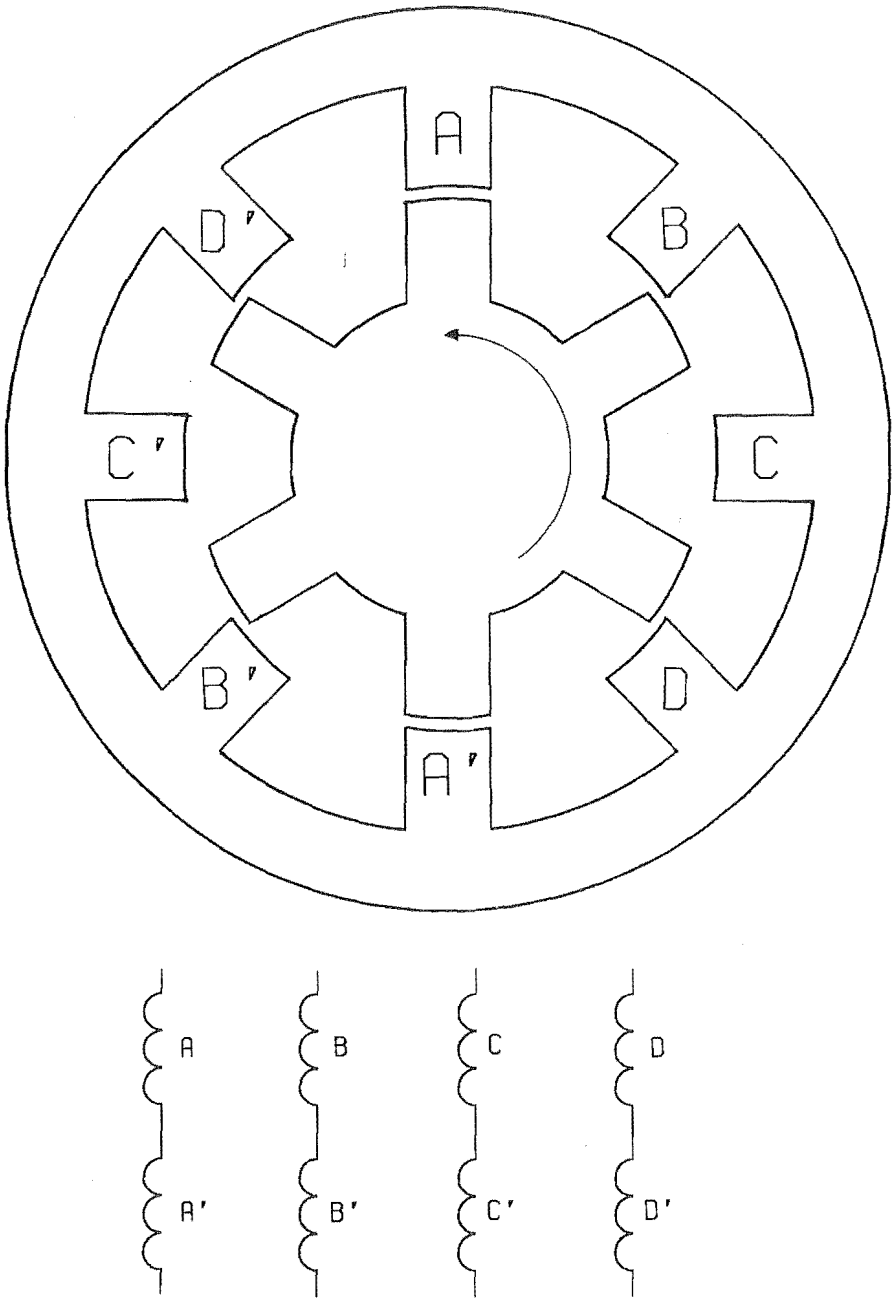

Fig. 3.1
The phase configuration viewed from the non drive end.

configuration produces 15 degree steps or 24 steps per revolution.

3.3 The Controller Architecture.

The preliminary work consisted of developing the circuitry necessary to drive the motor. Independent identical circuitry was constructed for each phase with the exception of the power supplies which are common to all four phases. A block diagram of the circuitry for one phase is shown in figure 3.2. This circuitry performs the active suppression and chopper current limiting but can be divided into three main sections. These are the current sensing circuitry, the active suppression drives and the power supplies. This circuitry is constructed in the form of an independent, slave drive unit which performs the chopper current limiting for each phase about an adjustable limit. The unit is operated by selecting the phase to be energised with external equipment. Communication is made with the unit via a 4 line connection in the form of a four element bit pattern. This arrangement offers complete versatility in the selection of the on phase. Furthermore, it was envisaged that the equipment used to control the slave unit would be subject to a number of developments and should therefore be externally situated.

3.3.1 Current Sensing.

The function of the current sensing circuitry is to control the current chopping. A schematic diagram is shown in figure 3.3.

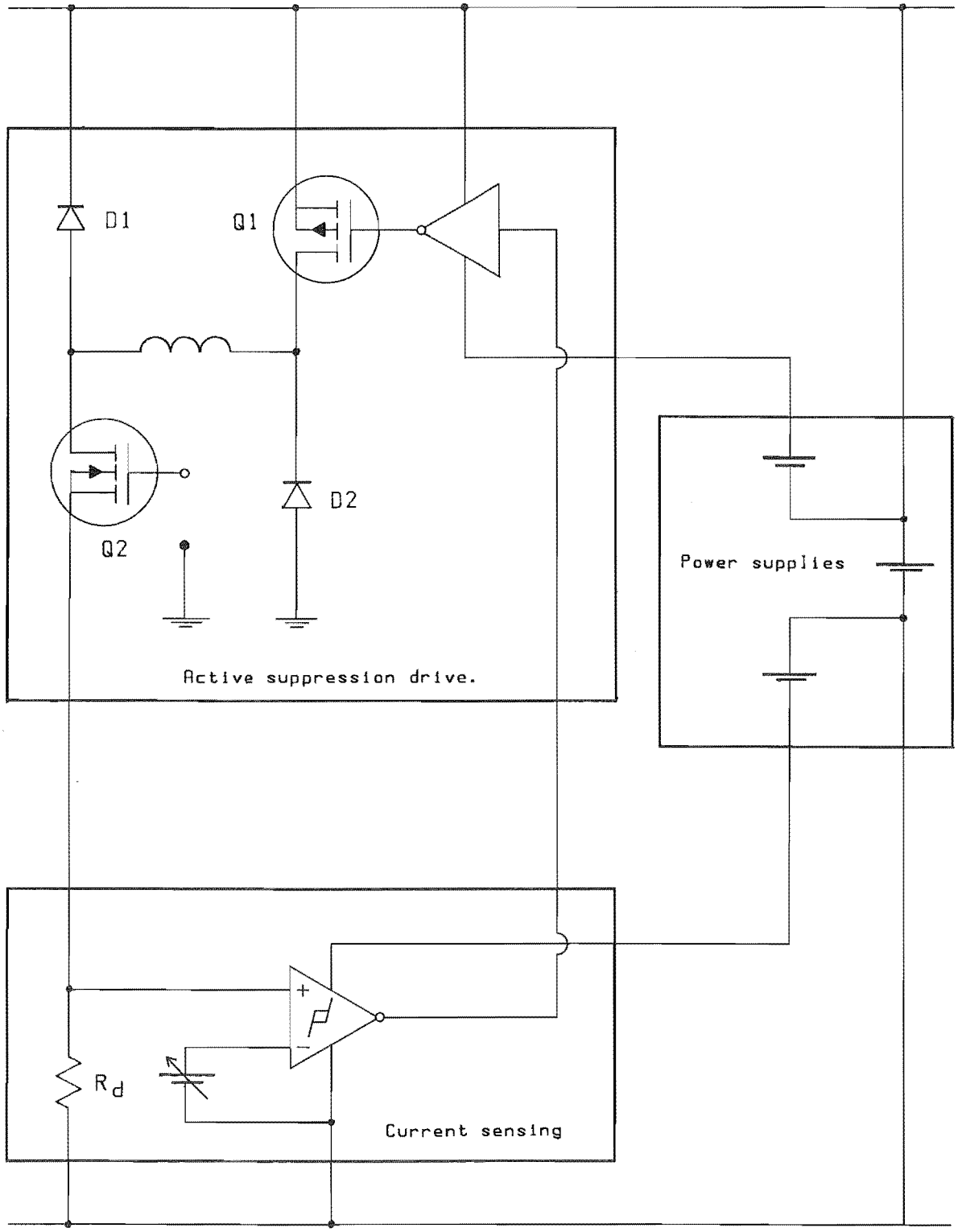

Fig. 3.2 The chopper current limiting circuitry.

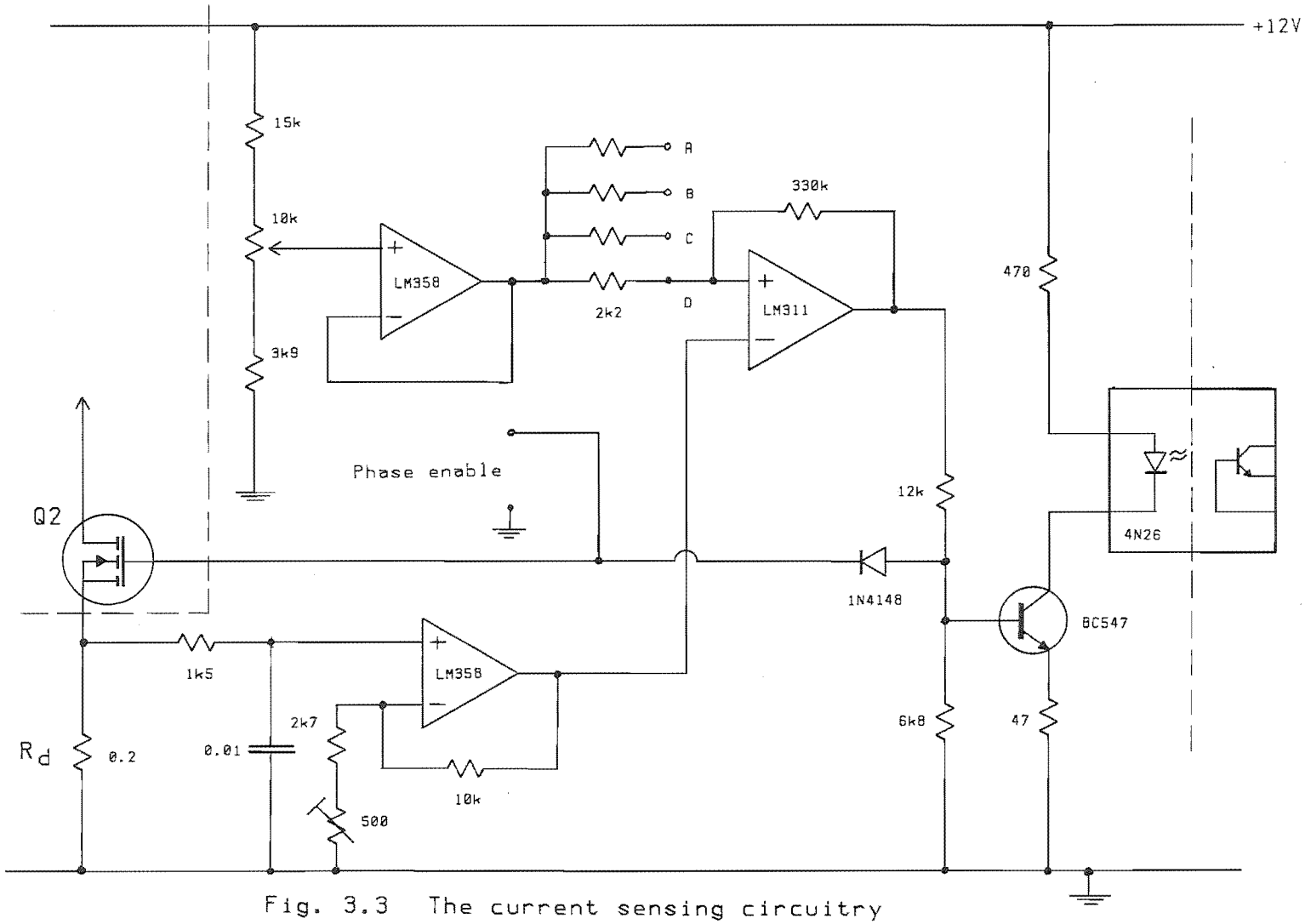

Fig. 3.3 The current sensing circuitry

Principally, it comprises a current sensing resistor R_d, voltage amplifier, reference voltage, comparator and a switching transistor. The voltage developed across the current sensing resistor is first amplified to a level where it can be more readily compared with the reference voltage by the comparator. The mean current during chopping is set to a specified level by varying the reference voltage at the non inverting input of the comparator. This reference voltage is produced by a potential divider then buffered by a voltage following amplifier which supplies the low source impedance necessary to accurately set the hysteresis levels. The comparator functions with hysteresis levels which set the chosen upper and lower current chopping levels. The difference between the hysteresis levels and the current rise and fall rates in the phase determine the frequency of chopping. The output state of the comparator is passed to the high voltage regions of the drive circuitry via the isolation of an optocoupler. The input to the optocoupler is buffered by the switching transistor which unloads the comparator output and passes the high currents necessary to minimise the propagation delay.

3.3.2 The Active Suppression Drives.

The drive circuitry is shown in figure 3.4. It has been designed using power MOSFETs as the switching devices. These devices were selected because of their high switching speed, high voltage ratings and the ease with which they can be driven. Further, MOSFETs can be paralleled without current hogging problems. Two configurations are possible with this type of drive circuit. Firstly, complementary

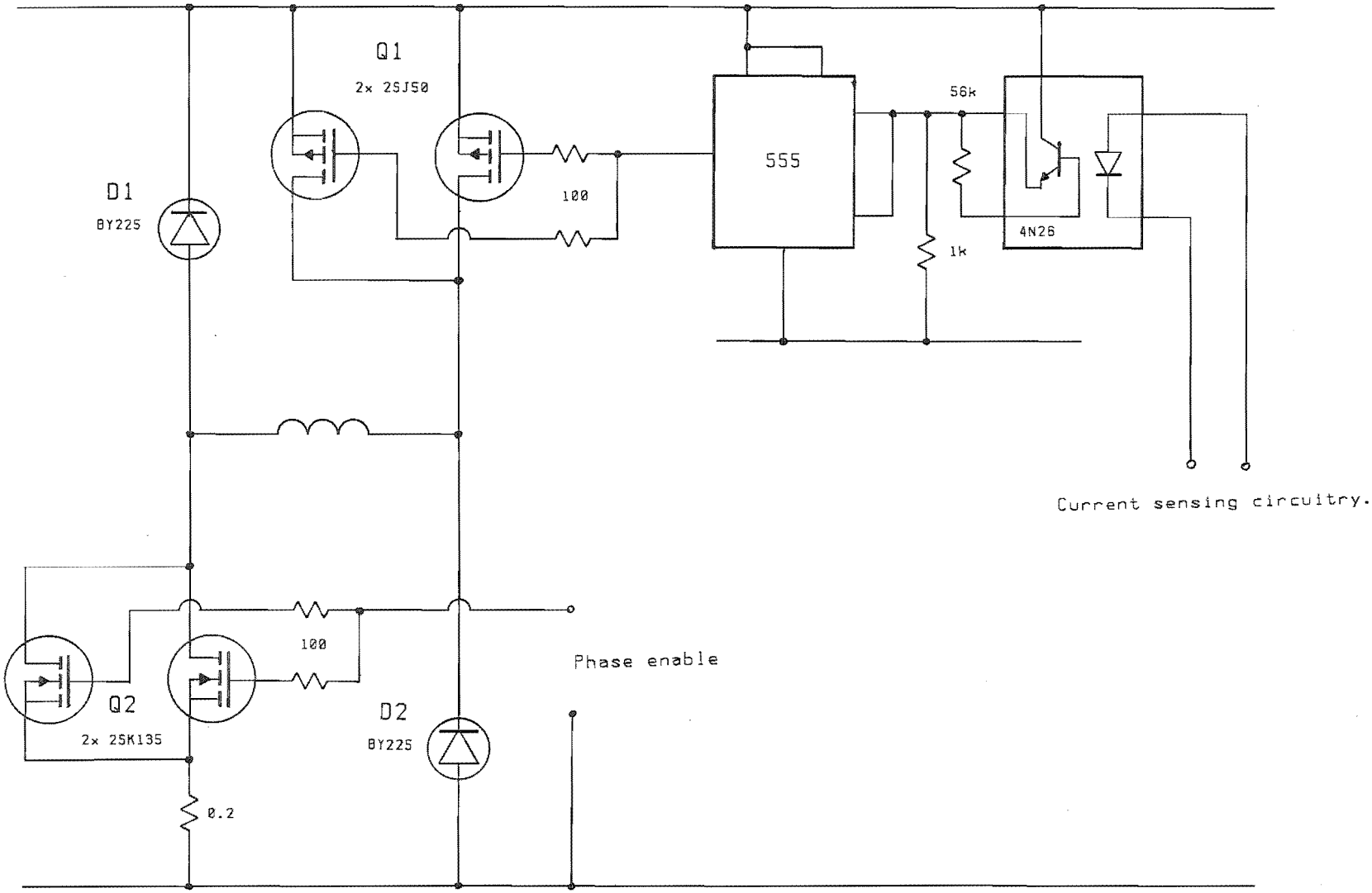

Fig. 3.4 The active suppression drive.

devices can be used for Q1 and Q2. The benefits of using the complementary configuration can be seen when driving of the MOSFETs is considered. The devices are biased on by applying a voltage of appropriate polarity between the gate and the source. When complementary devices are used, P channel devices are used for Q1 and their source terminals are connected to the power supply rail. The devices for all the phases can therefore be biased on by a common auxiliary supply voltage tied to the power supply rail. However the use of P channel MOSFETs limits the power the drive can deliver as at present the best readily available devices do not have the high voltage rating of N channel devices. The alternative is using N channel devices for Q1. However their sources would be at independent voltages which vary in accordance with the voltage across the phase they are energising. This necessitates independent supply voltages to bias Q1 for each phase. These voltages must be able to "float" with the source voltage of each Q1 and therefore must be isolated from each other and the power supply rail.

Despite the voltage rating limitation of the P channel devices, the complementary configuration was chosen because of its relative simplicity. Paralleled pairs have been used for both Q1 and Q2. The devices selected have a drain/source rating of -160 V. This is less than the voltage rating of the motor and limits the output power, but it still enables sufficient performance to fully investigate closed loop control using self positional feedback.

The output from the optocoupler is first buffered. The buffer is necessary in order to switch Q1 rapidly. Several specialist integrated buffering circuits suitable for driving Q1 were catalogued at the time, but future supply of any of these devices could not be

assured. It was therefore decided to develop a circuit using readily sourced components. The LM555 timer I.C. was found to function very effectively as a Schmidt trigger and buffer. Within the 555 are two comparators, a potential divider with junctions at 1/3 and 2/3 of supply voltage and an RS type flip-flop. The comparators can be configured to toggle the flip-flop when the input voltage passes through the 1/3 and 2/3 of supply voltage. The Q output of the flip-flop is buffered with a complementary output stage which enables the 555 to source and sink high currents. This makes it suitable for high speed driving of a capacitive load such as a MOSFET gate source junction.

3.3.3 Power Supplies.

The main power supply which is used for driving the motor is derived from full wave rectifying and smoothing of a 1.5 kVA single phase 85 volt A.C. supply. This produces the chosen rail voltage of 120 volts D.C. The reservoir capacitor inrush current at turn on is controlled. It is limited by a series resistor which is bypassed with a heavy duty relay when the supply voltage reaches 90 volts D.C. A second relay is needed to disconnect the power supply from the drive circuits until the first relay has been activated. The auxiliary supply voltage used for biasing the Q1 MOSFETs is obtained from an unearthed regulated 12 volt supply. The positive rail of this supply is connected to the main 120 volt supply rail. This enables the Q1 MOSFETs' gate-source voltage to be switched between limits close to those of the auxiliary supply voltage of -12 volts. A gate source

voltage in the region of -12 volts is sufficient to saturate the MOSFETs in the on state. A separate 12 volt power supply is used to power the sensing circuitry. Its ground rail is connected to the ground rail of the main power supply which forms the earth point for the controller as a whole.

3.4 Operation Of The Slave Drive Unit.

Initially no current flows in the on phase and the voltage across the current sensing resistor is zero. In response, the output from the current sensing comparator is high. This turns the optocoupler LED on via the switching transistor. The internal photo transistor is then biased on and a high output state results at the optocoupler output with respect to the ground rail of the auxiliary power supply. This forces the output of the buffer to a level close to the ground rail of the auxiliary supply voltage, biasing Q1 on and turning the supply to that phase on. When the upper limit to the energising current is reached, the output of the comparator goes low and a low output state results at the optocoupler output. This forces the output of the buffer to a level close to the main supply rail voltage, biasing the P channel MOSFET Q1 off and turning off the supply to that phase. The phase current is allowed to freewheel until the lower current limit is reached. At this point the voltage across the current sensing resistor after amplification has fallen to the lower hysteresis level. The process then repeats until Q2 is turned off and Q1 disabled.

The majority of the propagation delay of the circuit as a whole

is in the optocouplers. It was found necessary to optimise the forward current through the internal LED in order to minimise the high going propagation delay. The turn off time can be minimised by placing a base-emitter capacitance discharge resistor across the base-emitter junction of the phototransistor. By choosing appropriate values of forward current and base-emitter resistor, the rise and fall delay times have been made equal.

3.5 An Open Loop Control Scheme.

Experimentation began with open loop control of the motor. The drive unit was controlled by the first four outputs of a decade counter with ten parallel outputs. Resetting was performed on a high state at the fifth output. The device used was a CMOS 4017. The counter was clocked by a variable frequency signal generator. This scheme enabled the motor to be driven at a range of speeds and current levels. The effects of speed and current level on resonance and the ease with which synchronisation could be lost were observed. The initial application of open loop control proved that the current chopping and active suppression were operating correctly up to the rated current of the motor.

3.6 Self Synchronisation With A Position Encoder.

The next development was to obtain self synchronisation using the decoded outputs of the position encoder to provide the on phase

selection signals.

The motor was received with an optical position encoder factory fitted. This encoder is common to all the Oulton motors. The position encoder uses a shade ring with six slots which periodically enable four sensors as the ring rotates with the rotor. A hermetically sealed housing which is fixed relative to the motor frame contains four sets of detectors. These sets are angularly spaced in 7.5 degree intervals. With this spacing the encoder can resolve 7.5 degree increments in rotor position. As a result the four sensors produce eight different combinations of logical output states over the four step electrical cycle of the motor. Four output combinations coincide with the detent positions and the other four with the mid step positions. Table 3.1 lists all the encoder output combinations over an electrical cycle.

Table 3.1.

combination number.	sensor outputs. 1	2	3	4
1	0	0	0	0
2	0	0	0	1
3	0	0	1	1
4	0	1	1	1
5	1	1	1	1
6	1	1	1	0
7	1	1	0	0
8	1	0	0	0

The shade ring was noticed to have unequal regions of mark and space. The teeth each span 32 degrees of the shade ring periphery and the slots each span 28 degrees. It can only be concluded that this is to overcome the effects of photosensors with diffuse sensitivity. If a shade ring of 50% duty was used with these sensors then different rotor positions would correspond to the high going and low going outputs from each sensor. This would cause some phases to have longer step lengths than others.

Unfortunately, shortly after modification of the motor the encoder failed. A replacement was unavailable and the hermetic construction of the encoder made it unserviceable. It was therefore necessary to construct a new encoder. The new encoder was to be a close replacement so the same positioning was used for the optosensors as in the Oulton encoder. However the optosensors used in the construction of the new encoder have a narrower aperture and hence less sensitivity to edge effects than those used in the Oulton encoder. When used in conjunction with the Oulton shade ring they were found to produce unequal step lengths for each phase and rough running. The shade ring is an accurately manufactured and aligned component and it was decided not to modify it or to attempt producing another with the required unity mark space ratio. This necessitated repositioning the sensors. The sensors were spaced with one step intervals. This is the only positioning with the existing shade ring which will produced equal step lengths for each phase. However with such a spacing it is not possible to detect more than one rotor position per step as two output combinations correspond to every sensed rotor position. The reconstructed encoder can directly sense four discrete rotor positions in multiples of one step. This

arrangement however still provided the appropriate lead angles whenever the position encoder was required.

3.6.1 Decoding.

It is necessary to decode the sequence of encoder output combinations to provide the commutation signals. The decoding scheme developed enables the particular combination assigned to the energising of a given phase to be changed. This enables the energising of that phase at eight discrete rotor positions within the electrical cycle and hence the production of eight different lead angles. When starting from rest, four of these lead angles are positive and four are negative. This enables operation in either direction.

Circuit Operation:

The decoding circuit diagram is shown in figure 3.5. The decoding is performed with firmware as this provides a wider range of control facilities than can readily be achieved with hardware decoding. A program has been written to generate data (named "Decode") which contains the four element bit patterns necessary to control the slave drive unit. The bit patterns generated are stored in look up table form in an EPROM. Each encoder output combination is used to complete the address of a byte of memory which contains the required bit pattern. The bit patterns are generated according to the output state of the encoder, desired lead angle and other control commands.

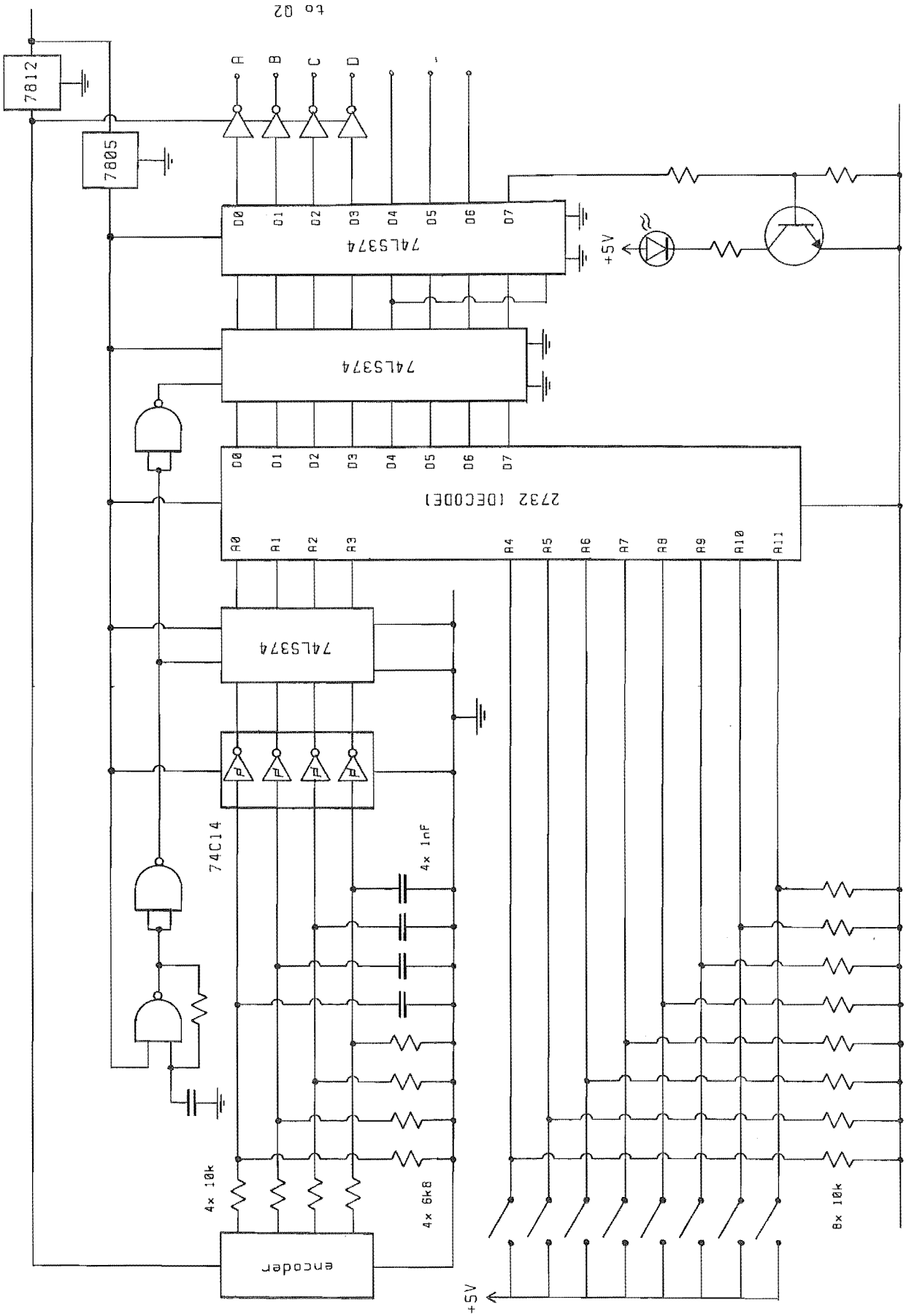

Fig. 3.5 The position encoder decoding circuitry

Before the outputs from the encoder are passed to the EPROM for decoding, they are first low pass filtered by a first order RC network. This is done to protect against the intrusion of radio frequency interference. The output leads from the encoder are necessarily long and exposed to an electrically noisy environment. The edges of the logic signals from the encoder are not visibly effected by this filtering but Schmidt trigger buffers are used to ensure that all the ongoing logic levels are well defined. The encoder signals are latched before they are fed to the EPROM address lines. The data lines are also latched. This avoids glitches which may occur as the output from the EPROM changes state from being passed on to the drive unit. The latching of the address and data lines is performed on the positive and negative going edges respectively of clock pulses. An extra latch was provided to enable a delay between encoder input and decoded output to enable a continuously variable lead angle if required. The clock frequency is approximately 500 kHz.

The Software:

A four kilobyte EPROM (2732) is used to store the bit patterns. The four kilobytes of memory require twelve address lines (A0 to A11). Four address lines are fed by the encoder and the remaining eight address lines can be used to select a range of useful control functions which have been programmed. Table 3.2 illustrates with some examples how the data has been determined in relation to the addresses of bytes of memory within the EPROM.

The four least significant bits (D0 to D3) of each byte are

Table 3.2.

address												data							
A11	A10	A9	A8	A7	A6	A5	A4	A3	A2	A1	A0	D7	D6	D5	D4	D3	D2	D1	D0
0	0	0	0	0	0	0	0	0	0	0	0	0	0	0	0	1	1	1	0
0	0	0	0	0	0	0	0	0	0	0	1	0	0	0	1	1	1	1	0
0	0	0	0	0	0	0	0	0	0	1	1	0	0	1	0	1	1	0	1
0	0	0	0	0	0	0	0	0	1	1	1	0	0	1	1	1	1	0	1
0	0	0	0	0	0	0	0	1	1	1	1	0	1	0	0	1	0	1	1
0	0	0	0	0	0	0	0	1	1	1	0	0	1	0	1	1	0	1	1
0	0	0	0	0	0	0	0	1	1	0	0	0	1	1	0	0	1	1	1
0	0	0	0	0	0	0	0	1	0	0	0	0	1	1	1	0	1	1	1
0	0	0	0	0	0	0	1	0	0	0	0	0	0	0	0	1	1	1	0
0	0	0	0	0	0	0	1	0	0	0	1	0	0	0	1	1	1	0	1
0	0	0	0	0	0	0	1	0	0	1	1	0	0	1	0	1	1	0	1
0	0	0	0	0	0	0	1	0	1	1	1	0	0	1	1	1	0	1	1
0	0	0	0	0	0	0	1	1	1	1	1	0	1	0	0	1	0	1	1
0	0	0	0	0	0	0	1	1	1	1	0	0	1	0	1	0	1	1	1
0	0	0	0	0	0	0	1	1	1	0	0	0	1	1	0	0	1	1	1
0	0	0	0	0	0	0	1	1	0	0	0	0	1	1	1	1	1	1	0
0	0	0	0	1												1	1	1	0
0	0	0	1	0												1	1	0	1
0	0	1	0	0												1	0	1	1
0	1	0	0	0												0	1	1	1
1	0	0	0	0												1	1	1	1
								0	0	1	0	1	0	0	0	1	1	1	1
								0	1	0	0	1	0	0	0	1	1	1	1

passed to the slave drive unit to select the on phase. Bits D4 to D6 indicate the current encoder output state in binary form. The last data line (D7) provides an error signal on receiving unrecognisable input combinations from the position encoder. In the corresponding memory locations D7 is set to 1, indicating an error. D0 to D3 are set to 1 in these memory locations, which when inverted by the buffers, turns all the phases off.

The inputs from the encoder are fed to the address lines A0 to A3. Sixteen binary input combinations are possible on these address lines. Only the eight generated by the encoder are shown. For each input combination there is a bit pattern in D0 to D3. Only one of these four bits is at logic level 0 at a time, this bit selects the on phase. At every second input combination there is a change in the on phase because of the half step between adjacent inputs.

The three address lines A4 to A6 are used to assign any of the eight encoder output combinations as the energisation point of a given phase. If line A4 is set to 1, the bit patterns are rotated one place in relation to the input combinations. If A4 is returned to a 0 and A5 is set to 1, the bit patterns are rotated another place. With three address lines (A4 to A6) eight shifts and hence eight lead angle changes are possible. There is no change in the data of D4 to D6 as this is tied to the encoder output.

The four address lines A7 to A10 are assigned to independently selecting the on phase. This feature was programmed to override the encoder output state, enabling either manually switched or alternatively triggered commutation. The twelfth address line A11 was used to turn all the phases of. The four address lines A7 to A10 when singly set to 1 call memory locations where D0 to D3 respectively, are

set to 0. The data lines D4 to D6 still represent the encoder output state. The software signals erroneous inputs on lines A7 to A10 but allows more than one on phase when selected via A7 to A10.

The position encoder and decoding circuitry functioned correctly. The resulting system was a self synchronised drive with incremental control over the lead angle and continuous control of the current limit. The system enabled variable speed control and offered all of the key features of the commercial controller.

3.7 Self Synchronisation With Self Positional Feedback.

The next development was the circuitry which implements the monitoring algorithm outlined in chapter two. The circuitry which derives the self positional feedback is in two parts. These are the switching circuitry which performs the monitoring chopping and the circuitry which interprets the monitoring waveforms and performs the phase commutation.

3.7.1 Modifications To The Drives.

The first requirement of position monitoring is to perform the monitoring phase current chopping simultaneously with the on phase current chopping but without interaction. The possibility of using the existing drives without modification, for position monitoring chopping as well as for on phase chopping was considered. This approach would require the minimum additions to the existing controlling circuitry.

However it was decided to perform the monitoring chopping independently with an additional switching device in parallel to Q2, as the low value of the on phase current sensing resistor would only develop a small signal voltage at the small current used for monitoring. Further, the extra device frees the monitoring circuit for experimentation with parameters such as the circuit time constant. It also allows modifications to be made more easily. This extra device and the associated circuitry, increases the complexity of the drive circuit and requires extra control but makes the circuitry controlling the monitoring independent of the drive circuitry. The schematic circuit diagram of the modified drive is shown in figure 3.6.

The modification required the construction of new drive circuitry as the extra components could not conveniently be included in the drive unit which had already been built. At this point other changes were made as well, the most major of these being an on phase current sensing circuit common to all phases. The EPROM based look up table approach was used again to perform the phase selection and chopping for both the monitoring and on phases.

3.7.2 Operation Of The Modified Drive Circuitry.

The operation of the drives has not been changed by the addition of Q3 and R_m. During driving, Q2 is switched on and the current level is sensed across R_d, with Q1 performing the chopping. During position monitoring in that phase, Q2 is switched off. The current path is through Q1, Q3 and the current sensing resistor R_m. As the current is not allowed to freewheel during monitoring, both Q1 and

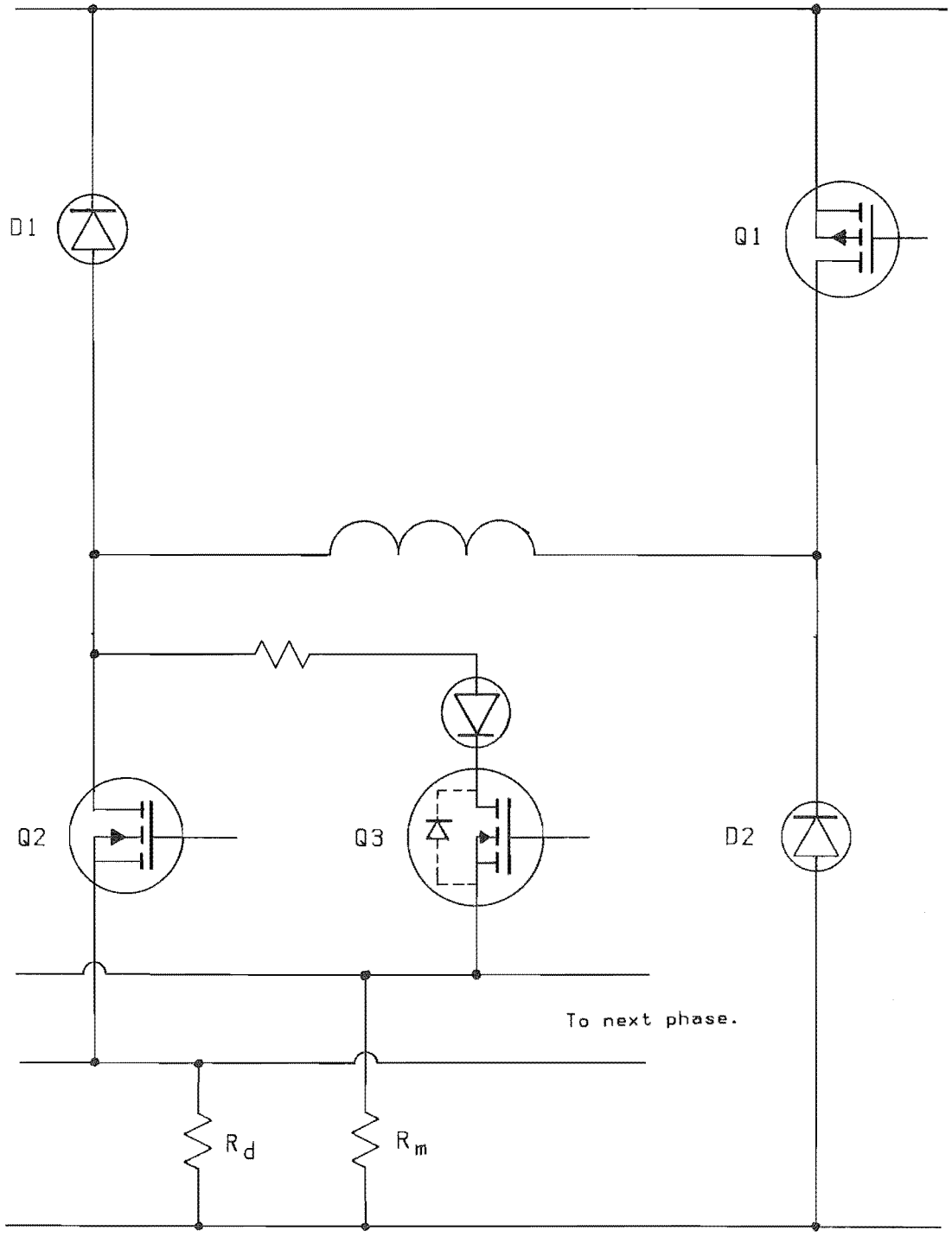

Fig. 3.6 The modified active suppression drive.

Q3 are turned off at the end of each monitoring period and the current is actively suppressed. The drive and monitoring currents share the same active suppression diodes.

An extra diode and resistor are shown separating the drain terminals of Q2 and Q3. The resistor has been included to show where extra resistance is placed if the monitoring circuit time constant is to be increased. If R_m is increased too much, the voltage rise across it during monitoring will rise to the maximum voltage obtainable at the source terminal of Q3 and the monitoring waveform will be clipped. It was found that the value of R_m required to set the Q3 operating conditions was not the optimum value for monitoring and the extra resistance was required.

The diode in the circuit is a critical component. It is necessitated by both R_m being common to all phases and the presence of a parasitic reverse biased diode across the Drain and Source of the MOSFET. This internal diode allows the monitoring phase current to pass through the Q3 of the on phase (which is ostensibly turned off) and then through Q2 of the on phase to ground. The extra diode blocks this alternative current path. If this current path is left open, the voltage at the Drain of Q2 of the on phase modulates the monitoring waveform giving the impression of coupling between the monitoring and on phases within the motor.

3.7.3 The Position Monitoring Circuitry.

The position monitoring algorithm is performed over a ten step cycle. The steps are defined by the outputs of a 4017 decade counter

which is clocked at 165 kHz from a 555 timer. This frequency assures fifteen monitoring cycles per step (one per degree) up to 3,000 rpm. The outputs are used to synchronise the operations which the monitoring circuit performs by controlling the monitoring chopping. The circuit diagram is shown in figure 3.7.

3.7.4 Operation Of The Position Monitoring Circuitry.

Counter Outputs 0 to 3;

The monitoring period is set by counter outputs 0 to 3. These four sequential outputs are gated together to produce a common chopping signal. The signal is used to time the switching of Q1 and Q3 and sets the monitoring period at 25 microseconds.

The current in the phase during this period is observed as a voltage across the current sensing resistor R_m. This signal voltage is filtered by a first order low pass filter comprised of R1 and C1. After the signal has been filtered, it is fed to the base of the bipolar transistor Q4. This transistor functions as a peak voltage detector. It is configured as an emitter follower and therefore provides current gain while following the input voltage. The absolute voltage at the emitter is not important but rather the variation. The emitter load is capacitor C2. The low output impedance and drive capability of Q4 allow it to charge C2 rapidly and still follow the signal voltage. When the voltage at the base is rising, the emitter voltage follows but is lower by the forward biased base-emitter junction voltage of close to 0.65 volts. The high transconductance of

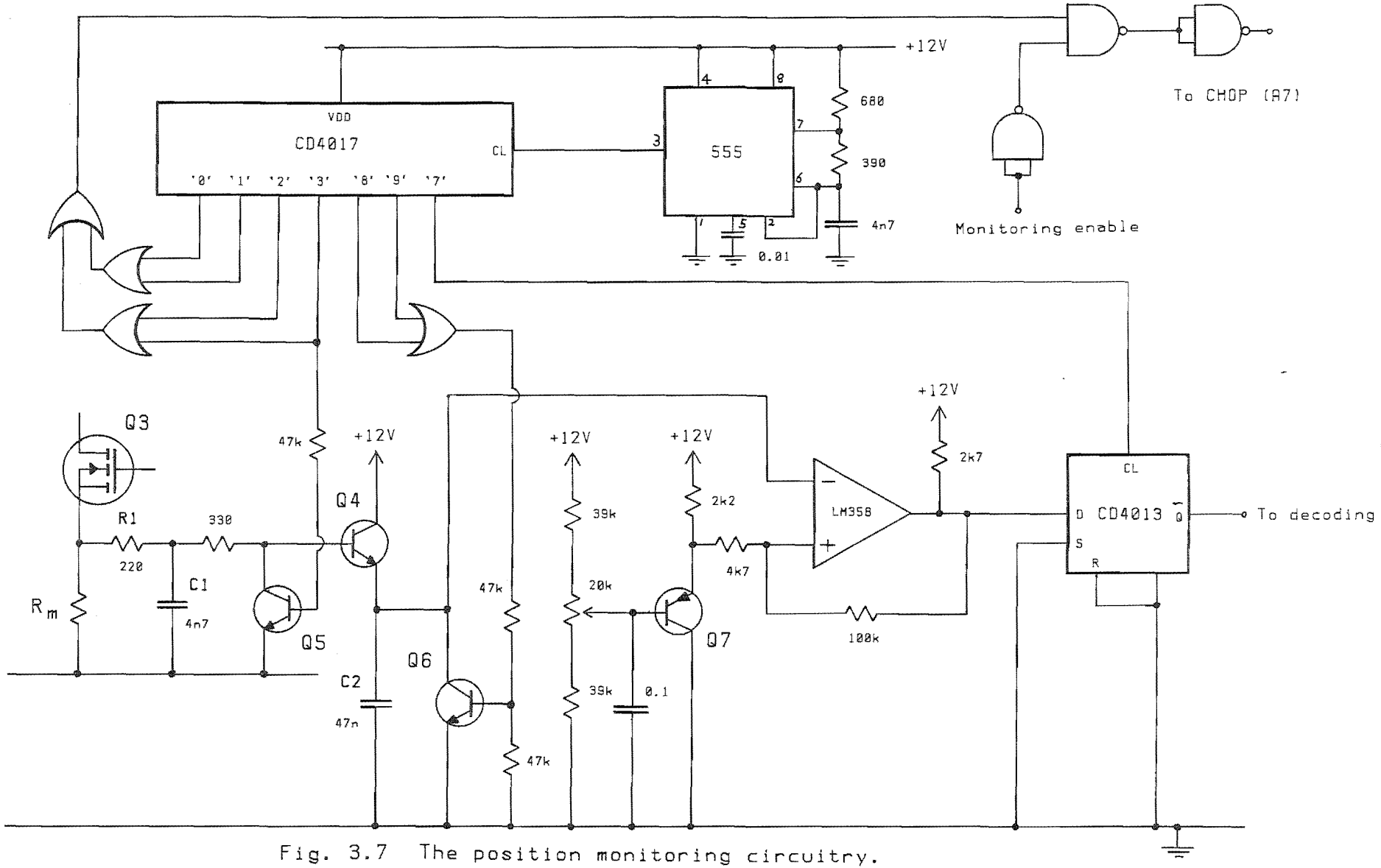

Fig. 3.7 The position monitoring circuitry.

the bipolar transistor maintains the base-emitter voltage close to 0.65 volts over the large variation of emitter current. The net result is that the voltage across C2 although 0.65 volts lower, closely follows the rise of the input voltage.

During counter output 0 the signal at the base of Q4 is shorted to the main power supply ground by Q5. This stops switching transients which occur when the phase is first energised from being interpreted as monitoring phase current. The monitoring circuit has an independent ground rail which is three volts negative with respect to the main power supply ground rail. This is necessary to avoid clipping of the small amplitude monitoring peaks which occur at maximum phase inductance. There is also the added advantage of reduced noise in the monitoring circuit, as its ground rail is not subject to the high level, rapidly changing currents which flow in the main power supply ground rail.

Counter Outputs 4 to 6;

The time during which one of the counter outputs 4 to 6 is high is used as a delay period in which to compare the peak voltage with the reference voltage. When counter output 4 goes high, the chopping signal goes low and Q1 and Q3 are turned off. The voltage across the current sensing resistor is then zero and the monitoring current begins falling to zero. The base of Q4 is now also at zero volts but C2 has been charged to the voltage reached at the end of the monitoring period. In this state the base-emitter junction of Q4 is reverse biased and C2 is isolated from the voltage at the base of Q4.

The peak voltage obtained during monitoring is now stored by C2 and available for comparison with the reference voltage by a comparator. The comparator has 18 microseconds if required, in which to change state and settle.

The reference voltage and the comparator together set the commutation points. The performance of the position monitoring circuitry as a whole is therefore governed by the performance of this section of circuitry. In analysing the suitability of a motor for providing self positional feedback, it is necessary to keep constant as many circuit performance parameters as possible.

A LM311 comparator is used to compare the voltage across C2 with the reference voltage. Hysteresis is used to ensure glitch free output state changes from the comparator. To avoid corrupting the voltage stored by C2 it is necessary to place minimal load on it. For this reason the comparator is configured in the inverting mode in preference to the non inverting mode. In the inverting mode the only load on C2 is the input bias current of the inverting input. The voltage across C2 is unaffected by the positive feedback of hysteresis.

The variable reference voltage is taken from a potential divider. This output of the potential divider is buffered by Q7. The output of Q7 in conjunction with the series resistance provides a reasonably constant source resistance with reference voltage. The amount of positive feedback is set by the ratio of the feedback resistance to the reference source resistance. In this circuit the amount of positive feedback remains relatively constant over the full range of the reference voltage.

Counter Output 7;

When the peak voltage exceeds the lower hysteresis level, the output of the comparator goes low. The output is read by a D type flip-flop when it is clocked by output 7 of the decade counter. The flip-flop stores its output state until it is clocked again ten clock cycles later. When motoring, the output from the flip-flop carries a train of commutation pulses. These pulses need to be demultiplexed to provide the commutation of the on and the monitoring phases. This operation is the function of decoding circuitry.

Counter Output 8 and 9;

Steps 8 and 9 are used to discharge C2 in preparation for the next monitoring cycle. These two outputs are gated together. A high state at either output forward biases transistor Q6 which discharges C2 to approximately -0.65 volts.

3.7.5 Decoding The Monitoring Circuit Output.

The commutation pulse train from the monitoring circuitry needs to be decoded into switching signals for the on and monitoring phases. This decoding is implemented by applying the same techniques used to decode the position encoder outputs. The decoding system developed provides control functions equivalent to those of the position encoder decoding circuitry.

Circuit Description:

The serial commutation pulse train from the position monitoring circuitry is first converted into a two bit signal. This signal provides the four output states necessary for phase selection. The circuitry which performs these functions is shown in figure 3.8. The conversion is performed by clocking a 4520 binary counter from the pulse train. The two least significant bits provide the four output states. The four states are then used to complete the address of data stored in look up table form in an EPROM. This data which has been named "Shift" controls the four Q2 and hence selects the on phase.

The Software:

Table 3.3 is a truth table showing a few examples of the relationship between "Shift" and its addressing. "Shift" provides the four element bit patterns necessary to control Q2 of the four active suppression drives. This bit pattern forms D0 to D3 of each byte. "Shift" also outputs two bits (D4 and D5) which represent the decoded outputs to Q2 in binary form and hence indicate the on phase. Address lines A0 and A1 receive the signal from the binary counter. Lines A2 to A5 are used for externally selecting the on phase and are equivalent to A7 to A10 of "Decode". This function was included to enable self synchronisation with the position encoder also. Reversing occurs when A6 is taken high. This reverses the order in which the bit patterns are produced and hence the motoring direction. When Line A7 is high D0 to D3 are high which turns all four Q2 off. Data bits D4

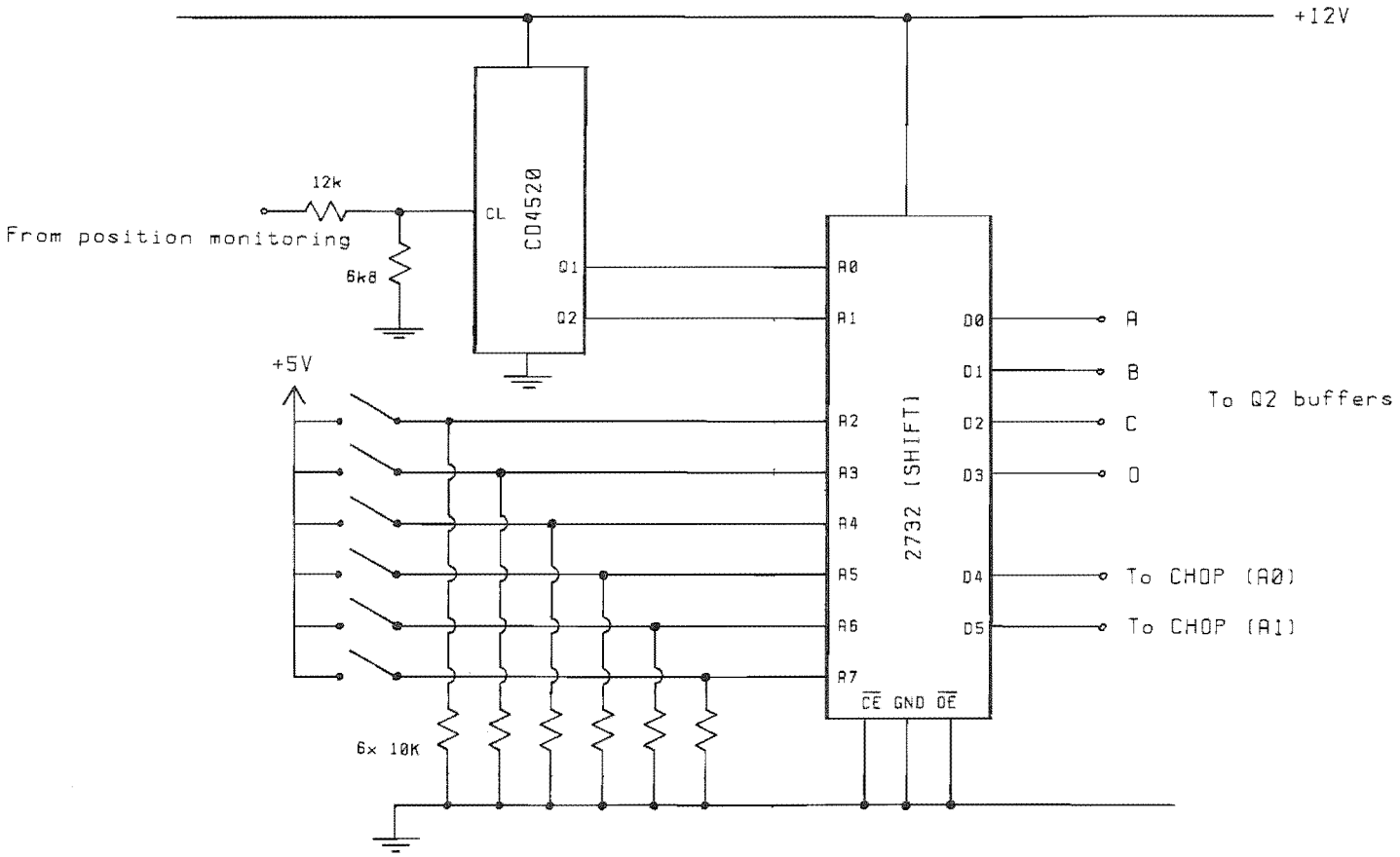

Fig. 3.8 The position monitoring decoding circuitry.

Table 3.3.

address								data							
A7	A6	A5	A4	A3	A2	A1	A0	D7	D6	D5	D4	D3	D2	D1	D0
0	0	0	0	0	0	0	0	0	0	0	0	1	1	1	0
0	0	0	0	0	0	0	1	0	0	0	1	1	1	0	1
0	0	0	0	0	0	1	0	0	0	1	0	1	0	1	1
0	0	0	0	0	0	1	1	0	0	1	1	0	1	1	1
0	0	0	0	0	1	X	X	0	0	0	0	1	1	1	0
0	0	0	0	1	0	X	X	0	0	0	1	1	1	0	1
0	0	0	1	0	0	X	X	0	0	1	0	1	0	1	1
0	0	1	0	0	0	X	X	0	0	1	1	0	1	1	1
0	0	0	0	1	1	X	X	0	0	0	0	1	1	1	1
0	1	0	0	0	0	0	0	0	0	0	0	1	1	1	0
0	1	0	0	0	0	0	1	0	0	1	1	0	1	1	1
0	1	0	0	0	0	1	0	0	0	1	0	1	0	1	1
0	1	0	0	0	0	1	1	0	0	0	1	1	1	0	1
1	0	0	0	0	0	0	0	0	0	0	0	1	1	1	1
1	0	0	0	0	0	0	1	0	0	0	1	1	1	1	1
1	0	0	0	0	0	1	0	0	0	1	0	1	1	1	1
1	0	0	0	0	0	1	1	0	0	1	1	1	1	1	1

X = either state.

and D5 relay the signal at A0 and A1 but if a high signal is registered on one of address lines A2 to A5, then D4 and D5 reflect the input to A2 to A5. In this way the position monitoring can be observed when commutation is self synchronised with either the position monitoring itself or the position encoder.

3.7.6 Coordinating Driving And Position Monitoring.

Additional circuitry is required to control the current chopping in both the on and monitoring phases. The net function of this circuitry is to control Q1 and Q3 of the drives. The control of the Q1 and Q3 is also software based and is performed by data called "Chop" resident in another EPROM. This EPROM and its supporting circuitry are shown in figure 3.9. The data responds to the phase selecting (D4 and D5) outputs of "Shift". Table 3.4 illustrates with a few examples the relationship between the addressing and the data.

The four least significant bits of "Chop" (D0 to D3) control the four Q1 and four most significant bits control the four Q3. The data is addressed by nine address lines. Address lines A0 and A1 read the D4 and D5 outputs respectively of "Shift". Line A2 reads the output state of the on phase current sensing comparator. Q1 of the on phase (selected by A0 and A1) is turned on when the comparator output into A2 is high. Line A3 when taken high turns Q1 of the monitoring phase off causing freewheeling of the current. Lines A4 and A5 when independently high shift the monitoring phase to the phase leading or lagging the on phase respectively, enabling monitoring of either

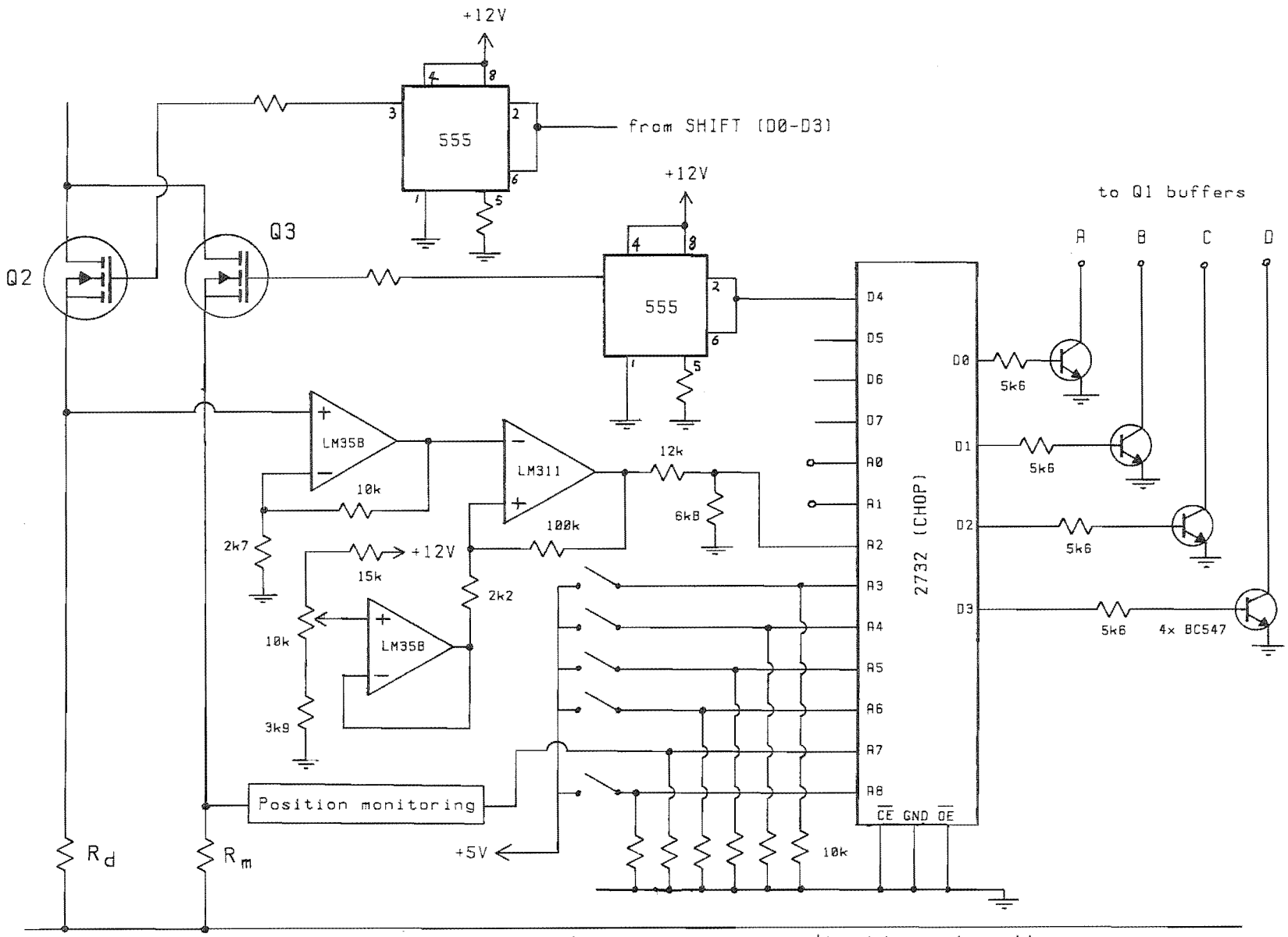

Fig. 3.9 The driving and monitoring coordinating circuitry.

Table 3.4.

address.								data.							
A7	A6	A5	A4	A3	A2	A1	A0	D7	D6	D5	D4	D3	D2	D1	D0
0	0	0	0	0	0	0	0	1	1	1	1	0	0	0	0
1	0	0	0	0	0	0	1	1	1	1	1	0	0	0	0
0	0	0	0	0	0	1	0	1	1	1	1	0	0	0	0
0	0	0	0	0	0	1	1	1	1	1	1	0	0	0	0
0	0	0	0	0	1	0	0	1	1	1	1	0	0	0	1
0	0	0	0	0	1	0	1	1	1	1	1	0	0	1	0
0	0	0	0	0	1	1	0	1	1	1	1	0	1	0	0
0	0	0	0	0	1	1	1	1	1	1	1	1	0	0	0
1	0	0	0	0	0	0	0	1	0	1	1	0	1	0	0
1	0	0	0	0	0	0	1	0	1	1	1	1	0	0	0
1	0	0	0	0	0	1	0	1	1	1	0	0	0	0	1
1	0	0	0	0	0	1	1	1	1	0	1	0	0	1	0
1	0	0	0	0	1	0	0	1	0	1	1	0	1	0	1
1	0	0	0	0	1	0	1	0	1	1	1	1	0	1	0
1	0	0	0	0	1	1	0	1	1	1	0	0	1	0	1
1	0	0	0	0	1	1	1	1	1	0	1	1	0	1	0

adjacent phase. The functions provided by lines A3 to A5 were subsequently not required and were hardwired to be inactive. Line A6 when high turns Q1 and Q3 of the monitoring phase off, disabling monitoring. The chopping signal from the position monitoring circuit (steps 0 to 3 of the monitoring cycle) is received at A7. When this signal is high, Q1 and Q3 of the monitoring phase are turned on and the monitoring cycle begins. When the signal is low the monitoring phase current is actively suppressed. Line A8 when high turns Q1 of the on phase off and when used with A7 of "Shift" isolates any on phase.

The programs "Decode", "Shift" and "Chop" are listed in appendix C.

3.8 Modifications.

When the circuitry already described was tested it was found that the monitoring current was not decaying as rapidly as expected, resulting in interference. This problem was traced to incomplete turn off of Q1 and Q3. The effect was too small to effect the performance of the on phase, but was sufficient to interfere with the monitoring. The solution is to reverse bias the MOSFETs with a gate-source voltage of opposite polarity when they are to be switched off. Bipolar power supplies are therefore required to supply the buffers which switch the MOSFETs.

The necessary power supplies were built but the LM555 timers were found to be unsuited to the bipolar supply and a number of switching glitches were noticed. The glitches were sporadic and

difficult to trace to these devices. Further it was also found that the unequal switching periods of Q1 and Q3 which result from the propagation delay in the optocouplers was effecting the monitoring phase chopping. The effects were insignificant in the on phase where the chopping frequency is low.

These findings lead to the complete replacement of the LM555 timers and the optocouplers with discrete bipolar transistor circuits.

The buffer circuit used to switch both Q2 and Q3 are as shown in figure 3.10. This circuit accepts a TTL input and inverts it, taking the gates to -3 volts with respect to the source terminal when the output is low, and to +9 volts when high. The circuit has active "pull up" and "pull down".

The circuit which replaces the optocoupler and Q1 buffer is shown in figure 3.11. An emitter follower complementary pair is used to swing the gate of the P channel MOSFET between 3 volts and -9 volts with respect to the source terminal, providing active "pull up" and "pull down". The pair is driven from a split in the collector load resistor of a high voltage switching transistor. This transistor is driven directly from a TTL output and replaces the transistor used previously to drive the optocouplers. Zener diodes are included to protect against damage caused by excessive voltages should they arise.

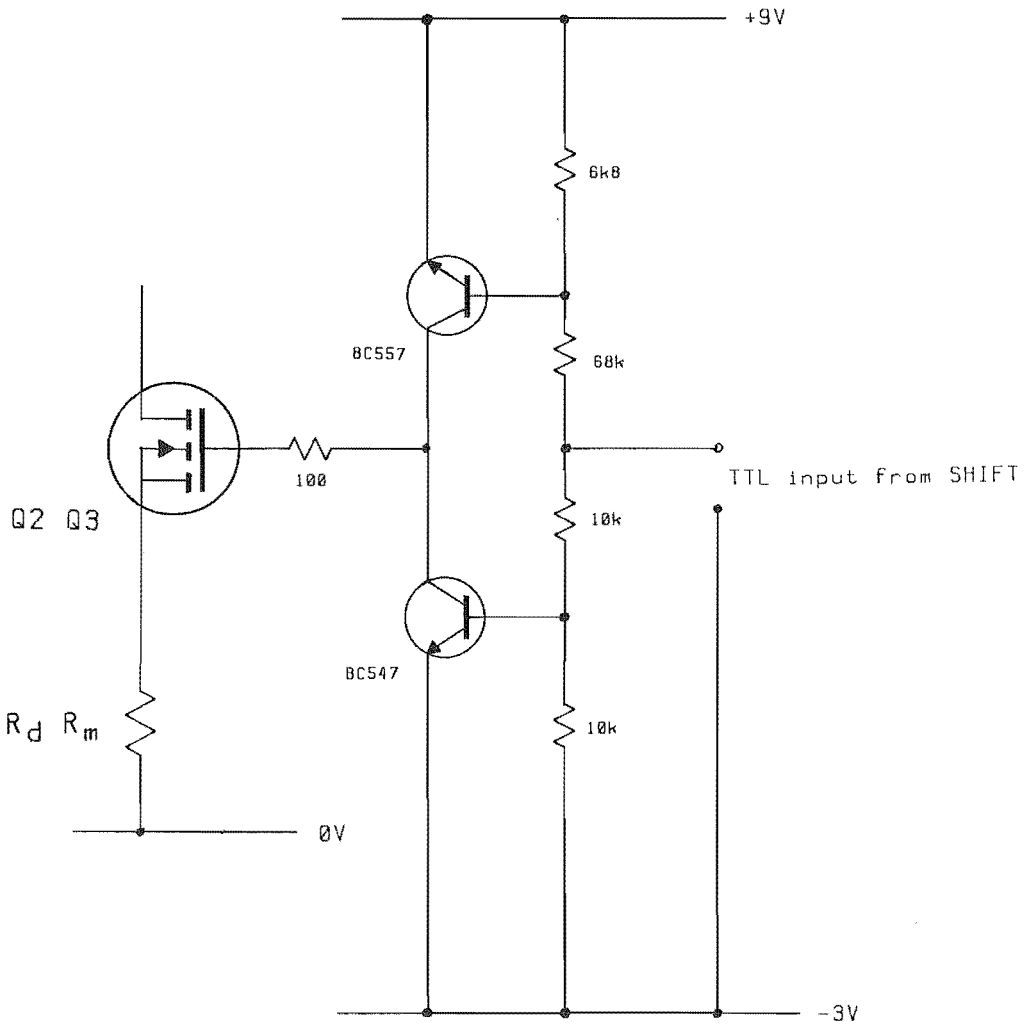

Fig. 3.10 The Q2 and Q3 buffer circuits.

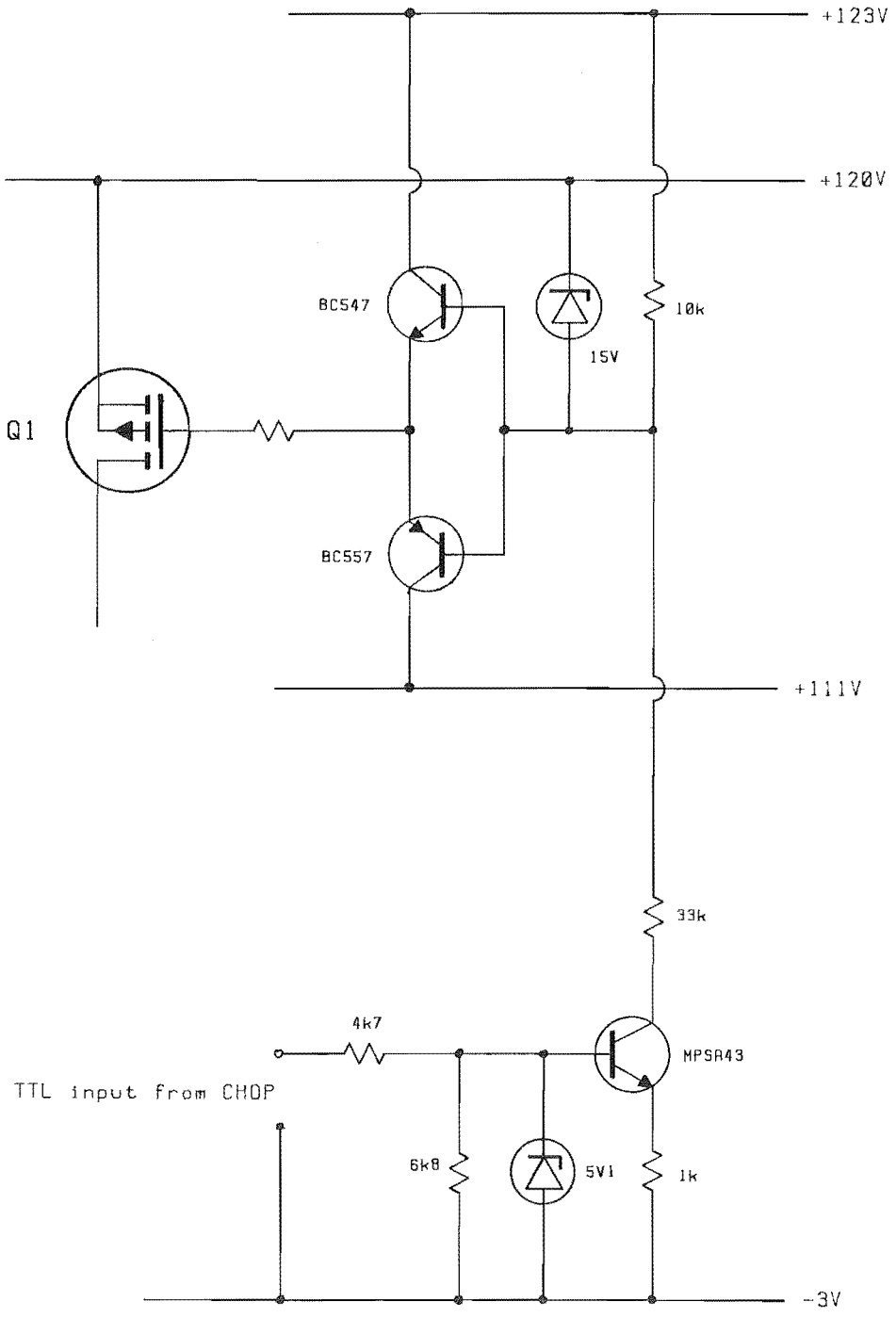

Fig. 3.11 The Q1 buffer circuits.

3.9 Summary.

The final circuitry proved very successful producing clean correctly timed switching of the MOSFETs in both the on and monitoring phases. The completed system has successfully implemented active suppression driving of the motor and the position monitoring algorithm discussed in the previous chapter.

CHAPTER 4.

THE RESULTS.

4.1 Introduction.

This chapter discusses the performance of the control system of chapter 3. Distinct performance attributes are shown to be linked to the susceptibility of the position monitoring algorithm to the unique electrical characteristics of the four phase single stack motor. Examples of the characteristic voltage and current waveforms encountered in the control system which illustrate the performance are presented.

Finally a measured torque output vs speed plot is presented to show the actual performance of the system.

4.2 The Motor.

The motor was disassembled to enable modification to the internal wiring. During this time measurements were made to determine the air gap between the stator and rotor poles. The diameter of the rotor was measured between the ends of opposite teeth to be 95.67 mm. This measurement is accurately maintained over the rotor's length as it has been cylindrically ground. Measurements of the stator's internal diameter between opposite teeth revealed appreciable variation. The mean air gaps for each phase over the length of the stator are;

Phase	air gap
A	0.87 mm
B	1.05 mm
C	0.85 mm
D	0.72 mm

4.2.1 Self Inductances.

The self inductance of phase A over a rotor movement of 180 degrees is shown in figures 4.1 and 4.2. The variation is relatively sinusoidal within one step either side of the detent positions. However in the misaligned tooth position, the salient nature of the poles causes the departure from the theoretical sinusoidal variation. The result is a fifteen degree region of rotor position at minimum inductance over which there is very little change in reluctance.

The phase inductances have been measured over 180 degrees of rotor movement in 2.5 degree intervals. The mean overall inductances, mean minimum inductances and the mean detent inductances over this range are as follows.

Table 4.1

Inductance (mH).

Phase	mean	minimum	detent
A	38.6	13.1	65.7
B	36.1	13.0	62.0
C	38.0	13.1	66.3
D	38.8	13.2	67.7

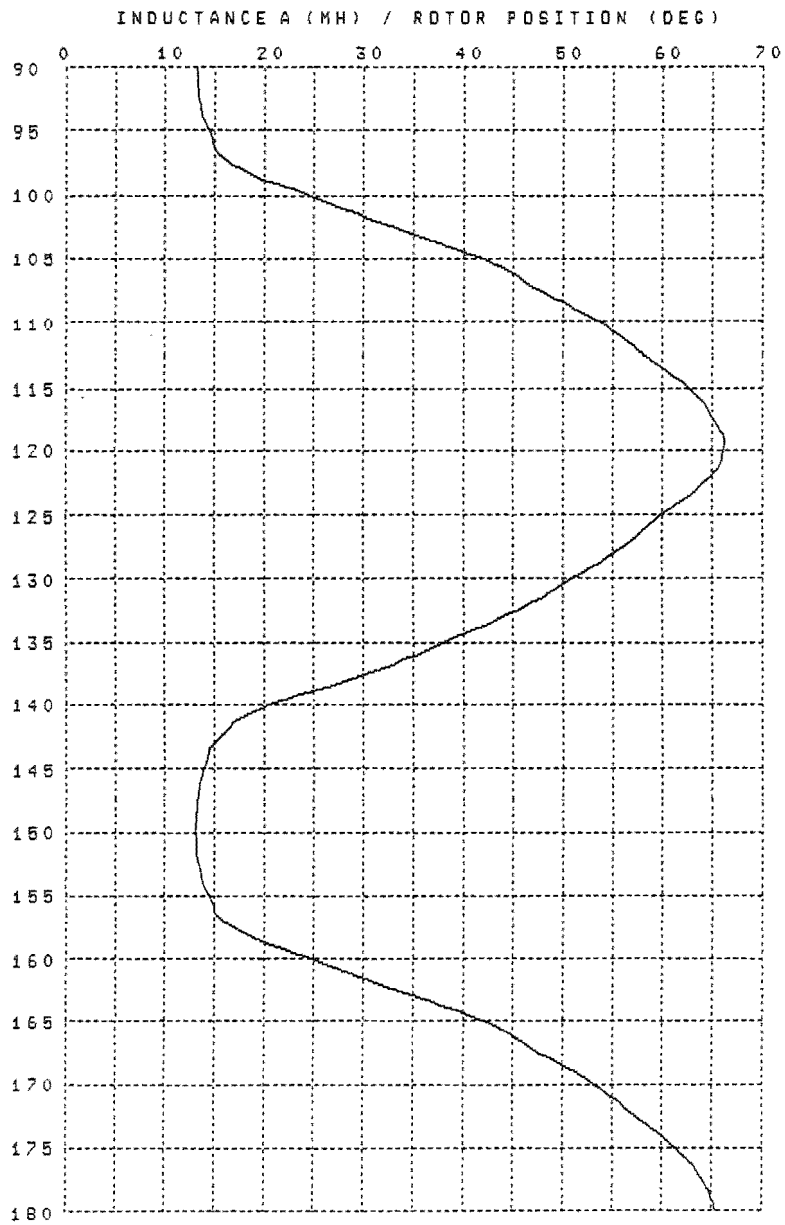
INDUCTANCE A (MH) / ROTOR POSITION (DEG)
0 10 20 30 40 50 60 70
90 95 100 105 110 115 120 125 130 135 140 145 150 155 160 165 170 175 180

Fig. 4.2

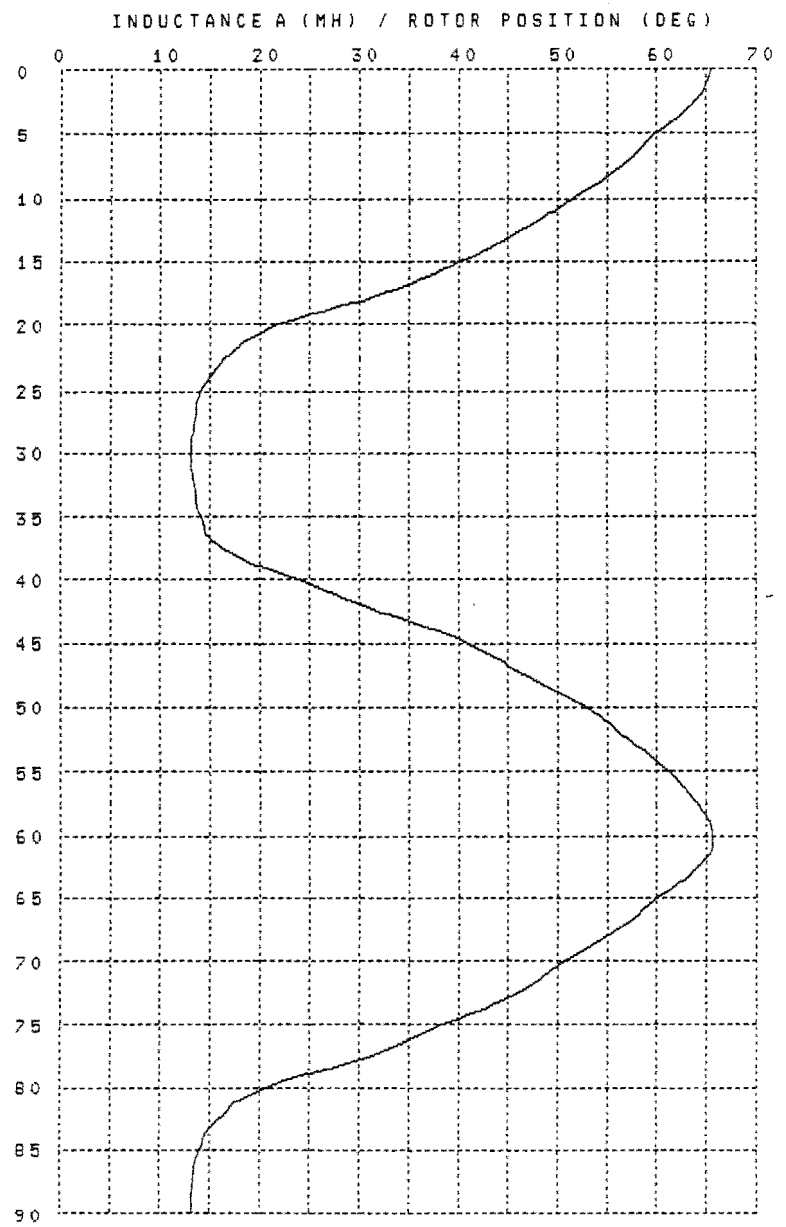
INDUCTANCE A (MH) / ROTOR POSITION (DEG)
0 10 20 30 40 50 60 70
0 5 10 15 20 25 30 35 40 45 50 55 60 65 70 75 80 85 90

Fig. 4.1

From the measurements of all four phases over 180 degrees of rotor movement;

mean overall inductance = 37.9 mH

mean minimum inductance = 13.1 mH

mean detent inductance = 65.2 mH

For any given phase, the inductances at its three detents within the 180 degrees of rotor movement are all within 1.2% of the mean for that phase. The maximum and minimum detent inductances measured are 68.0 mH (phase D) and 61.5 mH (phase B) respectively. These inductances differ by 10.0% of the mean detent inductance for all phases. These measurements show that the inductance variation within each phase is approaching an order of magnitude less than the variation between phases. The inductance measurements are consistent with the variation between phases in the air gap.

4.2.2 Adjacent Phase Mutual Inductances.

The mutual inductance between the adjacent phases A and B over 180 degrees of rotor position is plotted in figures 4.3 and 4.4. The form departs significantly from a pure sinusoid and there is some variation between the mutual inductances of adjacent phase pairs. However all these inductances have a similar form and show clearly defined periods. The form of mutual inductance AB can be seen to conform to the half step shift from the phase inductances, as the maximum of inductance AB is centrally located between the inductance maximums of

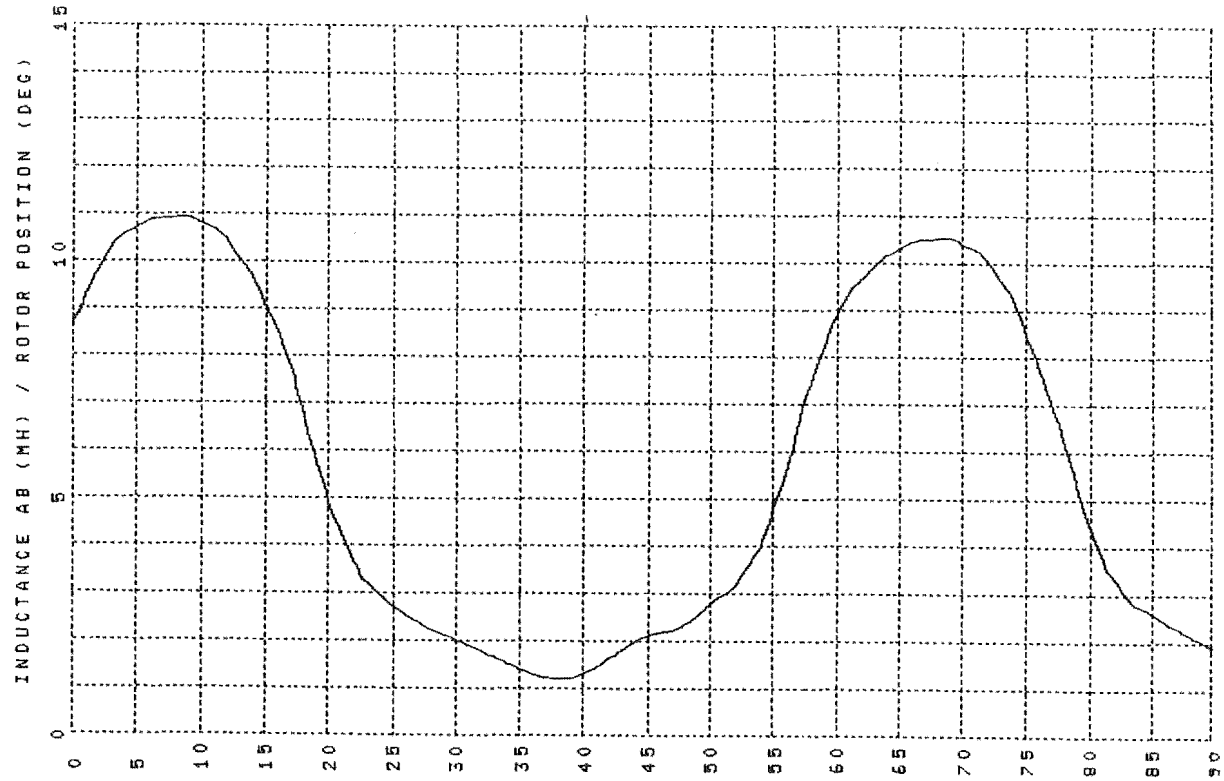
INDUCTANCE AB (MH) / ROTOR POSITION (DEG)
0
5
10
15
0
5
10
15
20
25
30
35
40
45
50
55
60
65
70
75
80
85
90

Fig. 4.3

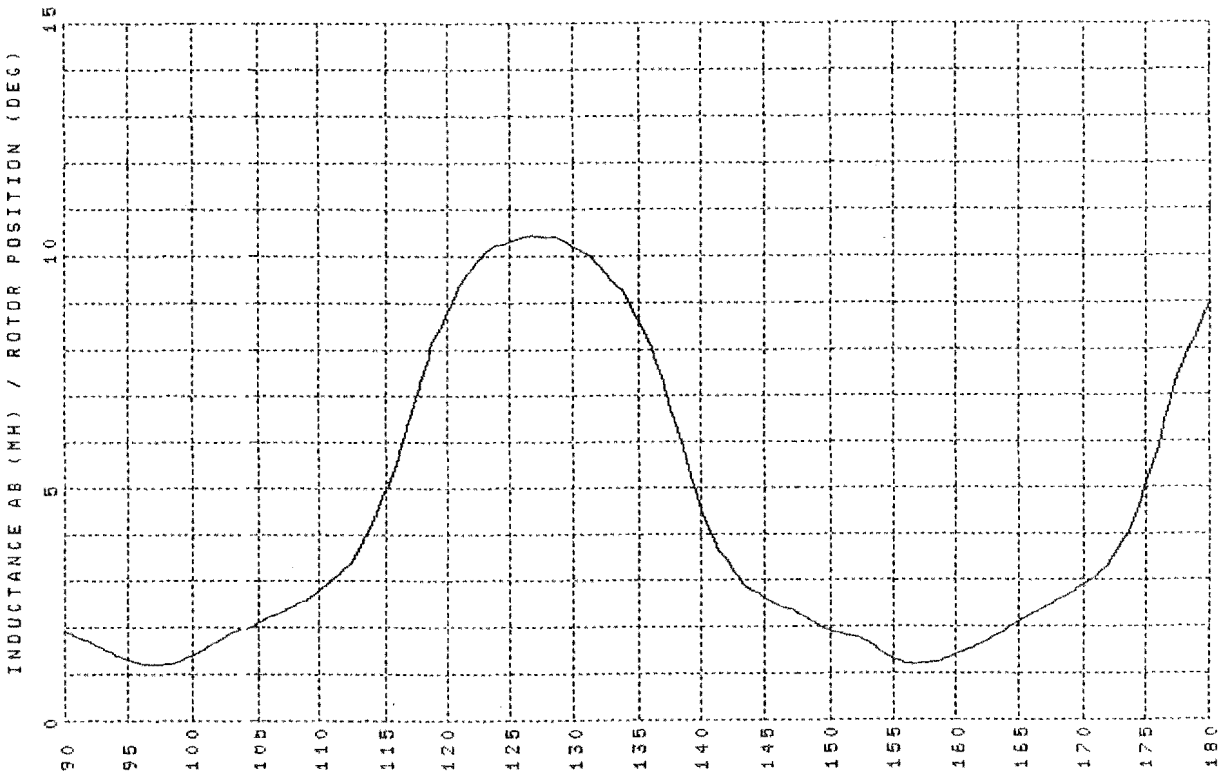
INDUCTANCE AB (MH) / ROTOR POSITION (DEG)
0
5
10
15
90
95
100
105
110
115
120
125
130
135
140
145
150
155
160
165
170
175
180

Fig. 4.4

phases A and B.

The mean overall inductance, the mean minimum inductance and the mean maximum inductance between adjacent phases have also been measured in 2.5 degree steps and are as follows.

Table 4.2

Inductance (mH)	mean	minimum	maximum
AB	5.1	1.2	10.5
BC	5.0	1.2	10.6
CD	6.1	1.3	13.5
DA	6.6	1.4	13.7

From the measurements of all four mutual inductances between adjacent phases over 180 degrees of rotor movement;

mean overall inductance = 5.7 mH

mean minimum inductance = 1.3 mH

mean maximum inductance = 12.1 mH

The effect the comparatively large air gap at the poles of phase B and the comparatively small air gap at the poles of phase D have on the mutual inductances can be seen in table 4.2. Both the mutual inductances formed with phase B are similar in their mean values and both the mutual inductances formed with phase D are also similar in their mean values. However, the mutual inductances formed with phase D are consistently larger than those formed with phase B. This result is in agreement with the self inductance measurements.

4.2.3 Orthogonal Phase Mutual Inductances.

The mutual inductance between the two orthogonal phase pairs AC and BD is plotted in figures 4.5. and 4.6. These inductances vary at twice the frequency of the self and adjacent phase mutual inductances. They are highly non sinusoidal in nature and are significantly different from each other. These inductances are comparatively small, peaking at slightly over 2 mH. At such low values, manufacturing tolerances such as the ovality encountered in the stator contribute significantly to the inductance variation associated with rotor movement. Short range non-periodic variations in the air gap dimensions would cause the irregular inductance plots.

The remaining self and mutual inductance plots are included in appendix A. Examples of the plotting routines written to produce these plots are listed in appendix D.

4.3 The On Phase Currents.

Current waveforms which are characteristic of current chopping and active suppression have been recorded. The plots of these current waveforms have been obtained by the measurement of the voltage across the on phase current sensing resistor.

Figure 4.7 is the current in the on phase with the rotor at rest in the detented position. The other extreme of fully misaligned stator and rotor teeth is shown in figure 4.8. The difference in these plots results solely from the difference in the phase inductance at the two points. These plots can be used to calculate the time constant

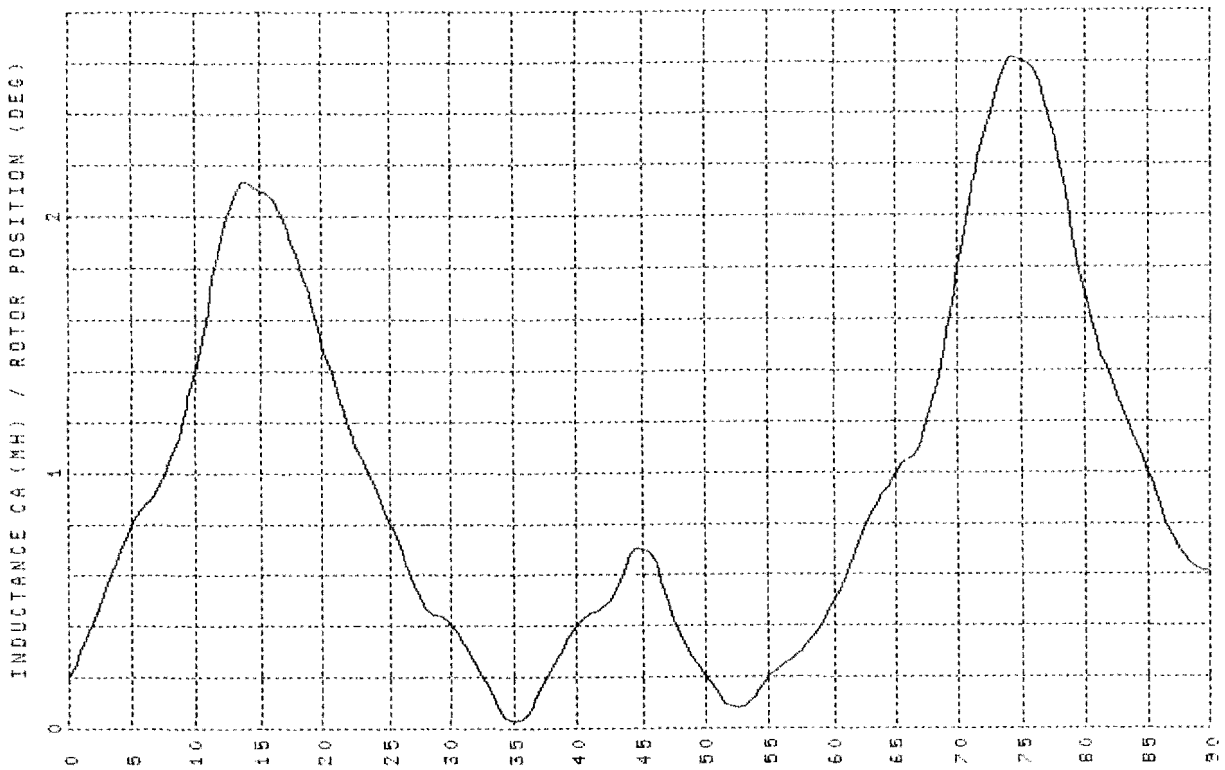
INDUCTANCE CA (MH) / ROTOR POSITION (DEG)
0
1
2
0 5 10 15 20 25 30 35 40 45 50 55 60 65 70 75 80 85 90

Fig. 4.5

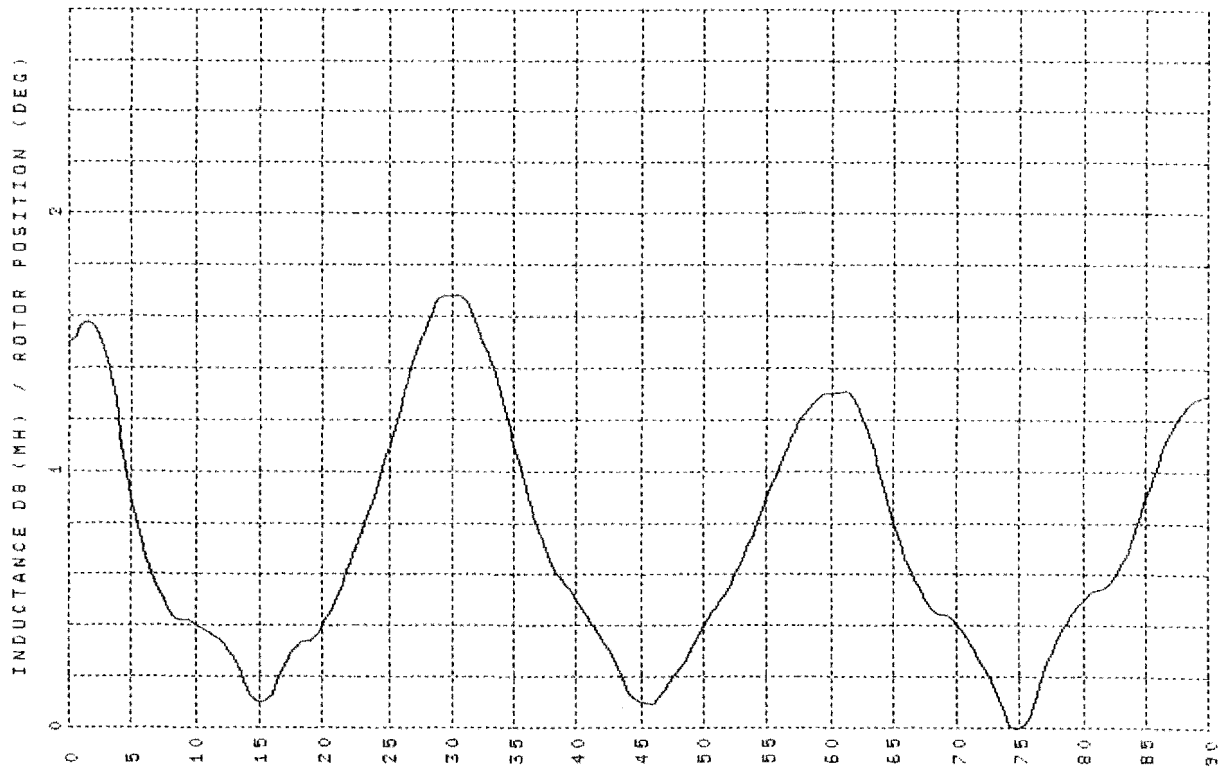
INDUCTANCE DB (MH) / ROTOR POSITION (DEG)
0
1
2
0 5 10 15 20 25 30 35 40 45 50 55 60 65 70 75 80 85 90

Fig. 4.6

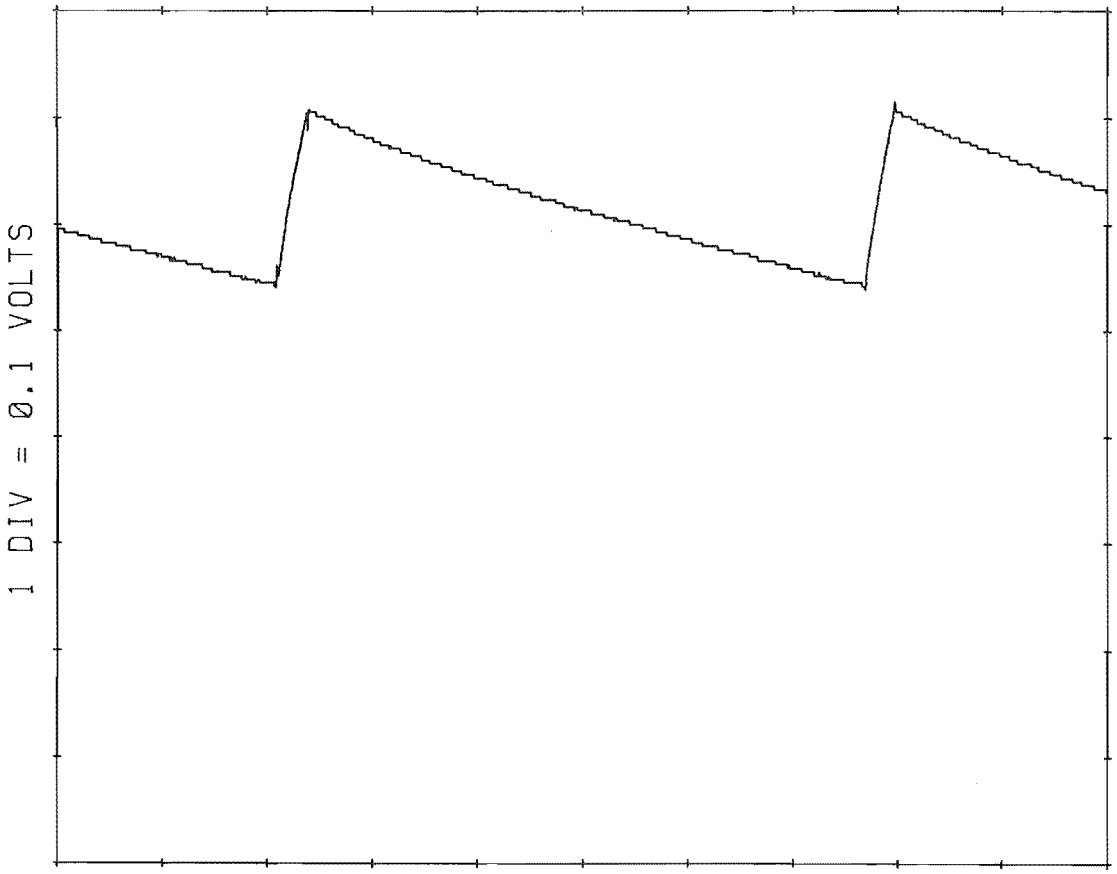

A:DVM3 Fig. 4.7

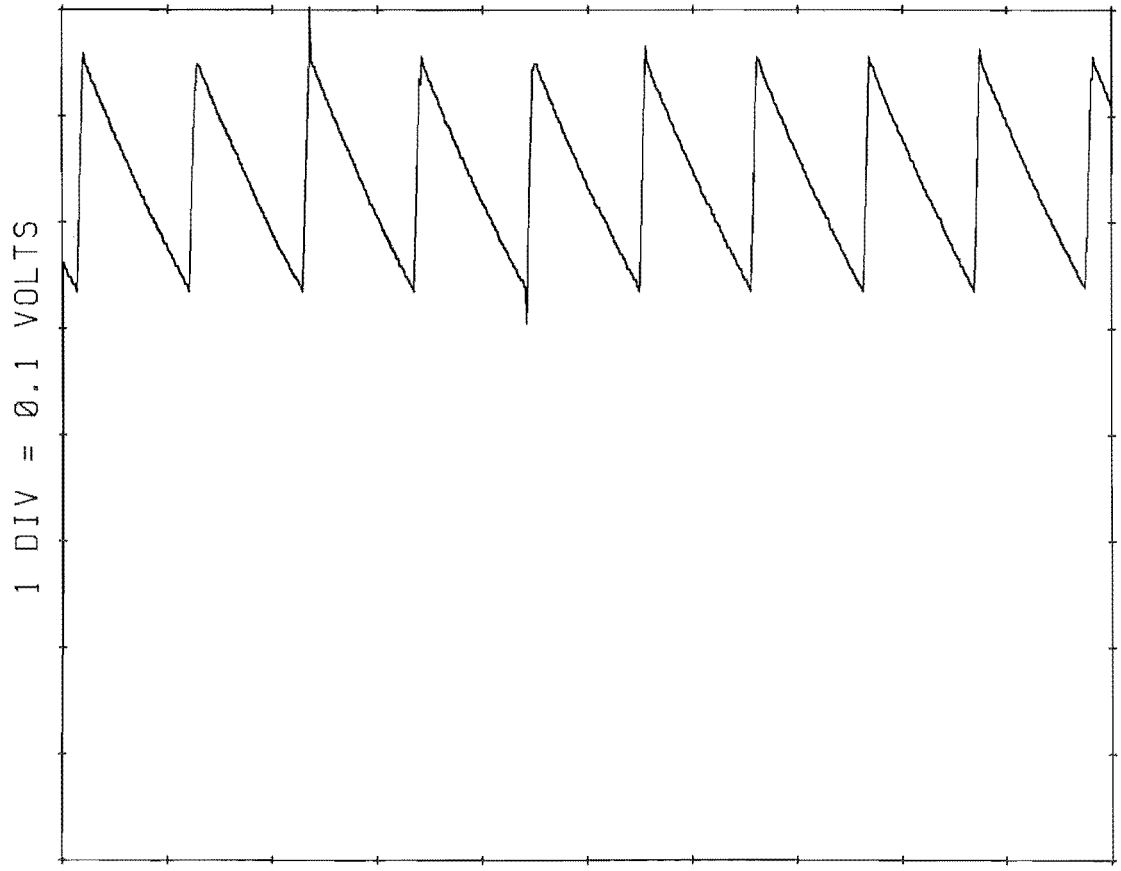

A:DVM4 Fig. 4.8

and circuit resistance of the energising and de-energising current paths.

Figure 4.9 is the on phase current waveform encountered at low speed. Here the current limit has been reached early in the step and the mean value is maintained by chopping. The rapid current rise to the upper current limit and the long time constant current decay to the lower limit are clearly visible. The effect of the changing phase inductance during the step can be seen. The frequency of chopping decreases throughout the step. Figure 4.10 shows the on phase current waveform measured at intermediate speed. At this speed the current limit is not reached until later in the step and the current is chopped only a few times. The effects of motional voltage are starting to become apparent in the current rise at the start of the step. Figure 4.11 shows the waveform recorded at high speed. Here the current limit is never reached during the step and no current chopping occurs. Maxima are visible in these waveforms. Figures 4.9 to 4.11 show the energising current only as the de-energising current does not pass through the current sensing resistor.

The energising and de-energising current waveforms are plotted together in figure 4.12. These have been recorded with separate oscilloscope traces because of the independent paths which these two currents flow in. Dual trace on phase current waveform traces have proved very susceptible to noise on the ground rail and very sensitive to the point where the oscilloscope is earthed to the drive circuitry. This is particularly evident in the traces of the de-energising current where transients are observed at the start of de-energisation. Figure 4.12 was recorded at a speed of 1380 rpm and a lead angle of 28 degrees. No chopping of the energising current occurs and the

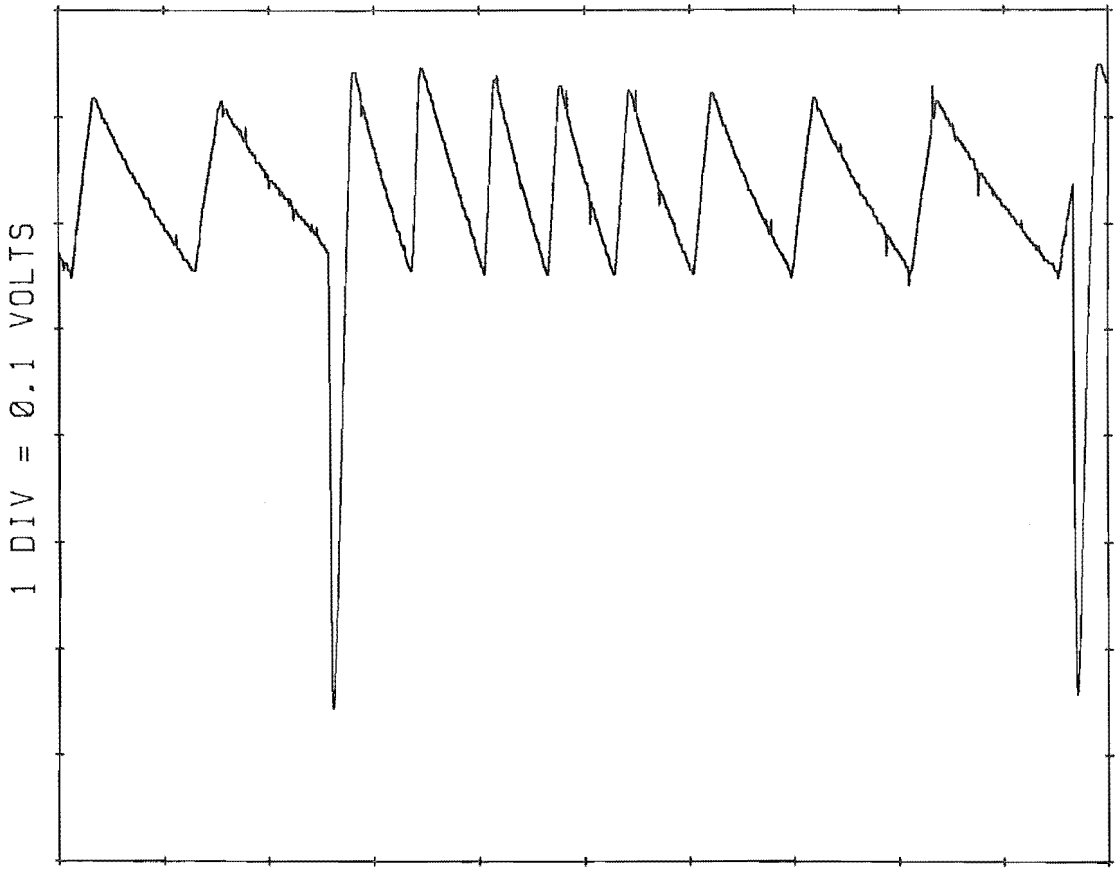

A:DVM5 Fig. 4.9

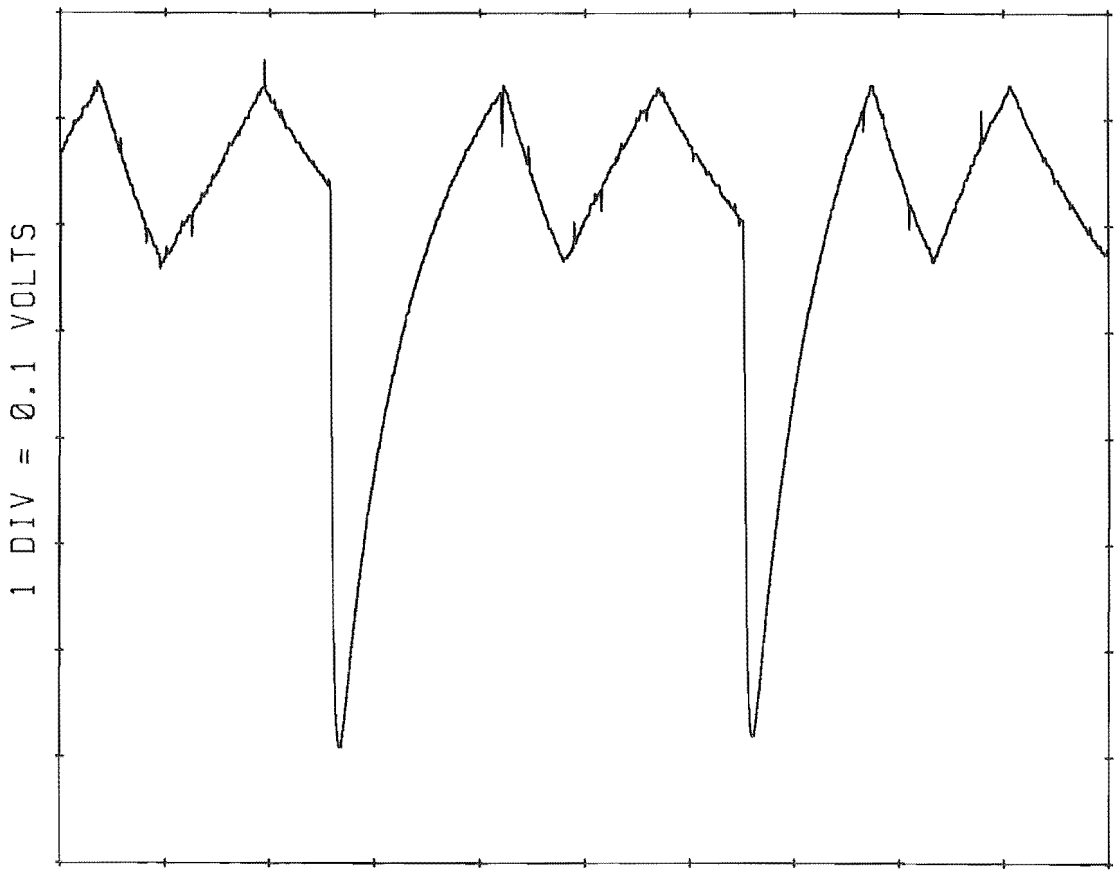

A:DVM6 Fig. 4.10

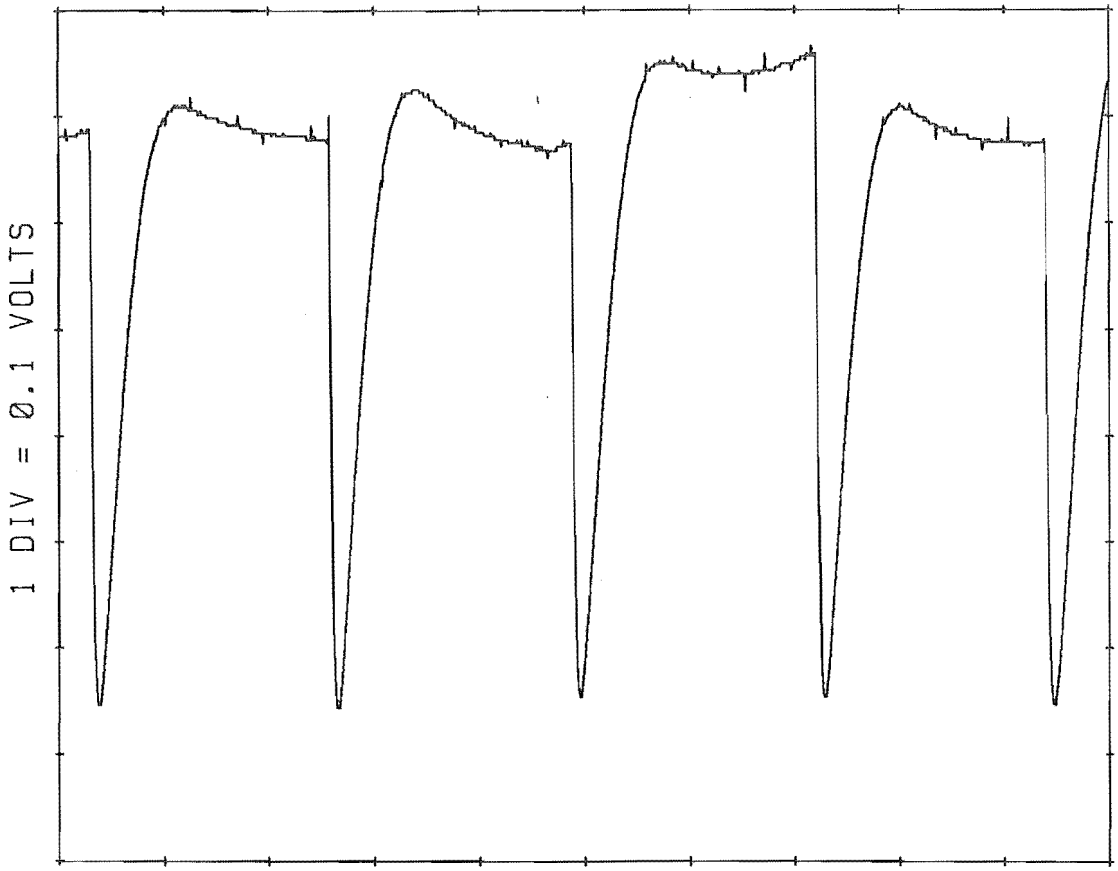

A:DVM7 Fig. 4.11

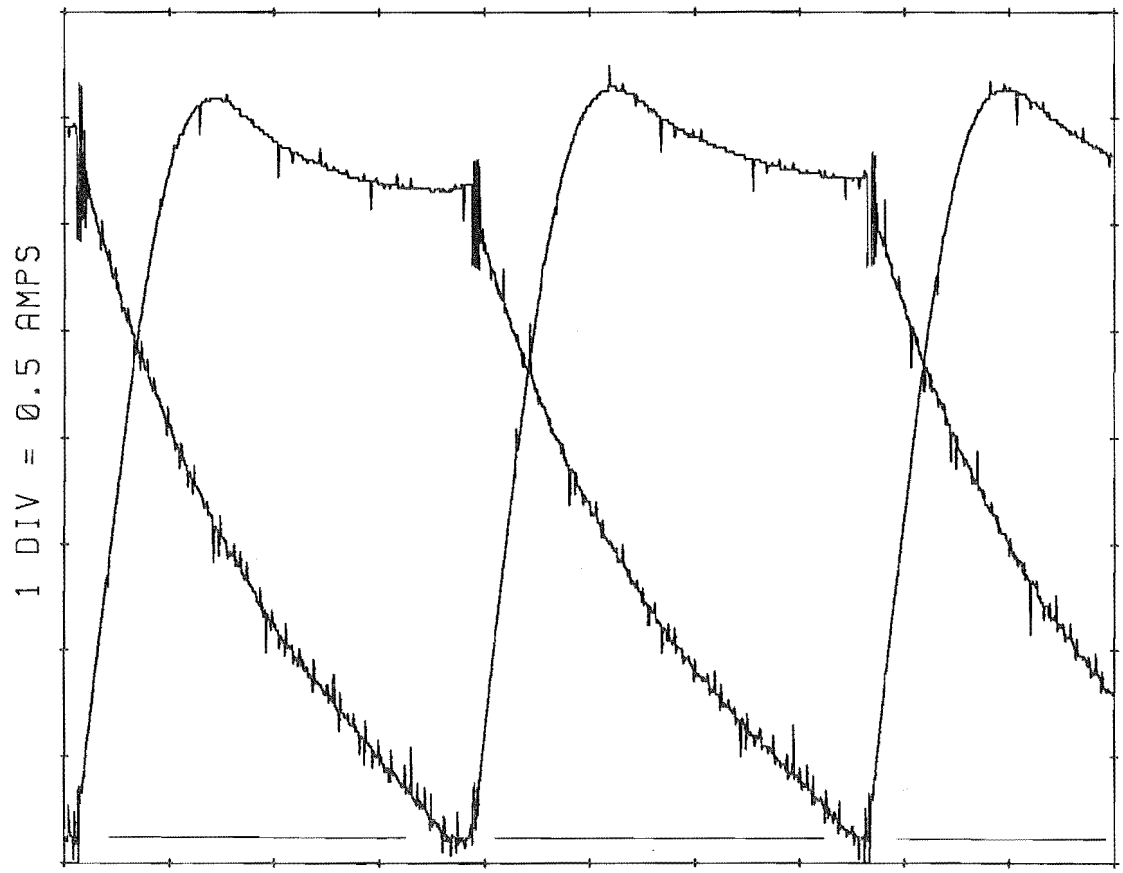

A:DVM20 Fig. 4.12

de-energising current decays to zero within one step as predicted by the circuit model of chapter 2.

4.4 The Monitoring Cycle.

The voltage waveform observed between positive end of the monitoring circuit resistance R and ground (figure 3.6) during the monitoring cycle has been recorded. Figure 4.13 is a plot of this voltage recorded at minimum phase inductance and shows two full cycles. When the phase is energised the voltage begins to rise and continues to rise for the duration of the monitoring period. The voltage rises to approximately 90 volts. At the instant the period is completed, the voltage at the positive end of the monitoring circuit resistance increases to the supply rail voltage of 120 volts. This sudden increase is the result of the active suppression returning the monitoring current to the power supply. Figure 4.14 shows the waveform when the phase inductance is at the maximum value. The effect of the increased monitoring circuit time constant is apparent in terms of the decreased voltage at the end of the monitoring period.

The current waveforms used directly to detect the rotor position are derived from a family of waveforms bounded by the waveforms illustrated in figures 4.13 and 4.14. The waveforms used to detect the rotor position are derived by observing the voltage across the current sensing resistor of the monitoring circuit. The voltage across the current sensing resistor is a fixed portion of the voltage across the complete circuit resistance R. This is because of the potential divider action of the two resistances which make up R.

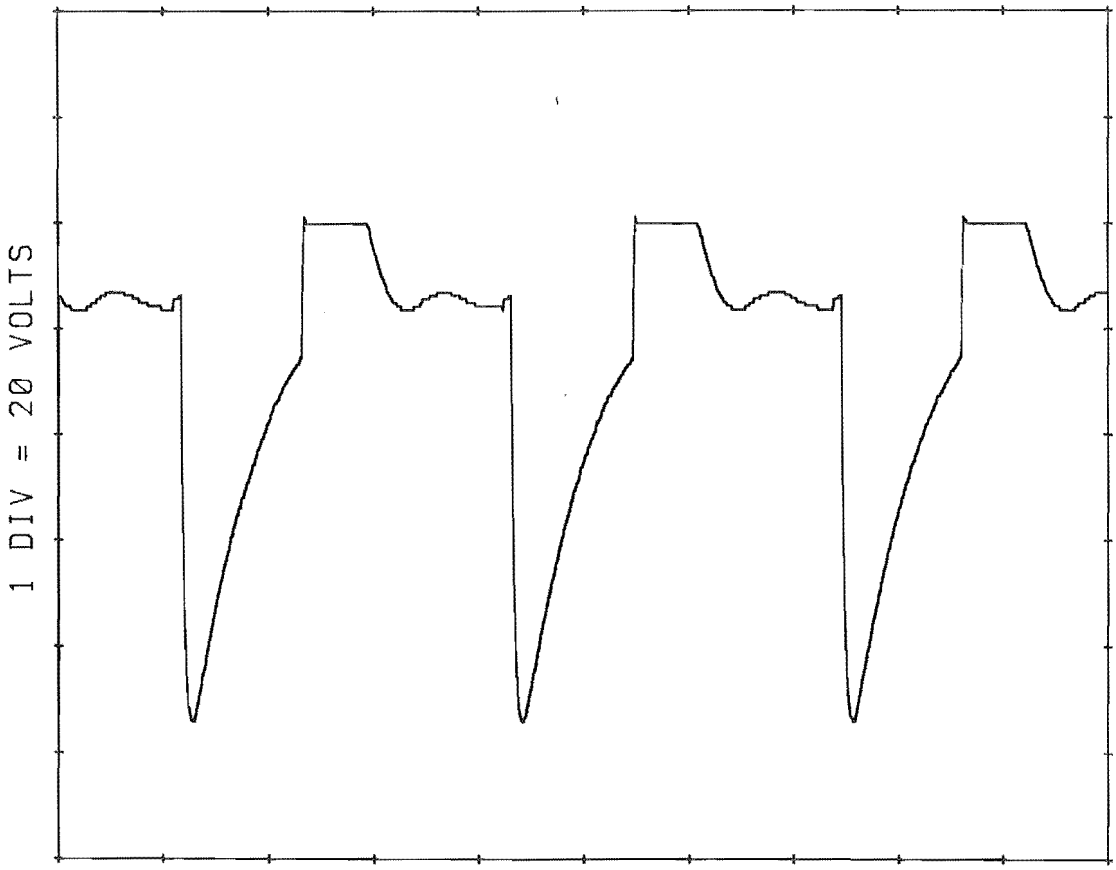

Fig. 4.13

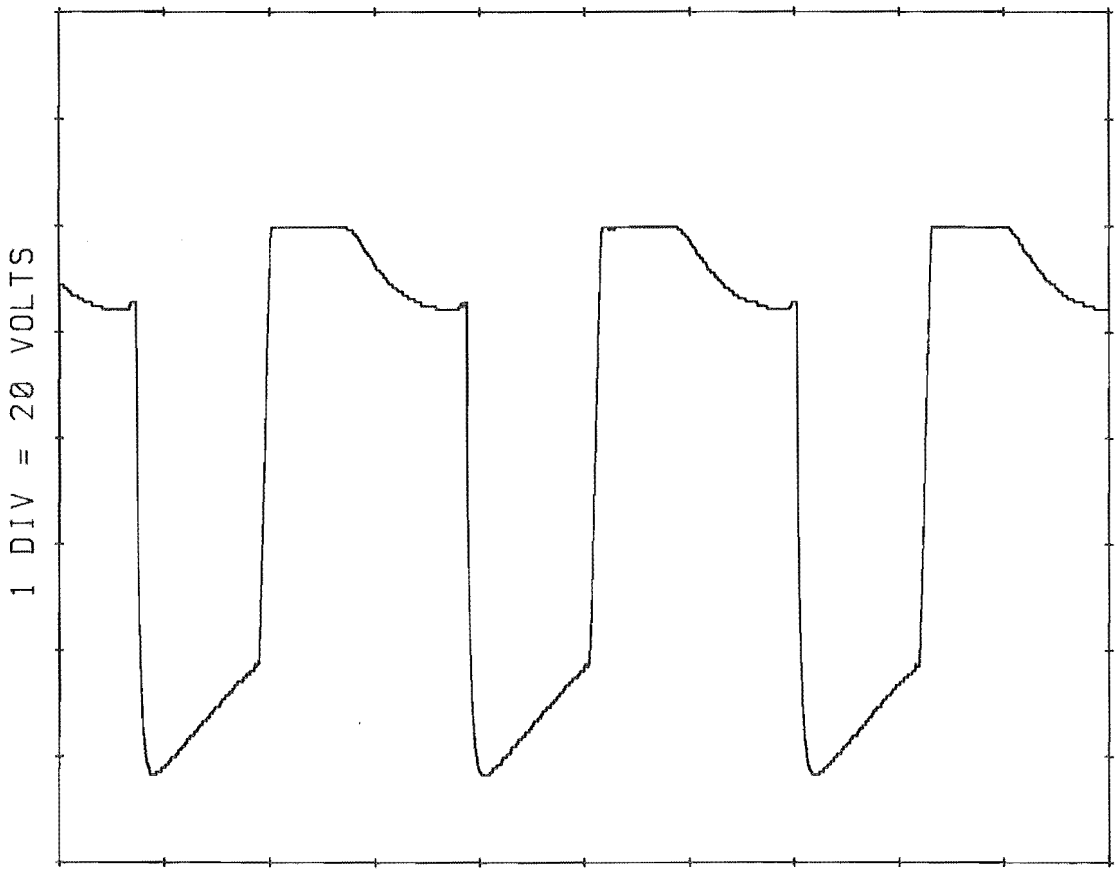

Fig. 4.14

The upper trace of figure 4.15 is one example of the waveforms used to detect the rotor position. This plot shows a monitoring cycle recorded at the output of the sampling circuit with minimum monitoring phase inductance. The ten intervals which define the monitoring cycle can be seen from the lower trace. This trace is a plot of the clock pulses to the 4017 counter. Comparison of the two traces shows the sampling circuit output voltage with respect to each interval within the monitoring cycle. As this minimum inductance case has the smallest time constant, it yields the largest peak voltage from the sampling circuit. As a result this case sets the upper limit to the output voltage range of the sampling circuit.

The other extreme of maximum monitoring phase inductance is illustrated in the plot of figure 4.16. This case sets the lower limit to the sampling circuit output voltage. The decrease in the amplitude of the sampled peak voltage with increase in inductance can be seen when comparing these plots.

4.5 The Monitoring Cycle Envelopes.

When the peak voltage measurement across R is repeated at intervals during a sweep in the rotor position, a plot of peak voltage against rotor position can be produced. The necessary measurements for such a plot have been made for each phase and plotted together in figure 4.17. Although generated manually by measuring the peak voltage at intervals, these plots represent the envelopes of the monitoring current peaks which should result during running.

Figure 4.17 verifies the regions predicted in chapter 2 where the

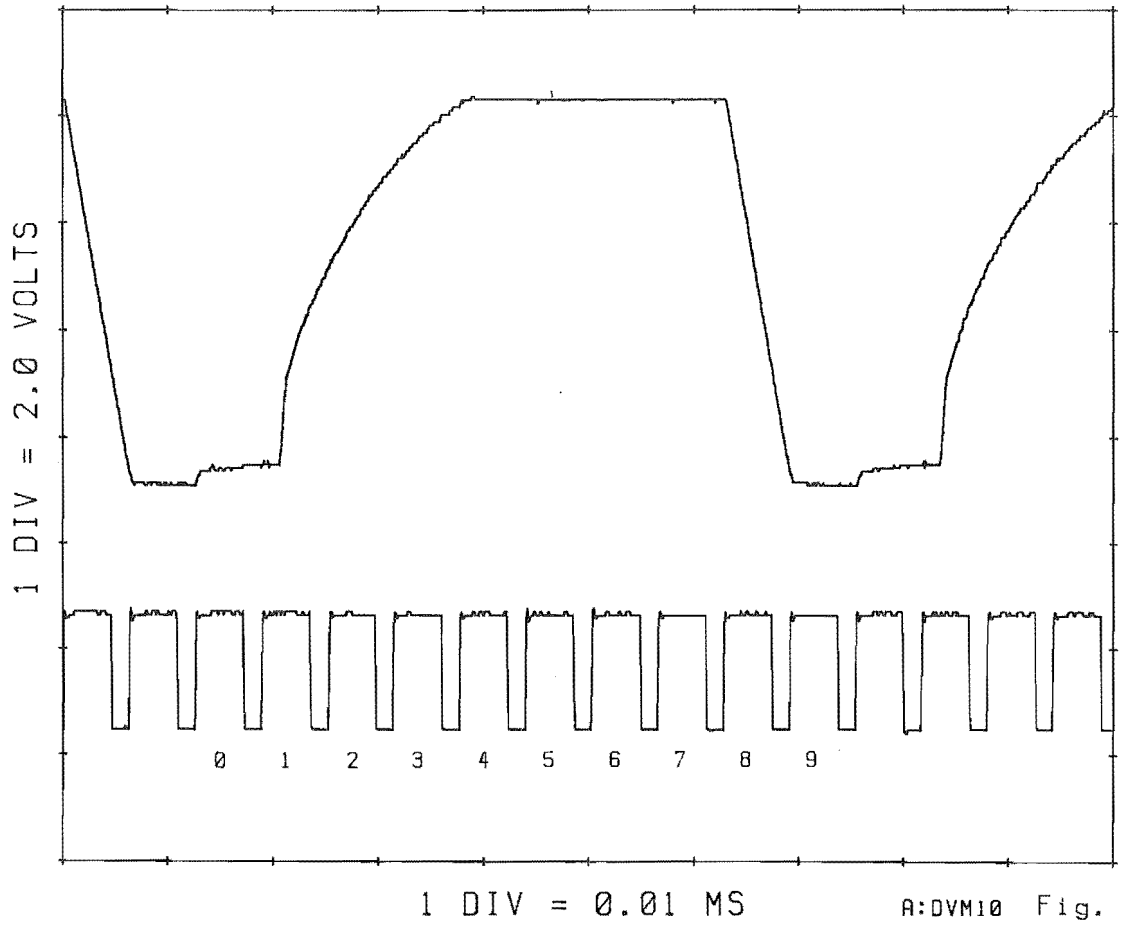

A:DVM10 Fig. 4.15

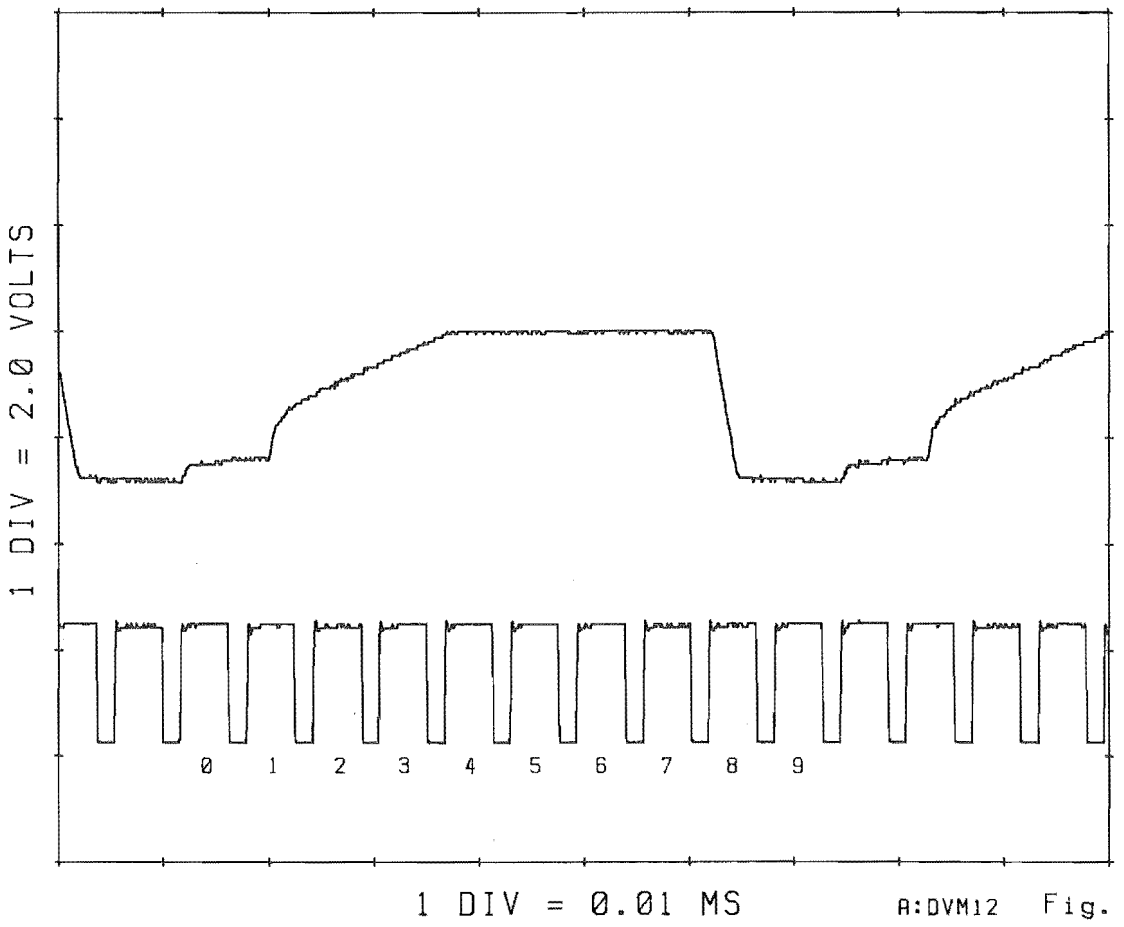

A:DVM12 Fig. 4.16

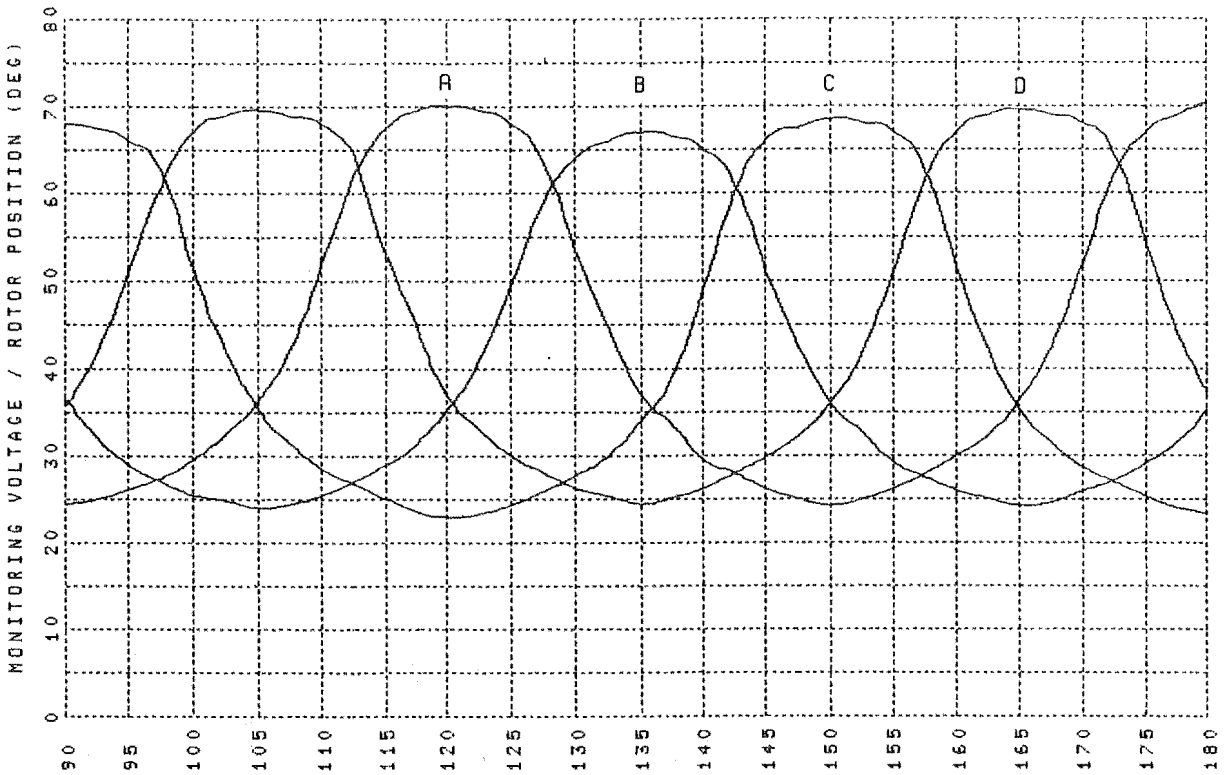

Fig. 4.17

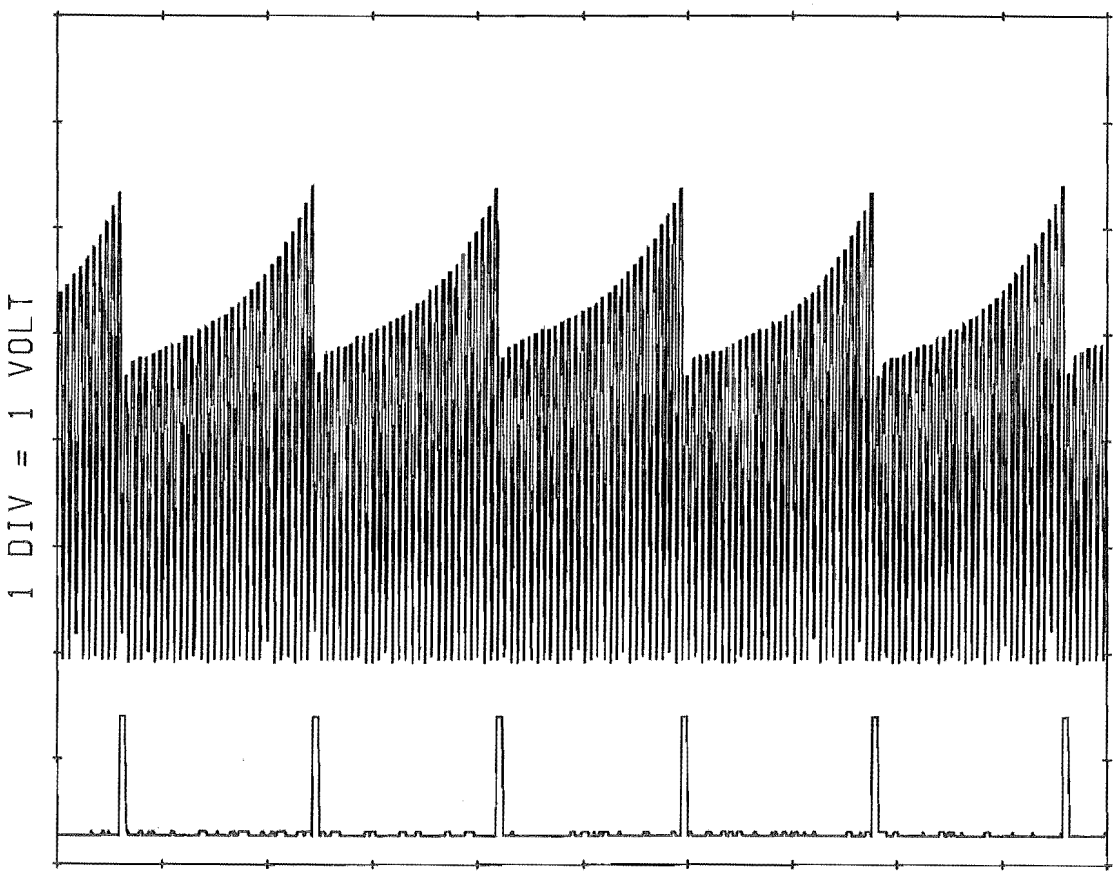

A:DVM14 Fig. 4.18

monitoring scheme will not correctly detect the rotor position. The intersections of the curves of adjacent phases show the bounds on the lead angle range. The 2.5 step lead angle limitation can be seen.

When a sequence of the monitoring waveforms are recorded during closed loop running, the peaks form envelopes which are successive single step portions of figure 4.17. The upper trace of figure 4.18 is such a plot. This trace was produced by monitoring with the on phase turned off and the rotor coasting down in speed from 1500 rpm. The lower trace was recorded with the second oscilloscope channel and shows the commutation pulses recorded at the output of the monitoring circuit flip-flop. The positive going edge of the commutation pulses identify the start of each step. The vertical scale refers to the upper trace only, the commutation pulses being in reality twelve volts in amplitude. Figure 4.18 was recorded at a speed of approximately 900 rpm and a lead angle of approximately 24 degrees. Here the on phase currents are zero. Ideal, solely rotor position dependant monitoring envelopes are obtained.

4.5.1 Monitoring Abnormalities.

When motoring, the waveforms of the monitoring cycles displayed major departures from the ideal waveforms of figure 4.18. Exhaustive testing of all the circuitry was carried out to ascertain if the interference of the drive currents on the monitoring behaviour was a result of a circuit malfunction. The switching scheme for the simultaneous on phase chopping and monitoring phase chopping is sufficiently complicated for an error or periodic glitch to manifest

itself in the form of a characteristic of the monitoring. An erroneous commutation caused by noise or a circuit malfunction could cause monitoring to occur at incorrect rotor positions for one or more phases. Further departures from the expected waveforms would then occur naturally.

No faults were discovered and the circuitry proved to be functioning as intended. Attention was then directed towards explaining the behaviour in terms of interaction of the fluxes in the on and monitoring phases.

The traces recorded while motoring at a constant speed of approximately 900 rpm are shown in figure 4.19. It can be seen that when motoring, significant distortions occur to the ideal envelopes of figure 4.18. The "saddle shaped" envelope is one example. During this step, the monitoring peaks are generally higher than those of figure 4.18. The "saddle shape" was at first thought to result from position monitoring at an incorrect rotor position in that phase. Such an envelope would occur when motoring at lead angles in the vicinity of 2.5 steps as shown in figure 4.17. However this behaviour has since been shown to result from flux leakage from the on phase adding to the self induced flux.

The large monitoring peaks which extend beyond the oscilloscope graticule occur on the first monitoring cycle of the following step. These monitoring peaks are significantly larger than normal current rise in the monitoring phase will produce. The envelope for the remainder of the step appears similar to the ideal envelope. The commutation pulses from the monitoring circuit (lower trace) are extended by two additional periods by the occurrence of the enlarged peak and the one which follows. Three adjacent monitoring peaks

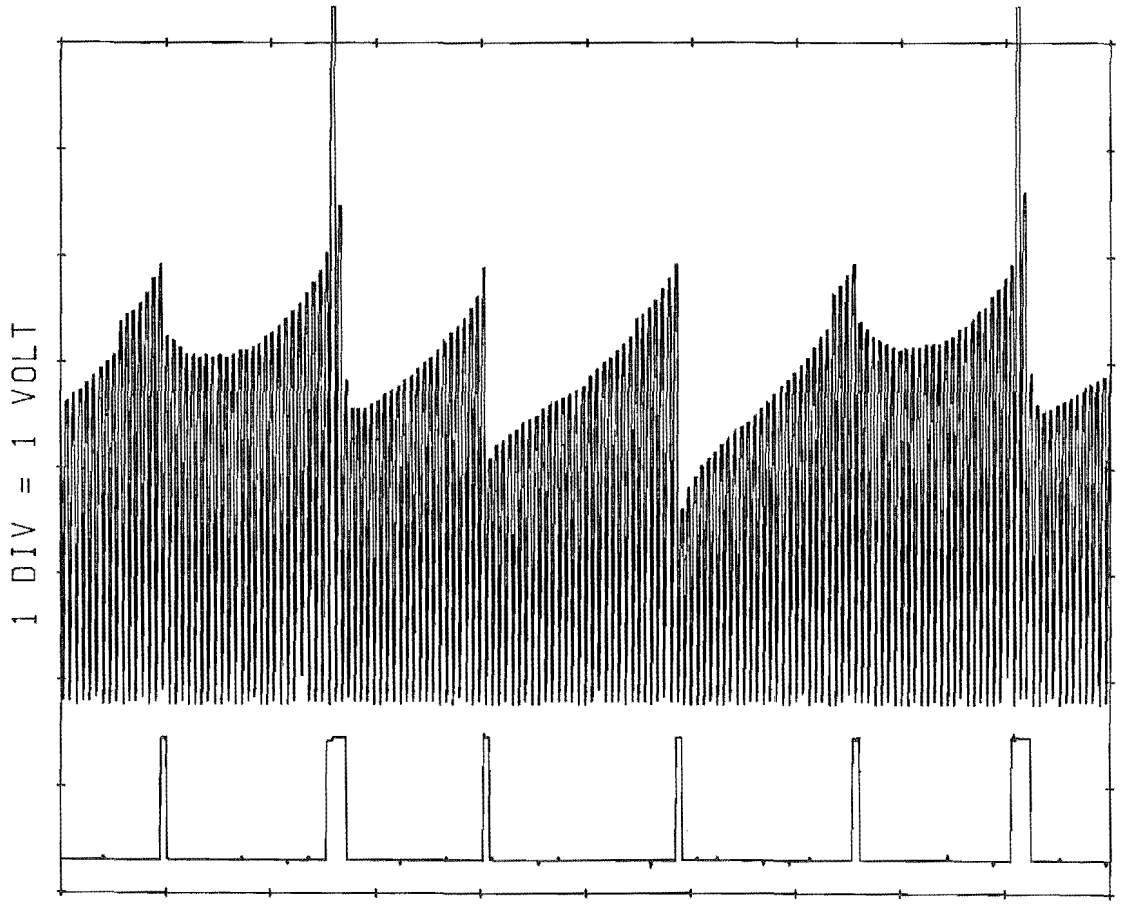

A:DVM18 Fig. 4.19

therefore exceed the reference voltage and the flip-flop output remains high for three times the usual period. These enlarged peaks are readily removed from the monitoring envelopes. This has been done by gating the monitoring pulses which are passed to "Chop". A comparator senses when the on phase current is below 2 amps and closes the gate. In this way no monitoring is performed in the early part of the step. The time required for the on phase current to exceed 2 amps is sufficient to delete these peaks from the envelope. This addition to the monitoring circuit however was found to offer no extension to its operating range or performance improvements.

Another distinguishing feature is the discontinuity in the envelope of the step preceding the first commutation pulse. The discontinuity appears as an upward step in a monotonically rising envelope. The monitoring peaks are of lower amplitude than the ideal envelope, particularly towards the beginning of the step. However the peaks in the elevated region at the end of the envelope fit the ideal envelope. It therefore appears that the peaks before the discontinuity have been "pulled down" with respect to the ideal envelope, whereas those occurring afterwards are comparatively uninfluenced. This behaviour reoccurs one electrical cycle later between the fourth and fifth commutation pulses. These abnormalities in the monitoring envelope also appear to be the result of flux leakage from the on phase.

4.6 Characterising the Observations.

Clearly the flux produced by the current in the on phase has a major influence on the monitoring envelopes. The form of the envelopes containing the monitoring waveforms is now no longer solely a function of rotor position. As has been shown, not all phases are affected equally. The waveform however repeats every four steps or one electrical cycle of the motor. This periodicity indicates that the magnetic design of the motor causes the departure from the solely rotor position dependant position monitoring behaviour.

4.6.1 Pole Configuration.

In analysing the performance of the monitoring scheme, the flux in the monitoring phase must be treated as the sum of the self induced flux and the flux exchanged between the monitoring phase and the other phases. Flux leakage into the monitoring phase inductance from another phase adds to the self induced flux in the monitoring phase. Flux may also leak from the monitoring phase to another phase thereby subtracting from the self induced flux. Which of these two cases occurs depends on the pole configuration within the motor. A qualitative analysis of the effects of pole configuration can be made by changing the relative polarities with which the phases are energised and comparing monitoring envelopes.

Under single phase excitation, the four phase motor requires that the diagonally opposite stator teeth ends (which are poles in the same phase), are of opposite magnetic pole. If the teeth ends are of like

pole the magneto-motive force applied across the air gap is only very small. Its magnitude will be approximately the difference between the fields created by the two windings which form the phase inductance. There are only two unique pole configurations which meet the above requirement. These configurations are shown in figure 4.20. The other configurations are merely rotations of these two with respect to the motor frame.

Analysis of the two different stator pole configurations reveals that between orthogonal phases the flux leakage from the on phase adds to the monitoring phase flux over the entire electrical cycle. This is the result of the symmetrical positioning of the on phase poles with respect to the monitoring phase poles. The poles of the on phase are equi-distant from each of the monitoring phase poles and flux exchange will always occur between opposite poles of the two phases.

The poles of the phases adjacent to the monitoring phase are not positioned symmetrically with respect to each of the monitoring phase poles. Consequently the nature of any flux exchange between the monitoring and adjacent phases, if it occurs, depends on whether like or opposing poles are adjacent to the monitoring phase poles.

Figure 4.20a is the configuration used in the generation of the position monitoring envelopes plot of figure 4.19. This configuration has four successive north poles followed by four successive south poles. Therefore there is one diameter line or interface across which a phase and an adjacent leading phase are of opposite polarity. The monitoring plot produced with this configuration has one saddle shaped envelope.

The alternative configuration of figure 4.20b yields the plot

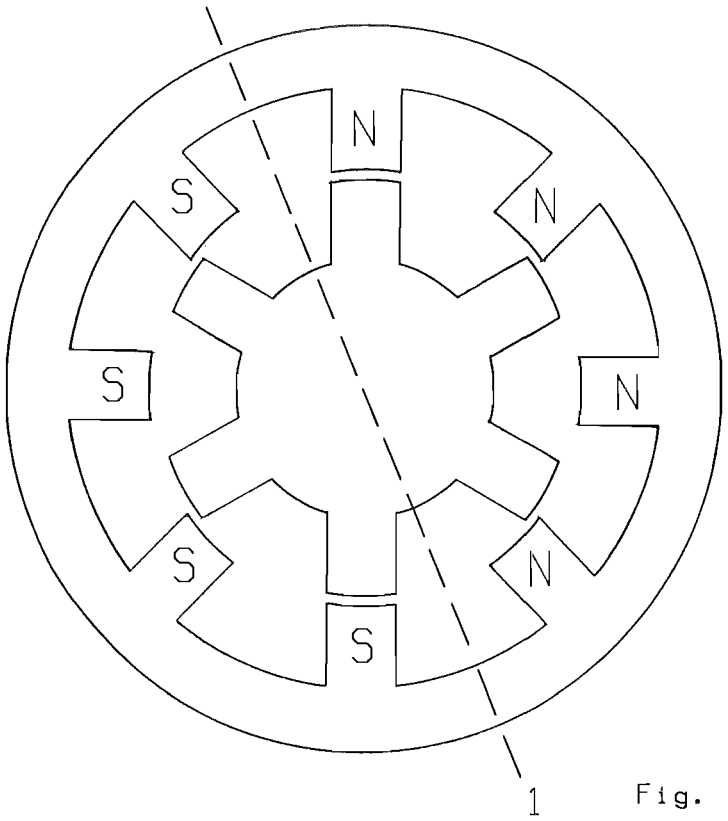

Fig. 4.20a

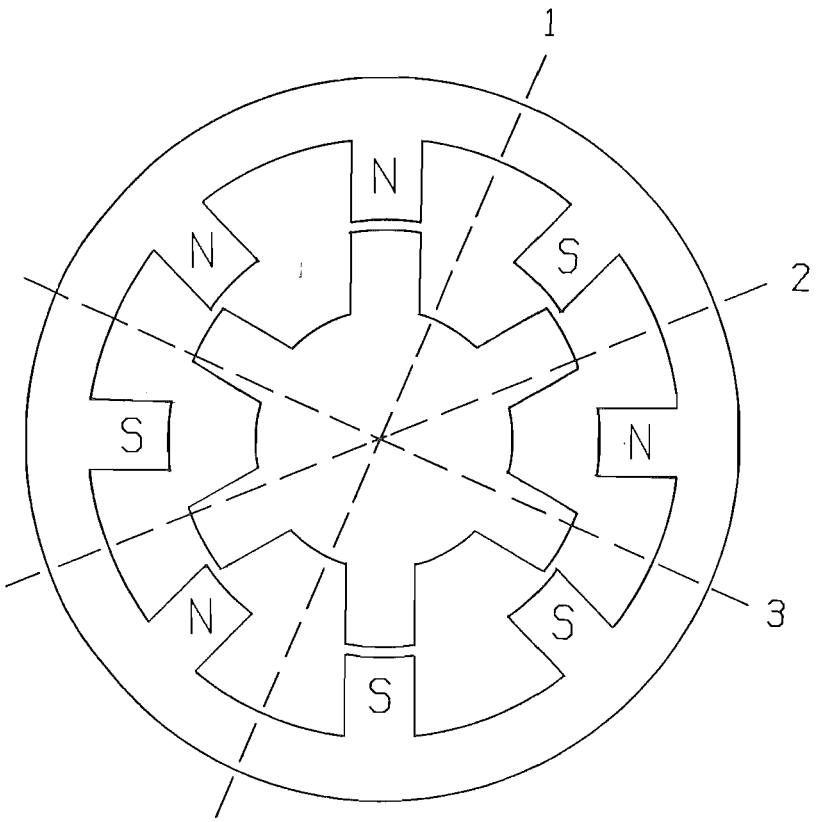

Fig. 4.20b

shown in figure 4.21. This configuration has three interfaces across which a phase and its adjacent leading phase are of opposite polarity. The plot of figure 4.21 is comprised of the same envelopes which occur in figure 4.19. The monotonically rising envelope with the discontinuity is once again present. However in one electrical cycle of the motor there are now three envelopes of the distinctive saddle shape. These envelopes now have a slight notch towards the end of the envelope followed by a steady rise towards commutation. It is shown numerically in the following chapter that the notch in the saddle shaped envelope is caused by the same phenomenon which causes the discontinuity in the monotonically rising envelope. Although no large amplitude monitoring peaks are present in figure 4.21, they can also occur when using the pole configuration of figure 4.20b.

With both configurations there is a direct correlation between the number of interfaces between adjacent phases of opposite polarity and the number of saddle shaped envelopes in one electrical cycle. The converse is found when the monotonic envelope is considered. There is a direct correlation between the number of interfaces between adjacent phases of like polarity and this type of envelope. These findings indicate that the main flux exchange with the monitoring phase is from the adjacent leading phase and not the on phase.

The de-energising phase is adjacent to and leads the monitoring phase. It is therefore the flux produced by the de-energising current which distorts the ideal position monitoring envelopes. As the monitoring peaks during the saddle shaped envelopes are higher than the ideal envelopes, flux is leaked into the monitoring phase and hence adds to the self induced flux during those steps. This has been shown to occur when the de-energising phase is of opposite polarity.

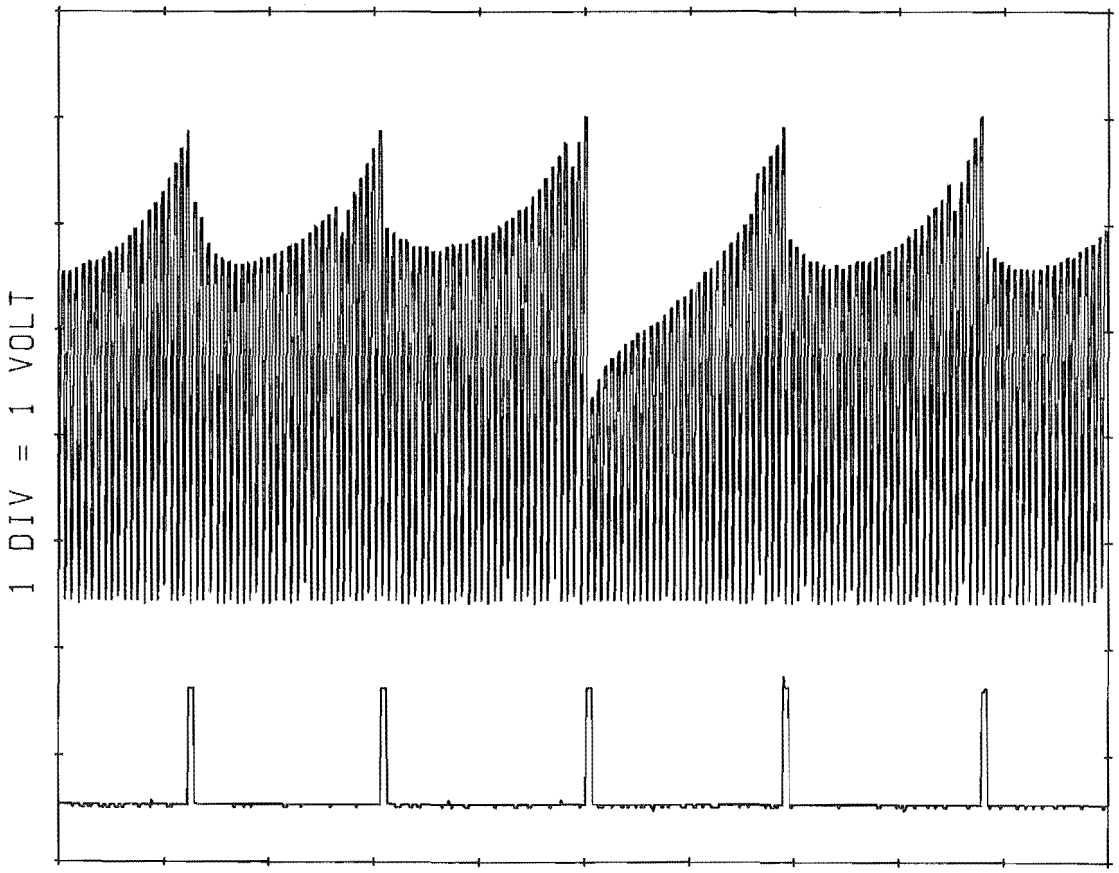

A:DVM19 Fig. 4.21

The monitoring peaks during the monotonic envelope are lower than the ideal envelopes, indicating that flux has leaked from the monitoring phase. This occurs when the de-energising phase is of like polarity.

Figures 4.22 and 4.23 are plots showing the interference of the monitoring waveforms (upper trace) in relation to the de-energising current (lower trace). In figure 4.22, the characteristic monotonic and saddle shaped waveforms are present. The discontinuities in these waveforms can be seen to coincide with the de-energising current decaying to zero. In figure 4.23 the de-energising current during the saddle shaped waveform does not reach zero as the envelope has been elevated to the commutation level and commutation has occurred prematurely. As a result, no discontinuity occurs in this envelope. The following envelope begins with two of the large monitoring peaks which extend beyond the oscilloscope graticule. These abnormal peaks are shown here to result from the residual flux in that phase when it is first position monitored.

The finding that the de-energising phase is the source of the interference and not the on phase is supported by the relative sizes of the mutual inductance these phases form with the monitoring phase. The current in the on and de-energising phases generate an approximately equal amount of flux. However the mutual inductance between adjacent phases is approaching an order of magnitude greater than the mutual inductance between orthogonal phases.

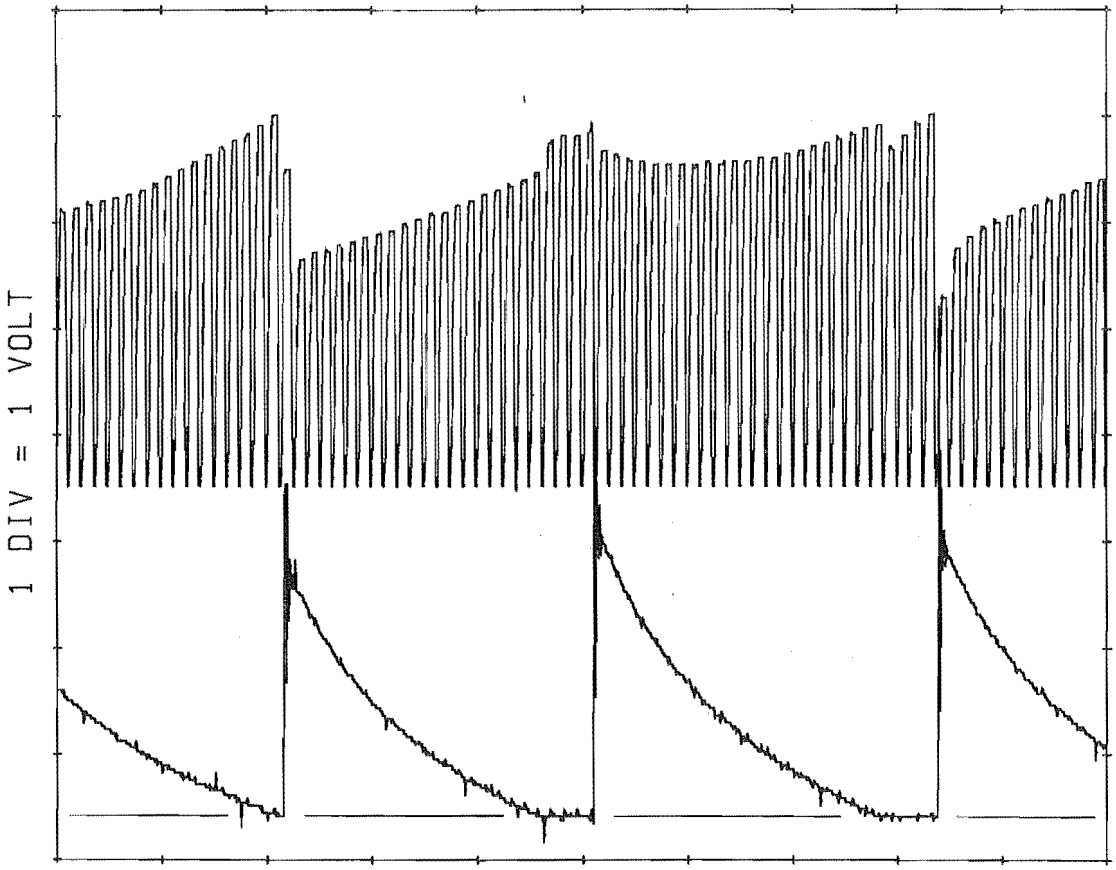

Fig. 4.22

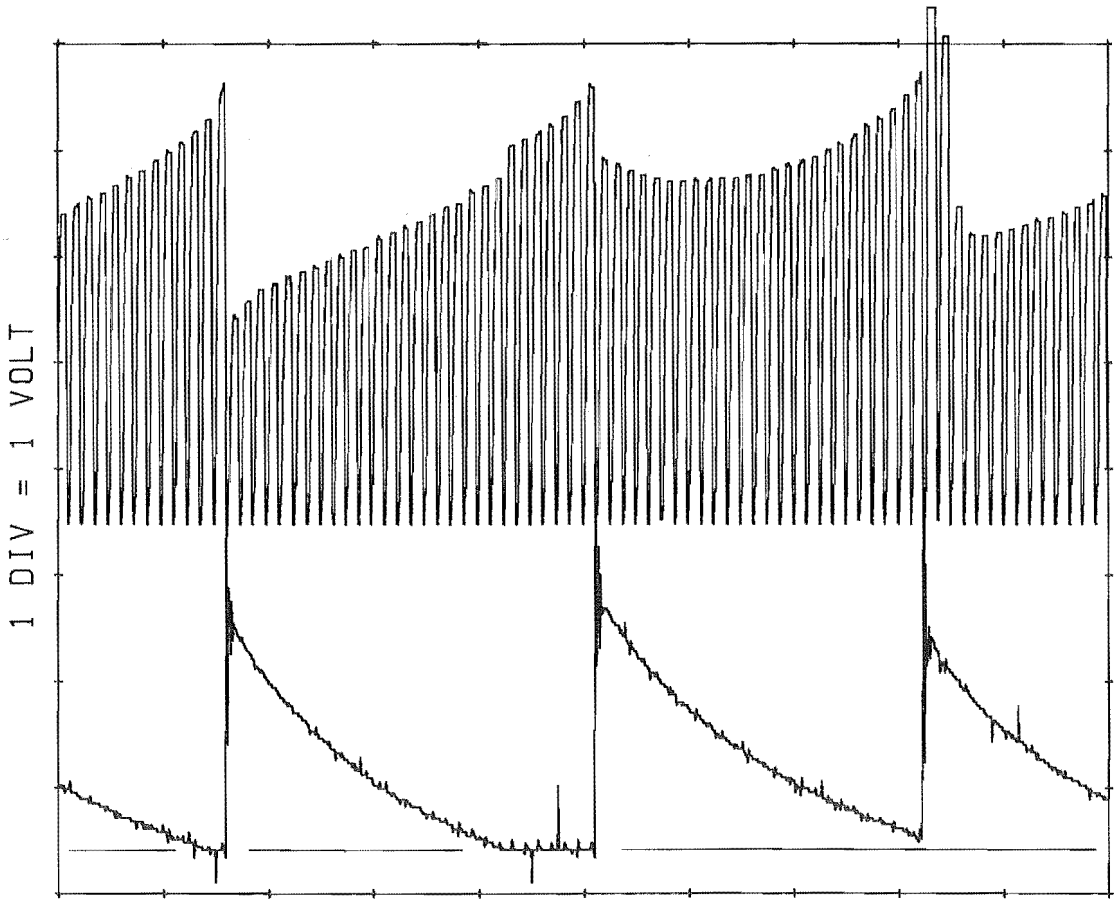

Fig. 4.23

4.6.2 The Effects Of Interference On Position Monitoring.

The reference voltage of the position monitoring circuitry is used to set the commutation positions for all phases. Therefore commutation is performed at the same level on each phase's monitoring envelope. As one monitoring envelope in four is effected differently, commutation occurs at a different rotor position for the consecutive phase. This effect is compounding, resulting in each phase operating at a different lead angle and producing a different torque. The difference in torque produced by each phase means that the motor will not run optimally.

Not only the difference between the envelopes over an electrical cycle poses position monitoring problems. Complications arise from the shapes of individual envelopes also. The saddle shaped envelope limits the maximum lead angle which can be obtained. The monitoring peaks at the beginning of the envelope are of similar amplitude to those at the end and the gradient at the point of commutation is shallow. This makes the commutation point less precisely defined with respect to rotor position. There is also the danger of the early monitoring peaks being elevated above those at commutation. If this occurs, commutation occurs immediately and the lead angle of the consecutive on phase is advanced by approximately one step. Such an advance will put the lead angle into the illegal operating range of 2.5 steps or greater if the initial lead angle is 1.5 steps or greater. As has already been shown, practical lead angles are always greater than 1.5 steps and occasionally 2.0 steps. The likely result of this unintentional lead angle increase to greater than 2.5 steps is loss of synchronisation. This mechanism of synchronisation loss has been observed in action and

is the principle restraint on the maximum lead angle. In the system developed the lead angle is limited by this mechanism to 27 degrees or 1.8 steps.

Like the saddle shaped waveform, the monotonic envelope makes absolute position detection very difficult, by being a function of the de-energising current waveform as well as of rotor position. However, absolute position detection is not necessary in obtaining speed control. A positional feedback system which consistently detects the same position within each step is sufficient. The control system can compensate for the non linearities in the positional feedback system by shifting the detected position until the performance is maximised.

The monotonic envelope is not subject to the premature commutation problem of the saddle shaped envelope and hence does not limit the maximum lead angle. It is possible that the reduced amplitude of the monitoring peaks may even extend the limit on maximum lead angle if the saddle shaped envelope was not present. However this effect has not been investigated.

The minimum lead angle is 19 degrees. The theoretical minimum is 1 step or 15 degrees and is based on sinusoidal phase inductance variation. As shown in figure 4.17 there is very little change in the monitoring voltage within a rotor position of approximately 5 degrees from the points of maximum monitoring peaks. As a result, position detection in these regions is uncertain and in practice the lead angle can only be reduced until the onset of these regions at approximately 20 degrees before detent.

4.7 Torque Measurement.

Torque measurements were made using a belt brake to supply the torque load. Spring balances were used in each end of the belt to measure the differential tension and enable torque calculations. Torque outputs were measured when the motor was running self synchronised. The measured torque output variation with speed is shown in figure 4.24. The characteristic reduction in the torque output with increasing speed can be seen. Torque outputs for speeds below 500 rpm have not been recorded as this is the lower working limit with the lead angles which can be produced. For a constant torque load the motor cannot sustain speeds below 500 rpm. With decreasing speed below 500 rpm, the torque output decreases also and a further reduction in the speed results. The process is degenerative and the motor speed continues to fall until the motor stalls. This is the result of a flat or positive torque vs speed gradient below this speed.

4.8 Summary.

Encoderless self synchronisation of the single stack four phase variable reluctance stepping motor has been achieved. However the research has shown the performance of the position monitoring algorithm is susceptible to interference from the de-energising phase. The interference is shown to be significant and to limit the maximum lead angle and therefore the high speed performance. The nature of the interference when using other motors could now be predicted by an analysis of the pole configuration.

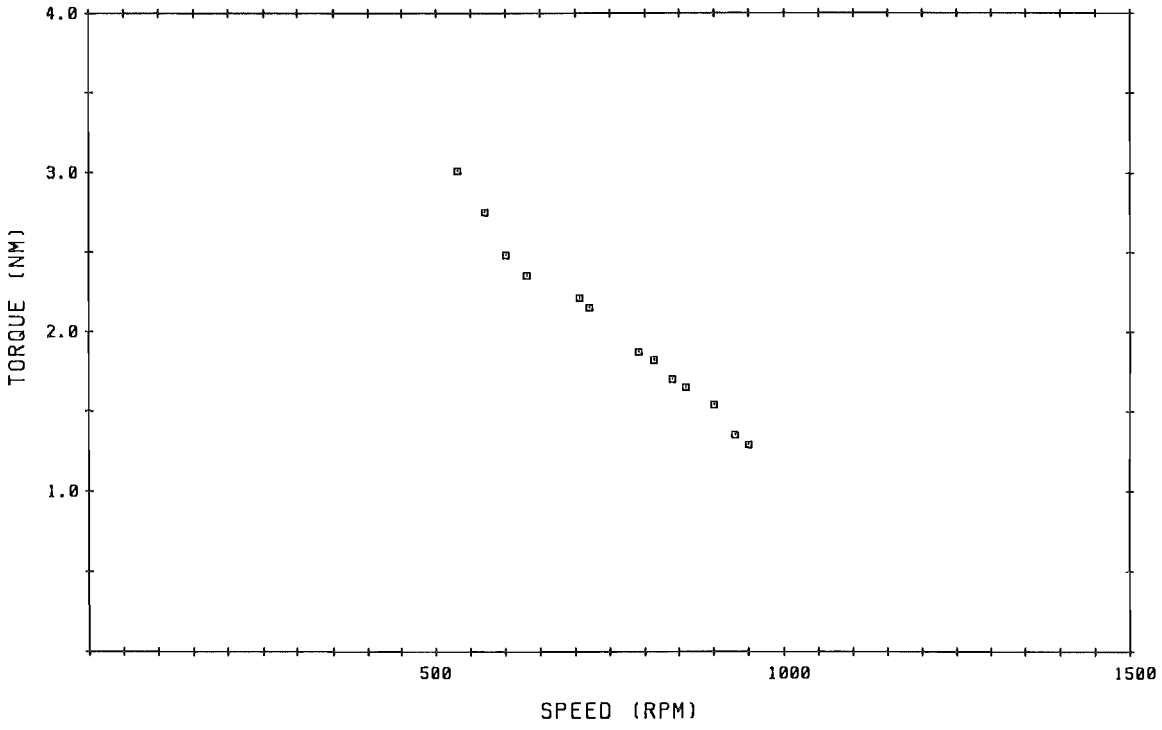

Fig. 4.24

CHAPTER 5.

MODELLING.

5.1 Introduction.

When the project was proposed and undertaken, the expectation was to achieve closed loop variable speed control of the single stack variable reluctance motor. This objective was achieved through the design and development of a waveform monitoring scheme which allowed operation over a limited range of lead angles. Through control over the level of the on phase current, variable speed control over a range of speeds was achieved. However, during motoring the waveforms of the monitoring cycles displayed major departures from the expected waveforms. The waveforms do not change solely in accordance with rotor position.

Much experimentation enabled these waveforms to be characterised in terms of the pole configuration of the motor. Having observed these effects it was decided to extend the scope of the project by mathematically simulating the monitoring characteristics. The aim was to gain insight into how certain variables effect performance and explain many of the phenomena observed during experimentation.

A simulation of the monitoring waveforms initially requires solutions for the phase current equations 2.6 and 2.10. These solutions are required to evaluate the flux exchange with the monitoring phase. The solutions not only enable a simulation of the monitoring waveforms, but also enable torque calculations and the generation of theoretical torque speed plots.

The on and monitoring phase equations are first order linear

differential equations with non constant coefficients. Initial attempts using analytical methods found them to be very unwieldy. As a result, numerical solutions were finally sought. The numerical method adopted was the fourth order Runge-Kutta method. It was chosen because of its accuracy and because it does not require higher derivatives of the expression it is integrating. A variety of methods of obtaining error estimates and interval size control are possible with the Runge-Kutta method. The method used in the simulations performed in the research is based on interval halving.

The operation of the fourth order Runge-Kutta method as a numerical solver of differential equations and the operation of interval halving based error control are well covered in the literature and are not reproduced here (cf. Conte and De Boor 1980).

5.2 Modelling The On Phase Currents.

In the interest of modelling continuous waveforms only the unchopped on phase currents are modelled. The same equations and algorithm can be used to model the chopped waveforms. However owing to the discontinuities in the on phase current during chopping a piecewise approach is required. The added complexity in performing this simulation would yield no benefits in identifying the source and extent of interference of the monitoring waveforms. Further, torque calculations can be made by calculating the torque developed by the constant mean current of the chopped waveform without the need to reproduce the small amplitude current variation of chopping.

The on phase current equations 2.6 and 2.10 are derived as

functions of time, but are more conveniently solved as functions of rotor position. They must also be re-expressed in terms of the differential of current before the Runge-Kutta method can be applied. The form which the energising current equation 2.6 takes is shown by,

$$\left(\frac{di}{d\theta}\right) = \frac{V - i\left(R + \omega\left(\frac{dL(\theta)}{d\theta}\right)\right)}{\omega L(\theta)} \qquad (5.1).$$

The required form of the de-energising current equation 2.10 is shown by,

$$\left(\frac{di}{d\theta}\right) = \frac{-\left(V + i\left(R + \omega\left(\frac{dL(\theta)}{d\theta}\right)\right)\right)}{\omega L(\theta)} \qquad (5.2).$$

When the current has been calculated at a given rotor position, the torque equation 2.5 can be applied minus the mutual terms. This equation then takes the from,

$$T = \tfrac{1}{2}\left(\frac{dL}{d\theta}\right)i^2 \qquad (5.3).$$

When the current is evaluated at a sufficient number of positions a plot of torque variation with rotor position can be produced.

5.3 Solving The On Phase Current Equations.

A FORTRAN program (VRM1) was written to apply the fourth order Runge-Kutta algorithm to equations 5.1 and 5.2. The operating conditions to be simulated are defined by the lead angle, speed, supply voltage, energising circuit source impedance and imposed

current limit.

The energising current equation 5.1 is evaluated at discrete rotor positions over one step starting at zero current. The spacing between these positions is adjusted in accordance with the error estimate. The current is successively evaluated at the rotor positions until the end of the step. At the end of the step, the de-energising current equation 5.2 is evaluated similarly for an extra step. The phase inductance range over which equations 5.1 and 5.2 are evaluated is set by the lead angle. If the current rises to above the prescribed current limit then the current limit is used in the following torque calculations and as the starting current for the de-energising step. The effect of active suppression is incorporated into the program by only evaluating equation 5.2 until the current falls to zero, as the de-energising current is never negative in practice.

Figure 5.1 is the computer simulation of the phase current arising from the operating conditions of figure 4.12 (speed 1380 rpm, lead angle 28 degrees). The simulation is plotted with the first waveform of figure 4.12 in figure 5.2. The initial current rises are of similar gradient and the de-energising currents are close throughout. The simulated waveform shows a slight extremum but it is not as large or acute as the one recorded in figure 4.12. Despite the difference here the modelled current is sufficiently representative of the actual to enable worthwhile torque calculations to be made.

Attempts were made to identify the cause of the extremum. The equations 5.1 and 5.2 were extended to include the effects of interaction of the fluxes produced by the energising and de-energising currents.

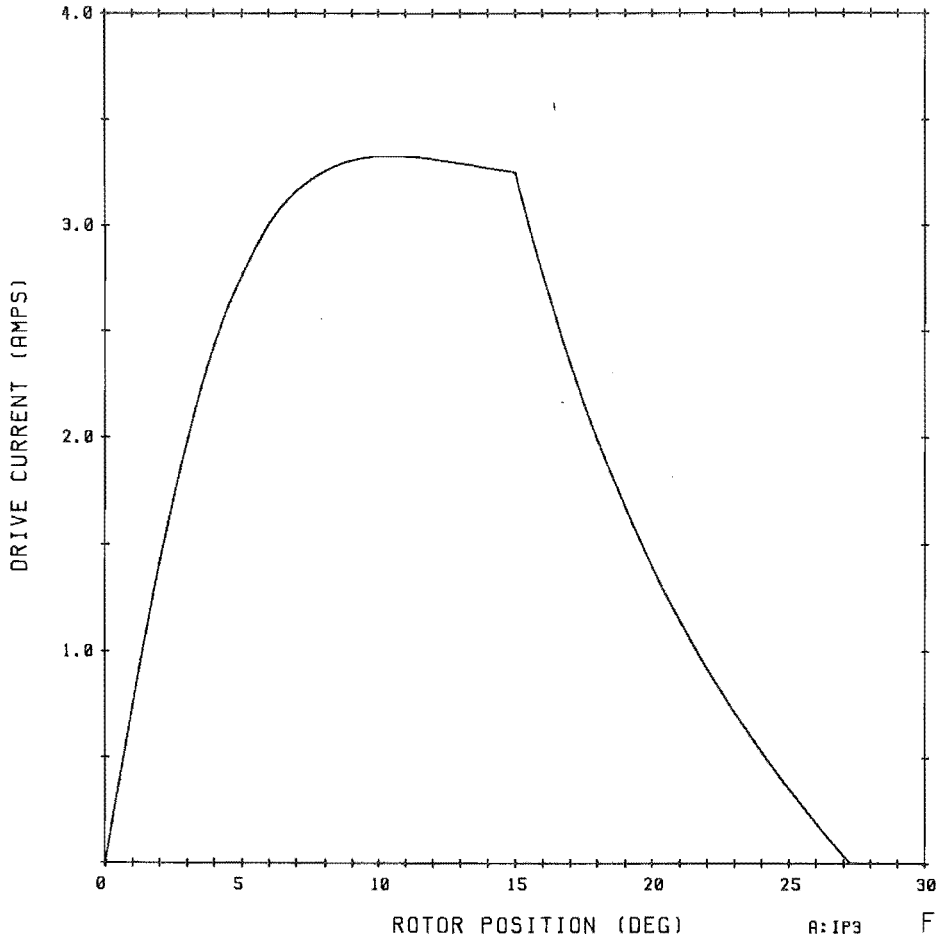
4.0
3.0
2.0
1.0
DRIVE CURRENT (AMPS)
0
5
10
15
20
25
30
ROTOR POSITION (DEG)
A:IP3

Fig. 5.1

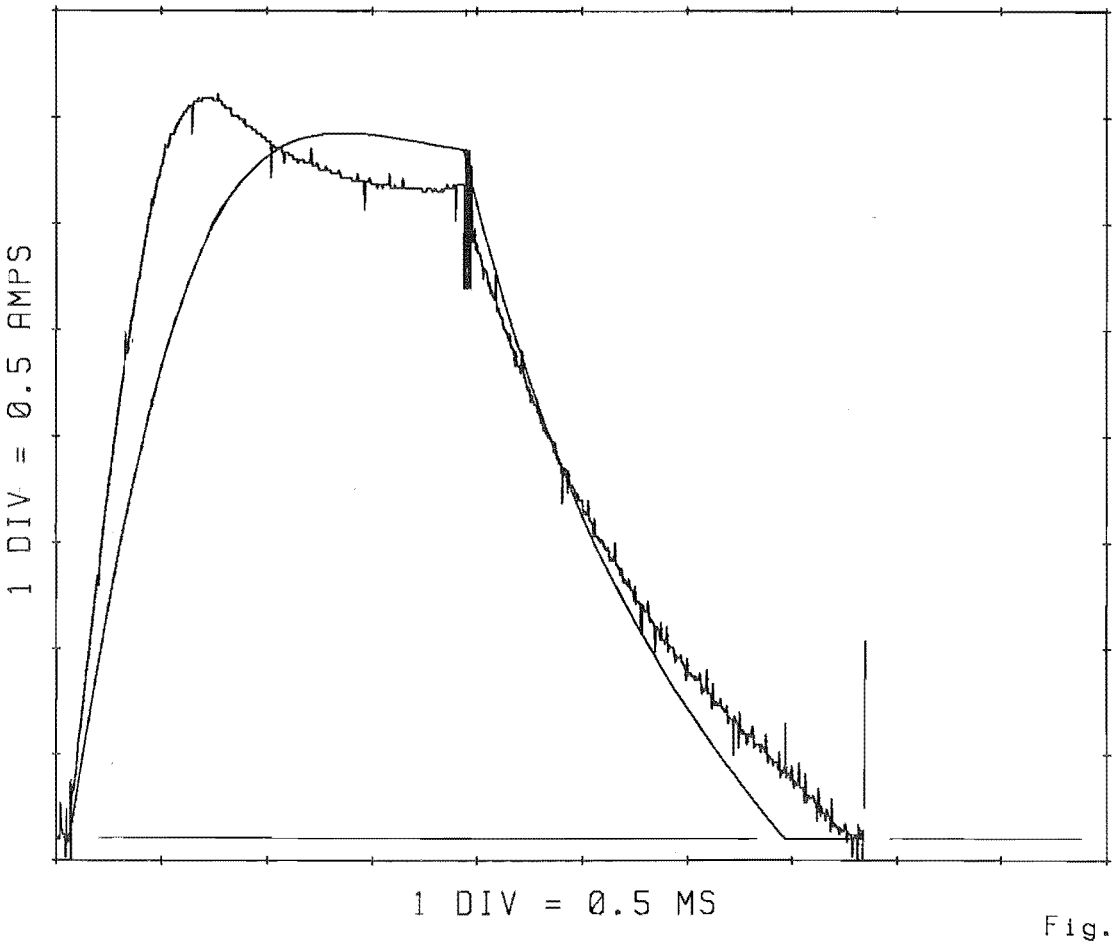
1 DIV = 0.5 AMPS
1 DIV = 0.5 MS

Fig. 5.2

Equation 5.1 becomes,

$$\left(\frac{di_A}{d\theta}\right) = \frac{V - i_A\left(R + \omega\left(\frac{dL_A}{d\theta}\right)\right) + i_B\omega\left(\frac{dL_{AB}}{d\theta}\right) + \omega L_{AB}\left(\frac{di_B}{d\theta}\right)}{\omega L_A(\theta)} \quad (5.4).$$

Equation 5.2 becomes,

$$\left(\frac{di_A}{d\theta}\right) = \frac{V - i_A\left(R + \omega\left(\frac{dL_A}{d\theta}\right)\right) - i_B\omega\left(\frac{dL_{AB}}{d\theta}\right) - \omega L_{AB}\left(\frac{di_B}{d\theta}\right)}{\omega L_A(\theta)} \quad (5.5).$$

A Program (VRM2) was written to obtain approximate solutions to these equations. This program uses VRM1 to evaluate equations 5.1 and 5.2 at specified rotor positions first. The currents calculated are used as initial values in evaluating equations 5.4 and 5.5 at those rotor positions. In this way the solutions for equations 5.4 and 5.5 are obtained iteratively. The process can be repeated to obtain progressive refinements of previous values. However, it was found on the single iteration performed by VRM2 that the energising and de-energising currents have only a small influence on each other. For a converging process, subsequent iterations would yield progressively smaller changes. The plots of these currents differ very little in form and magnitude from those calculated from equations 5.1 and 5.2, hence the results are not included.

These two on phase current simulations imply that the extremum is not caused directly by the motional voltage or interaction between energising and de-energising currents. The extremum is most likely the result of non linear magnetic properties of the stator and rotor giving rise to effects not included in the analyses. These effects are saturation, hysteresis and eddy current loss.

The phase currents simulated by VRM1 can be used in conjunction

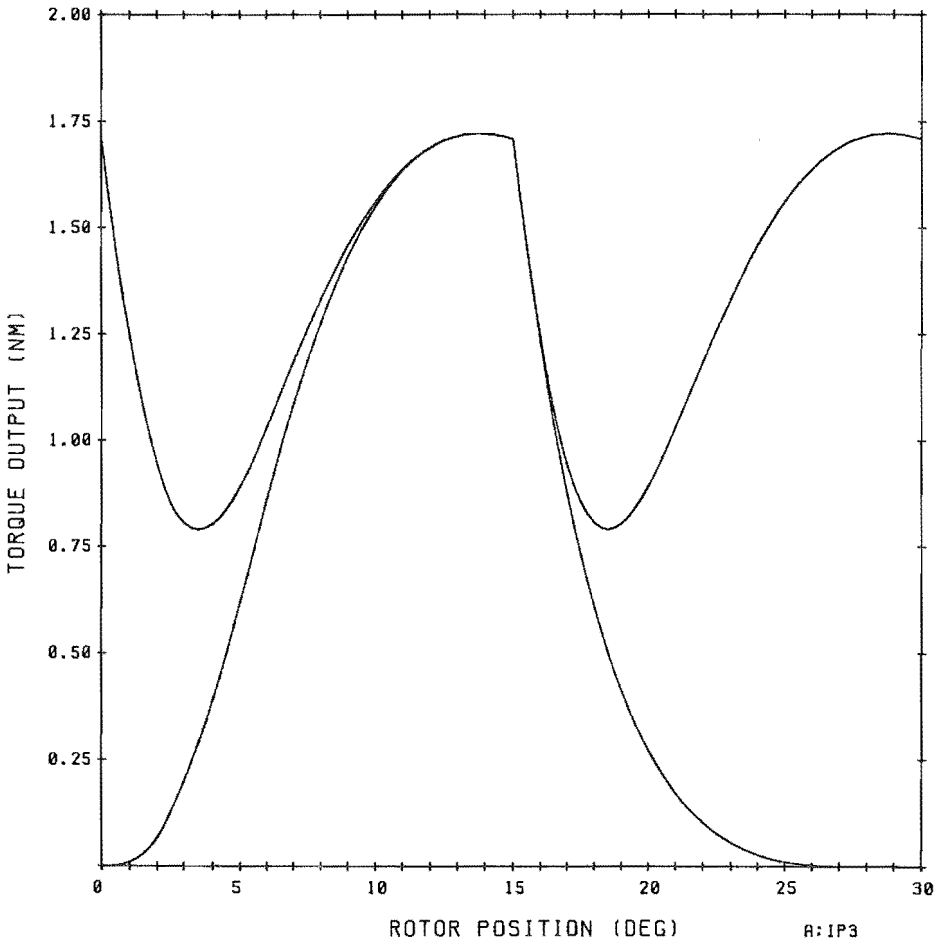
2.00
1.75
1.50
1.25
1.00
0.75
0.50
0.25
TORQUE OUTPUT (NM)
0
5
10
15
20
25
30
ROTOR POSITION (DEG)
A:IP3

Fig. 5.3

with equation 5.3 to calculate the torque developed. This enables a calculation of the instantaneous torque output against rotor position of the motor in motion. These are difficult torque measurements to make as they are dynamic. Figure 5.3 contains two torque plots derived from the simulated current waveform of figure 5.1. The lower plot is the torque calculated directly from the current plot. The upper plot is the superposition of a series of the lower torque plots shifted by one step. Torque is produced by both the energising and de-energising currents simultaneously. Therefore the torque produced the by two phases are summed. This plot shows the cyclic variation in the torque developed during motoring. When the mean torque output is calculated from a number of these plots produced at different speeds then torque vs speed plots can be compiled. These plots serve as a graphical representation of the drive's performance.

5.4 Generating Theoretical Torque vs Speed Plots.

The torque vs speed plots are generated by plotting the mean torque output at increments in speed over the full speed range. Other than speed, each plot is produced under fixed operating conditions.

Figure 5.4 is the computed torque speed plot obtained for a supply voltage of 120 volts and a current limit of 7.0 amps. As expected, at very low speed the smallest lead angle of 22.5 degrees provides the greatest torque. At a speed of approximately 220 rpm the next lead angle of 25.0 degrees provides the greatest torque output and continues to do so until a speed of 620 rpm. From 620 rpm to 920 rpm a 27.5 degree lead angle provides the greatest torque output and so on.

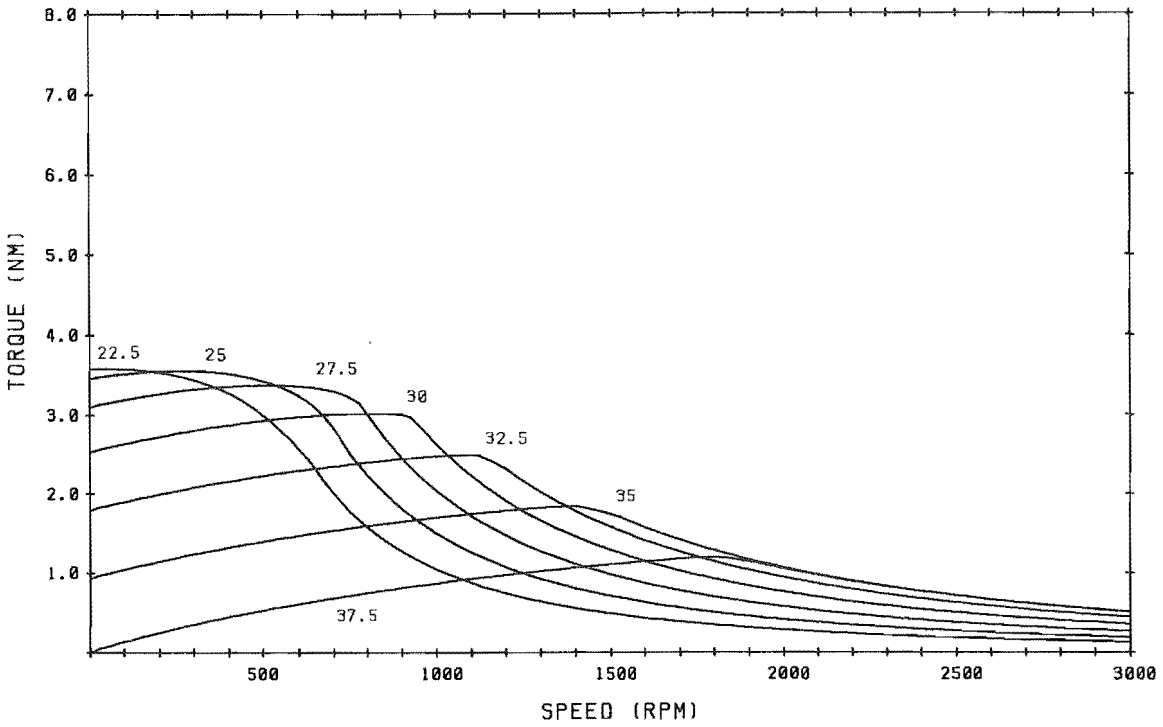
8.0
7.0
6.0
5.0
4.0
3.0
2.0
1.0
TORQUE (NM)
22.5
25
27.5
30
32.5
35
37.5
500
1000
1500
2000
2500
3000
SPEED (RPM)

Fig. 5.4

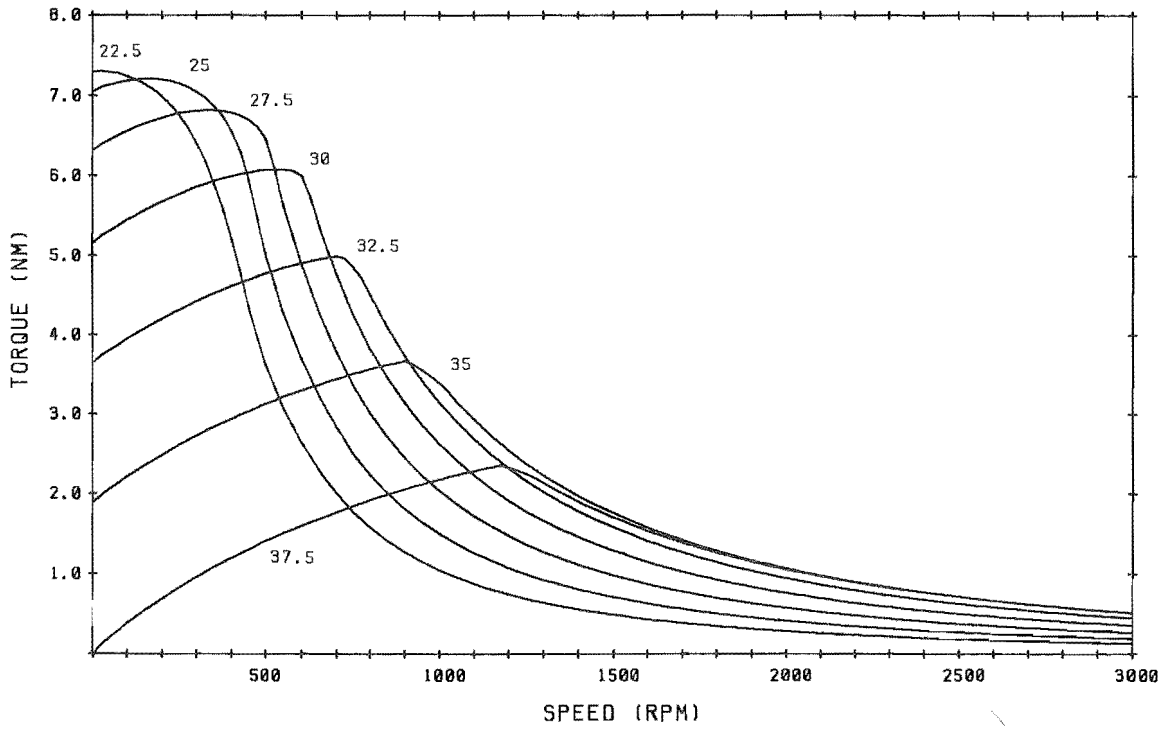
8.0
7.0
6.0
5.0
4.0
3.0
2.0
1.0
TORQUE (NM)
22.5
25
27.5
30
32.5
35
37.5
500
1000
1500
2000
2500
3000
SPEED (RPM)

Fig. 5.5

It can be seen that the five lead angles which are in increments of 2.5 degrees starting from 22.5 degrees will provide near maximum torque output up to a speed of 1500 rpm. This is illustrated by the nearly continuous torque envelope which these plots form. The envelope of maximum torque output is continuous and as shown by figure 5.4, a control system would require a continuously variable lead angle to produce it. Figure 5.5 is the plot obtained with a supply voltage of 120 volts and a current limit of 10.0 amps. The torque outputs at zero speed are now double those obtained with a 7.0 amp current limit. This results from the static torque developed being proportional to the current squared. However as the speed increases, the motional voltage increases limiting the current level in the phase. The extent to which the motional voltage limits the phase current is governed by the supply voltage, as these two voltages are in opposition.

To obtain near maximum torque up to a speed of 1500 rpm, six of the seven lead angles shown are required. As in figure 5.4 the lead angles are in increments of 2.5 degrees starting at 22.5 degrees. Below a speed of 1900 rpm the envelope of maximum torque is greater than that obtained with a 7.0 amp current limit. Above this speed however the envelopes are coincident. The maximum torque envelopes for the two current limits are shown together in figure 5.6. At zero speed the torque is entirely current limited and at 1900 rpm and beyond it is entirely voltage limited with respect to a current limit of 7.0 amps or greater. This is the speed where the maximum phase current falls below 7.0 amps and ceases to be chopped for the largest lead angle of 37.5 degrees (2.5 steps). Beyond this speed the on phase current waveforms for 7.0 amp and 10.0 amp current limits are then identical.

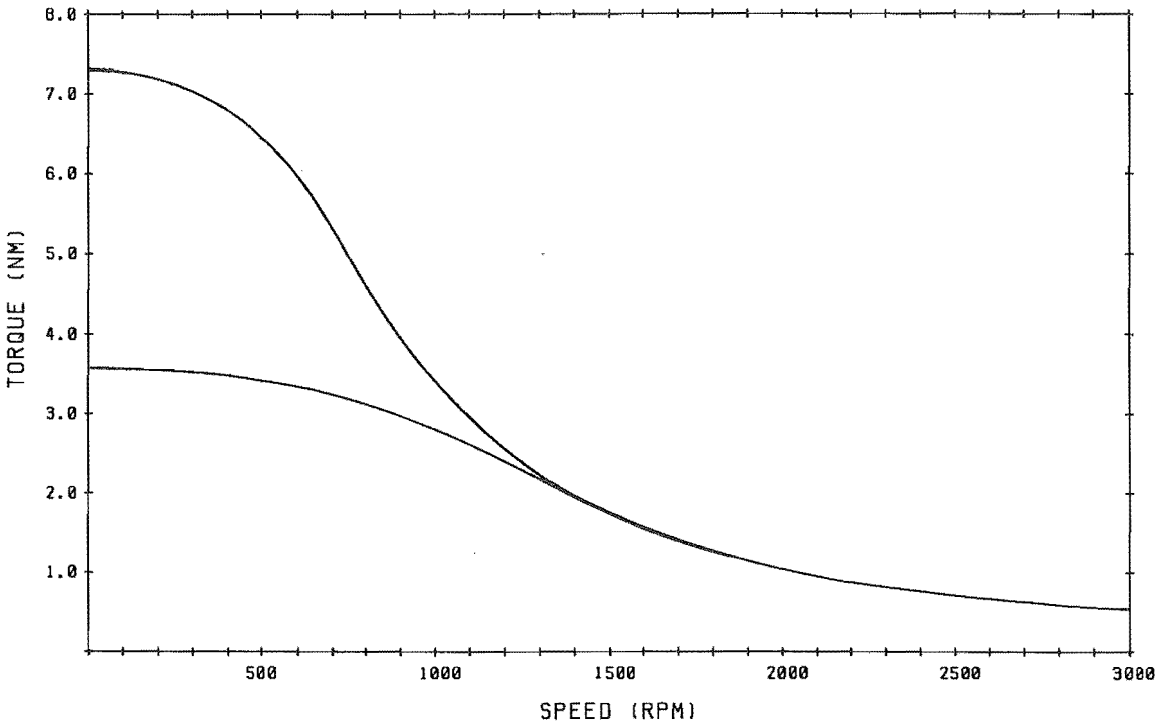
8.0
7.0
6.0
5.0
4.0
3.0
2.0
1.0
TORQUE (NM)
500
1000
1500
2000
2500
3000
SPEED (RPM)

Fig. 5.6

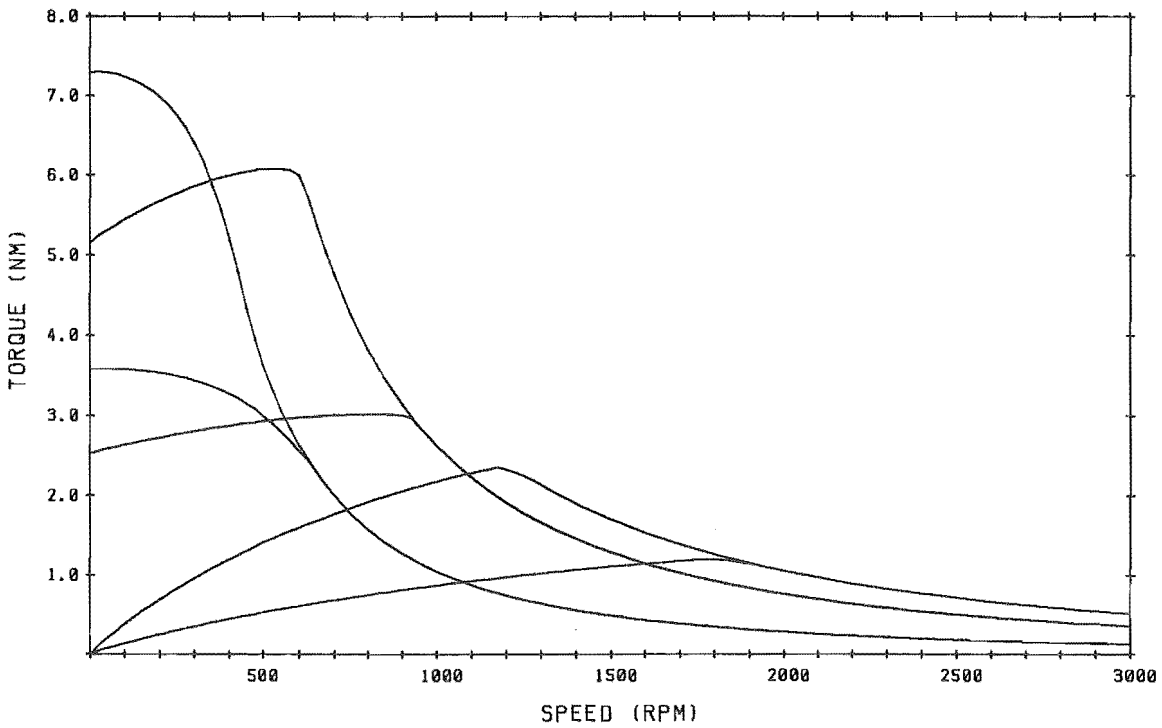
8.0
7.0
6.0
5.0
4.0
3.0
2.0
1.0
TORQUE (NM)
500
1000
1500
2000
2500
3000
SPEED (RPM)

Fig. 5.7

When comparing individual plots of the same lead angle from figures 5.4 and 5.5 it is seen that each plot shows similar characteristics to the maximum torque envelope. The speed beyond which the two plots coincide is the speed where the torque is entirely voltage limited (with respect to a 7.0 amp current limit) for that lead angle. The speed where the two plots coincide increases with increasing lead angle. This phenomenon is illustrated in figure 5.7 where for clarity only three of the seven plots in figures 5.4 and 5.5 are shown. Clearly the shift from current limit based to supply voltage based torque limiting is a progressive one.

Up to 1900 rpm the gradient of the plots are greater than in figure 5.5. These plots display particularly high gradients between 500 and 1000 rpm. The gradient is a measure of the drive system's ability to maintain constant speed. With a high gradient a small decrease in speed causes a comparatively large increase in the torque output, restoring the original speed. The analogous response occurs with small increases in speed.

Figure 5.8 is the plot obtained with a supply voltage of 240 volts and a current limit of 10 amps. As required the zero speed torque outputs are the same as for the plots of figure 5.5. However the doubling of the supply voltage significantly increases the high speed performance of the drive. The torque envelope of figure 5.8 exceeds the envelope of figure 5.5 at approximately 250 rpm. This observation illustrates the low speeds at which the motional voltage becomes important. Now only four of the seven lead angles are required to nearly maximise the torque output up to a speed of 1500 rpm. The doubling of the supply voltage has reduced the gradients of the plots and hence reduced the speed regulation of the drive system. From

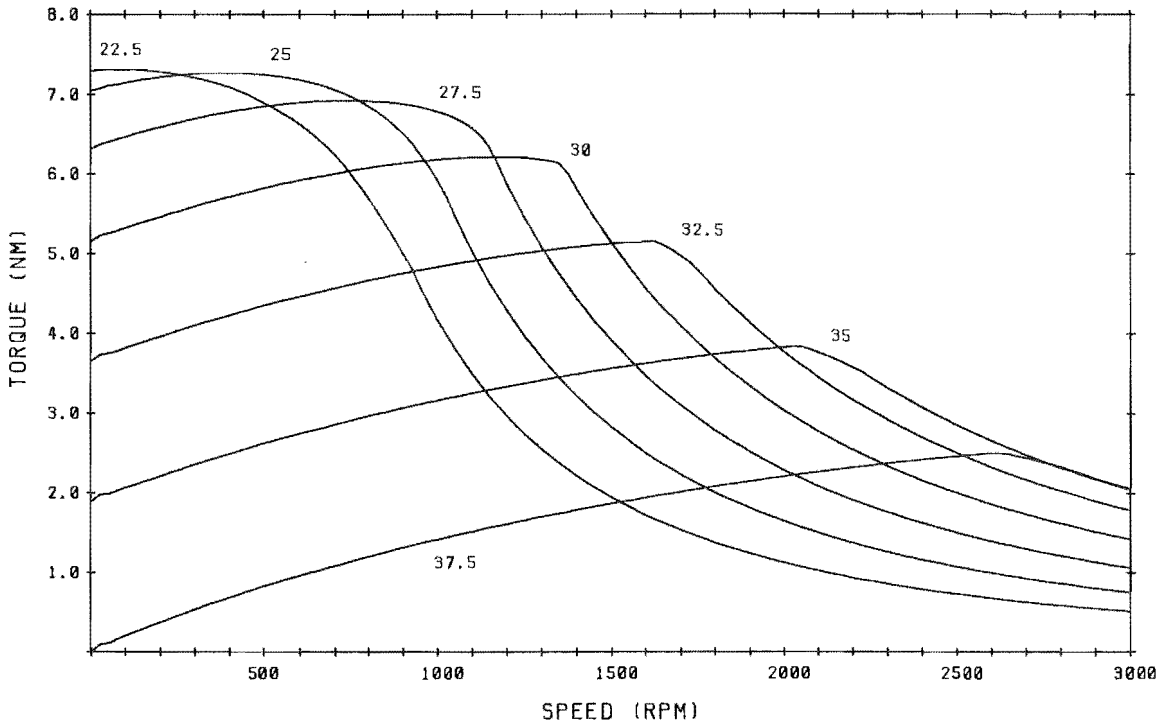
8.0
7.0
6.0
5.0
4.0
3.0
2.0
1.0
TORQUE (NM)
22.5
25
27.5
30
32.5
35
37.5
500
1000
1500
2000
2500
3000
SPEED (RPM)

Fig. 5.8

comparison of figures 5.4, 5.5 and 5.8 it appears that this ability is a function of the ratio of current limit to supply voltage.

When comparing the data plotted in figures 5.5 and 5.8, it was found that for any given lead angle, the torque plots of figure 5.8 tend towards four times those of figure 5.5 as the speed increases. This torque ratio becomes four at a speed where both plots become entirely supply voltage limited. This relationship between figures 5.5 and 5.8 holds for all seven lead angles. The motor speed at which the torque becomes four times the original increases with increasing lead angle. For the minimum lead angle of 22.5 degrees this speed is 925 rpm and for the maximum of 37.5 degrees the speed is 2775 rpm. It therefore appears that at speeds greater than or equal to the speed where the torque is entirely supply voltage limited, the torque developed is proportional to the supply voltage squared.

5.5 Comparison With The Experimental Torque Measurements.

The torque vs speed performance of the drive system as plotted in figure 4.22 has been simulated. Figure 5.9 shows the torque vs speed simulation plotted with the measured torque outputs. The operating parameters are;

lead angle: 24 degrees

supply voltage: 120 volts

current limit: 7 amps.

The torque vs speed simulation shows generally good agreement with the measured torque vs speed performance. The errors increase at the extremes of the speed range. At low speed a fall off in the measured

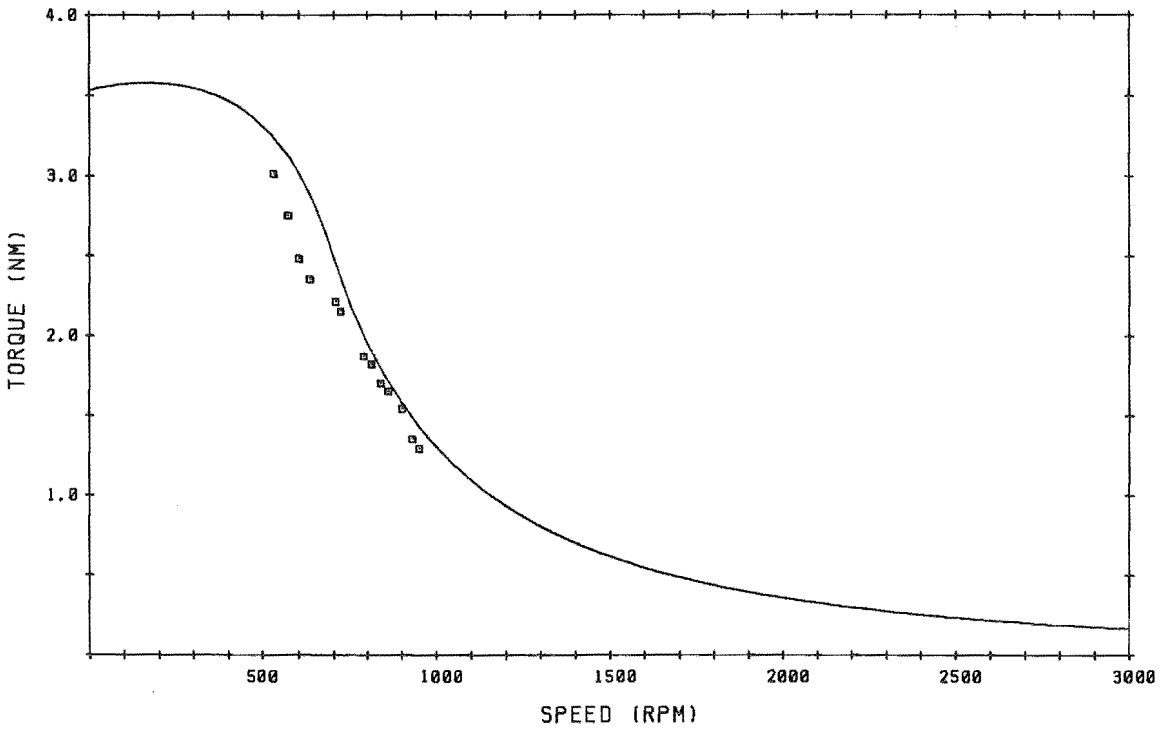

Fig. 5.9

torque output with respect to the calculated torque can be seen. This is probably caused by the increase in the effects of saturation and hysteresis which occur at lower speeds where the average phase current is typically higher. In the middle of the range the agreement is particularly good. At high speed there is another fall off in the measured torque. This is possibly the result of increasing losses through windage.

5.6 The Monitoring Current Model.

The techniques used in simulating the on phase currents are also applicable to simulating the monitoring envelopes. Linear expressions for the monitoring phase current have been derived from the general phase voltage equation 2.1. The schematic representation of the monitoring phase voltage components is shown in figure 5.10. The effect of flux linkage from the energising current in the orthogonal phase has been neglected in accordance with the observation that the most significant flux exchange occurs between the monitoring phase and the de-energising phase.

5.6.1 The Saddle Shaped Envelope.

The saddle shaped waveform occurs when there is flux leakage into the monitoring phase. Therefore the flux terms involving mutual inductances are positive.

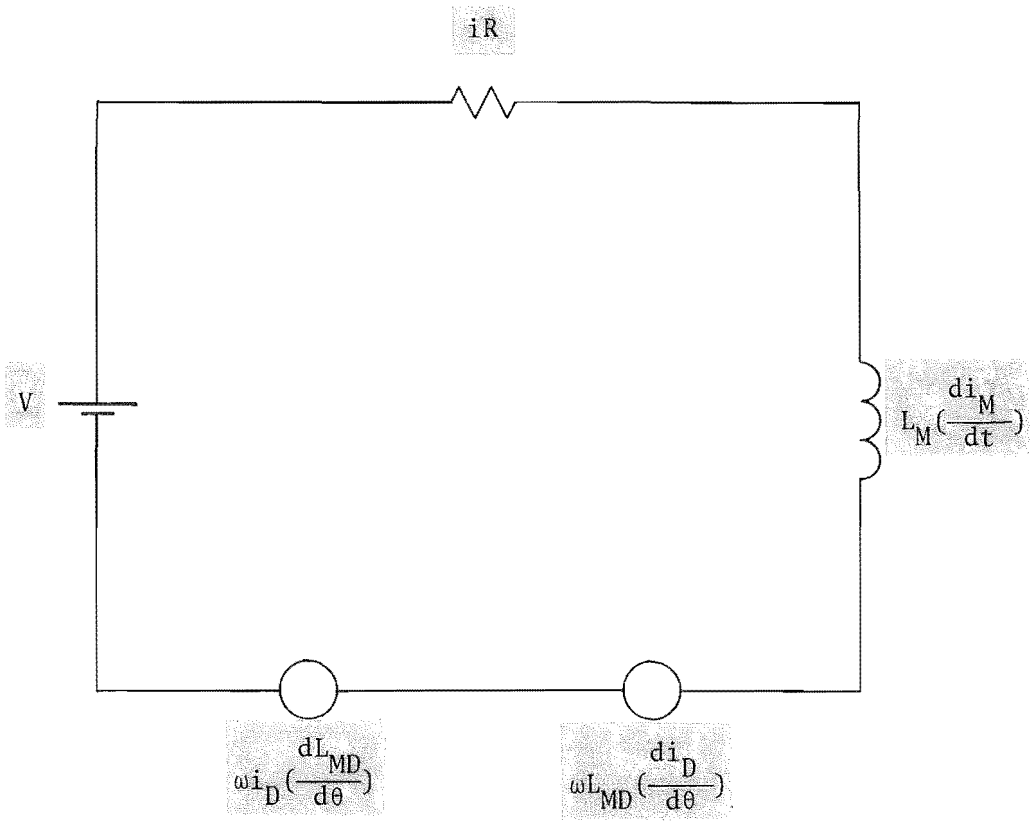

Fig 5.10 The monitoring current path.

The derived expression is,

$$\left(\frac{di_M}{d\theta}\right) = \frac{V - i_M\left(R_M + \omega\left(\frac{dL_M}{d\theta}\right)\right) + \omega\left(\frac{di_D}{d\theta}\right)L_{MD} + i_D\omega\left(\frac{dL_{MD}}{d\theta}\right)}{\omega L_M(\theta)} \quad (5.6).$$

A program VRM4 has been written to evaluate the monitoring phase current from equation 5.6. This program utilises the on phase current modelling results of VRM1. Evaluating equation 5.6 at set rotor positions requires values for the de-energising phase current and its gradient at those positions. The energising current in the on phase is calculated at set rotor positions until the end of the step. The number of intervals between adjacent set rotor positions is adjusted to meet a specified accuracy. The de-energising current and its gradient are then calculated at rotor positions of the same spacing but they are also determined at additional rotor positions where their value is required. Equation 5.6 is necessarily evaluated in piecewise fashion, as the monitoring current is actively suppressed to zero at the end of each monitoring cycle. The evaluation is performed over the angle of rotor rotation which occurs during each monitoring cycle at the specified speed.

The simulation of the solely rotor position dependant and saddle shaped envelopes are shown together in figure 5.11. Also plotted is the de-energising current simulation although not to the scale of the vertical axis. The solely rotor position dependant or ideal envelope begins at a current of 0.08 amps and rises monotonically to 0.106 amps. The gradient increases during the step in the manner observed in the measured envelopes of figure 4.17.

The saddle shaped envelope has been well reproduced by obtaining a large number of solutions to equation 5.6 over one step. As

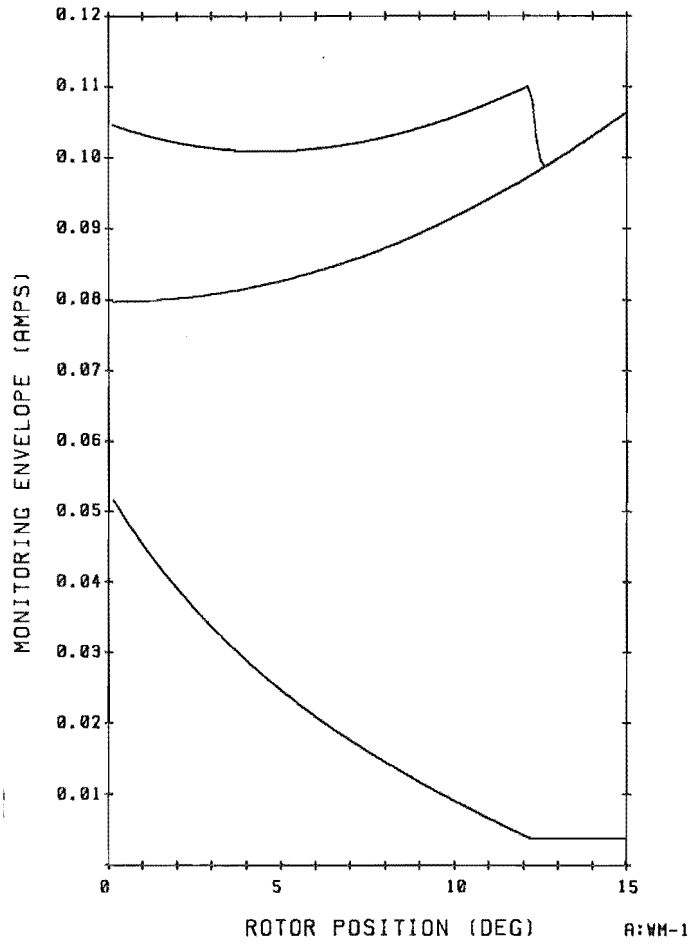
0.12
0.11
0.10
0.09
0.08
0.07
0.06
0.05
0.04
0.03
0.02
0.01
MONITORING ENVELOPE (AMPS)
0
5
10
15
ROTOR POSITION (DEG)
A:WM-1

Fig. 5.11

experimentally observed, this type of envelope is elevated with respect to the ideal envelope. The simulated envelope displays the characteristic notch observed in figure 4.22 near the end of the envelope. The simulation also conforms with the observation that the saddle shaped envelope is only elevated until the notch, after which the saddle shaped and ideal envelopes coincide.

The envelope is elevated beyond the detent level approximately four degrees in advance. The consecutive phase will therefore be energised with a lead angle this amount larger and before the de-energising current has reached zero. This effect is observed experimentally and shown in figure 4.23.

When examining the saddle shaped envelope in relation to the de-energising current it can be seen that the notch coincides with the de-energising current reaching zero. Because the interference ceases abruptly at the point of zero current, it appears the flux leakage into the monitoring phase is more dependant on the gradient of the de-energising current than the magnitude. The extent to which the saddle shaped envelope is elevated decreases as the notch is approached. However the decrease is small in relation to the large change in the de-energising current. By comparison, up to the point of zero de-energising current, the change in its gradient is small. But upon the gradient becoming zero there is a sudden reduction in interference which is the cause of the notch.

There are two terms in equation 5.6 which express the interference on the monitoring phase. These are,

$$+ \omega\left(\frac{di_D}{d\theta}\right) L_{MD} \qquad (5.7)$$

which represents the transformation induced flux leakage and,

$$+ i_D\omega\left(\frac{dL_{MD}}{d\theta}\right) \qquad (5.8)$$

which represents the motion induced flux leakage. Clearly the majority of the flux leakage and hence interference is the result of the current gradient or transformational term.

5.6.2 The Monotonic Envelope.

The monotonic envelope occurs when there is flux leakage out of the monitoring phase. A monitoring phase current expression analogous to equation 5.6 results but the flux terms envolving mutual inductances are now negative. The expression is,

$$\left(\frac{di_M}{d\theta}\right) = \frac{V - i_M\left(R_M + \omega\left(\frac{dL_M}{d\theta}\right)\right) - \omega\left(\frac{di_D}{d\theta}\right)L_{MD} - i_D\omega\left(\frac{dL_{MD}}{d\theta}\right)}{\omega L_M(\theta)} \qquad (5.9).$$

Program VRM4 was used again in the solution of equation 5.9. The simulation of the monotonic envelope is shown in figure 5.12. Also plotted are the ideal envelope and the de-energising current. The simulation displays the characteristic behaviour of the observed envelopes of figures 4.22 and 4.23. The interference causes this envelope to be "pulled down" with respect to the ideal envelope. Once again the interference decreases as the de-energising current decreases. At the point where the current and its gradient become zero there is no further interference and the envelope becomes ideal. As with the saddle shaped envelope, the most significant interfering flux

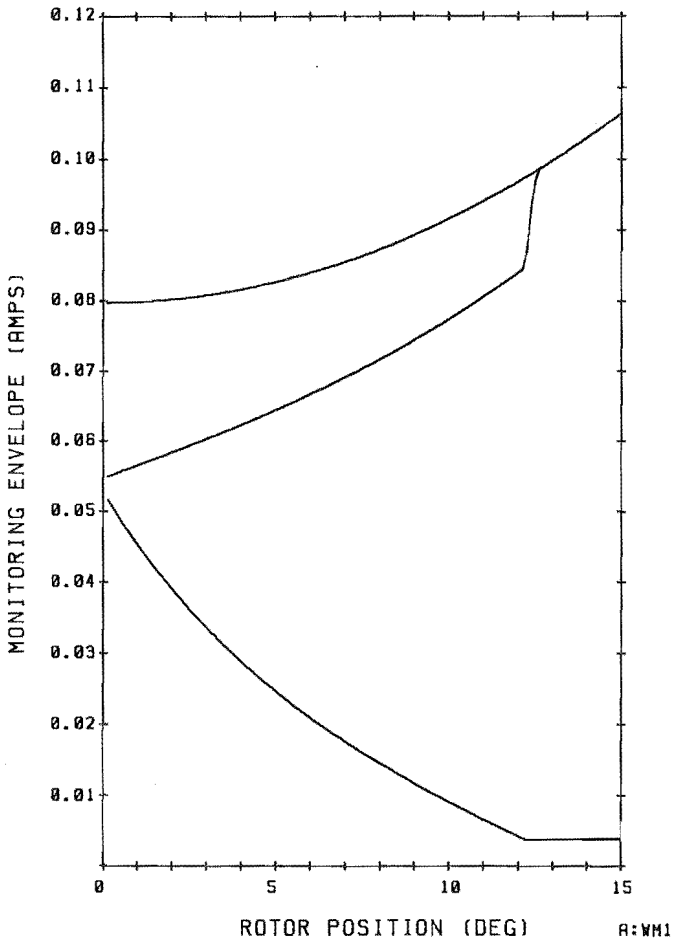
0.12
0.11
0.10
0.09
0.08
0.07
0.06
0.05
0.04
0.03
0.02
0.01
MONITORING ENVELOPE (AMPS)
0
5
10
15
ROTOR POSITION (DEG)
A:WM1

Fig. 5.12

component is the transformational one. The two terms which express the interference are the transformational term,

$$-\omega\left(\frac{di_D}{d\theta}\right)L_{MD} \tag{5.10}$$

and the motional term,

$$-i_D\omega\left(\frac{dL_{MD}}{d\theta}\right) \tag{5.11}.$$

Programs VRM1, VRM2 and VRM4 are listed in appendix B.

5.7 Summary.

The results of the simulations presented in this chapter illustrate the value of a mathematical model as a tool in analysing experimental observations. The simulations have shown that although the performance of the variable reluctance stepping motor is subject to a number of non linear effects, the performance can be simulated well with linear models.

The simulated on phase current waveforms show good agreement with the measured waveforms over most of a step. Some non linear effects are apparent in the experimental waveforms which have not been simulated. However, these effects could be incorporated empirically after being measured.

The torque vs speed performance simulation accurately predicts the measured performance. The discrepancy at the speed extremes can be plausibly explained in terms of magnetic effects at low speed and

windage losses at high speed. Inter detent torque predictions are easily performed as an extension to the on phase current simulation. Experimental measurements of this kind are dynamic and therefore difficult to make.

The nature of the monitoring waveform interference has been accurately reproduced. The source of the monitoring envelope interference was first discussed in the preceding chapter. However it was the results of the position monitoring simulation which identified the de-energising phase as the source of the interference and lead to the qualitative analysis of the effects of pole configuration.

The simulations developed have been used to explain the experimental observations in terms of governing equations set up by the author. However, the closeness of simulated and measured performances in many areas means that the programs written could used to predict performance limitations as well. It is in this area that further application of this work would prove most useful.

CHAPTER 6.

CONCLUSION.

Literature:

The first literature on achieving closed loop control of the variable reluctance stepping motor from self positional feedback was published in 1975. The algorithms in these early publications were based on the L/R drive. More recent work has revealed the improved performance of the drive which employs both chopper current limiting and active suppression. Publication of algorithms for obtaining self positional feedback with this type of drive has followed naturally.

The Development Of An Algorithm:

The advances made by this research have been explicitly directed at investigating the suitability of these position monitoring algorithms to control of the single stack motor. The research started with the further development of an algorithm published in 1985 to a more readily implemented form.

The Implementation:

Conventional drive circuits which employ both chopper current limiting and active suppression have been built and refined. Additional circuitry has been added to these drives to perform the

monitoring phase current chopping independently. The control of the drives has been performed with firmware as this provides flexibility and enables closed loop control from either the position monitoring circuitry or a position encoder. Circuitry which implements the position monitoring algorithm has been developed.

The final control system was very successful, in enabling a detailed study of the four phase single stack motor's response to the position monitoring algorithm.

The Results:

Characteristic on phase current waveforms have been obtained under closed loop control with both the position encoder and the position monitoring circuitry. However the waveforms of the position monitoring system displayed distinct aberrations from the expected or ideal waveforms. The aberrations have been conclusively linked to interference caused by the significant mutual inductance between the de-energising phase and the monitoring phase inherent in the four phase single stack motor. The nature of the interference has been explained in terms of the pole configuration within the motor.

The interference restricts the operating speed range through limiting the maximum lead angle. The position monitoring system provided consistent position detection over the limited lead angle range. The algorithm developed is capable of providing absolute inter detent positional feedback over a wide lead angle range, but only when the monitoring phase has negligible interference or linkage with external flux sources. This implies negligible mutual inductance

between the monitoring phases and other phases carrying appreciable currents. This environment is only found in the multiple stack motor.

Modelling:

Numerical simulations of the on phase current have enabled calculations of the torque output against rotor position. The results have been used in the preparation of torque vs speed plots which compare well with the measured torque outputs. From these plots it has been possible to make inferences on the performance of the system as a variable speed drive and assess the effect on the performance by varying the parameters of lead angle, supply voltage and current limit on the performance.

The monitoring phase current expressions have been derived and the results of the on phase current simulations applied to solving them. The solutions have yielded position monitoring waveform simulations which have accurately reproduced the form of the position monitoring interference. The simulations identified the relationship between the interference and the pole configuration of the motor. The relationship was subsequently observed experimentally.

Future Research:

The author believes continuation of this research in application to the three phase single stack motor may yield significant results. It is probable that the three phase single stack motor is better

suited to encoderless self synchronisation.

The three phase motor has a more favourable pole configuration as the relationship between the poles of the monitoring phase and the other phases is fixed. There is now the added complication of interference from both the on and de-energising phases. However there is the major advantage of consistency in the monitoring waveforms between phases. This leads to consistency in the point of commutation and therefore little chance of synchronisation loss at large lead angles and high speed.

The adaption of the monitoring waveform simulations to the three phase motor will provide some insight into its suitability to encoderless self synchronisation and the likely problems.

REFERENCES.

1. Acarnley P.P., Hill R.J., Hooper C.W. (1985).
"Detection or rotor position in stepping and switched motors by monitoring of current waveforms." IEEE Transactions of Industrial Electronics August 1985, vol IE-32, p215.

2. Acarnley P.P. and Gibbons P. (1982).
"Closed Loop control of stepping motors: prediction and realisation of optimum switching angle." Proc. IEE, 129, Part B, No.4

3. Cassat A. (1977).
"A high performance active suppression driver for variable reluctance step motors."
6th ann. symposium on incremental motion control systems and devices.

4. Conte S.D. and Carl de Boor.
"Elementary numerical analysis an algorithmic approach." Third edition 1980.
McGraw-Hill Kogakusha, Ltd.

5. Ferris T.A., Palombo G.A., Fortescue S.M. (1981).
"A low cost, high performance incremental motion system using a closed loop stepping motor."
Proceedings of the tenth annual symposium on incremental motion control systems and devices.

6. Hammad A.E. and Mathur R.M. (1977).
"Dynamic performance of permanent magnet stepping motors." Proc. IEE, vol. 124, no. 7. July 1977.

7. Jufer M. (1976).
"Self-synchronisation of stepping motors."
Proceedings of the international conference on stepping motors and systems, University of Leeds.

8. Jufer M. and Campiche S. (1976).
"Self-synchronisation of a one phase stepping motor by a bridge circuit of its coil." Proceedings of the international conference on stepping motors and systems, University of Leeds.

9. Kille E.J. and Klein S.M. (1980).
"A microcomputer controlled optimum sequenced stepper motor using phase-plane techniques." Proceedings of the ninth annual symposium on incremental motion control systems and devices.

10. Kuo B.C. (1979).
"Incremental motion control systems and devices. sixth annual symposium." vol. 2. SRL publishing company.

11. Rahman M.F. and Bell R. (1984).
"Loading characteristics and optimum switching conditions of multistack variable reluctance type stepping motors." IEEE transactions on industrial electronics. Vol. IE-31, no.1, Feb. 1984.

12. Taft C.K., Dietz P.S., Harned T.J. (1981).
Development of no overshoot open-loop step motor control strategies using the velocity-error plane. Proc. 10th annual symposium on incremental motion control systems and devices.

13. Taft C.K. and Gauthier R.G. (1975).
Stepping motor failure model. (1975).
IEE Transactions of industrial control instrumentation, vol 22, no. 3, August 1975.

14. Tal J. (1982).
"Optimal commutation of brushless motors."
Proceedings of the seventh annual symposium on incremental motion control systems and devices, University of Illinois.

15. Vallon B. and Jufer M. (1981).
"Microprocessor optimisation of stepping motor dynamic performance." Dept. of Electrical Engineering, Swiss Federal Institute of Technology.


INDUCTANCE b (MH) / ROTOR POSITION (DEG)
0 10 20 30 40 50 60 70
90 95 100 105 110 115 120 125 130 135 140 145 150 155 160 165 170 175 180

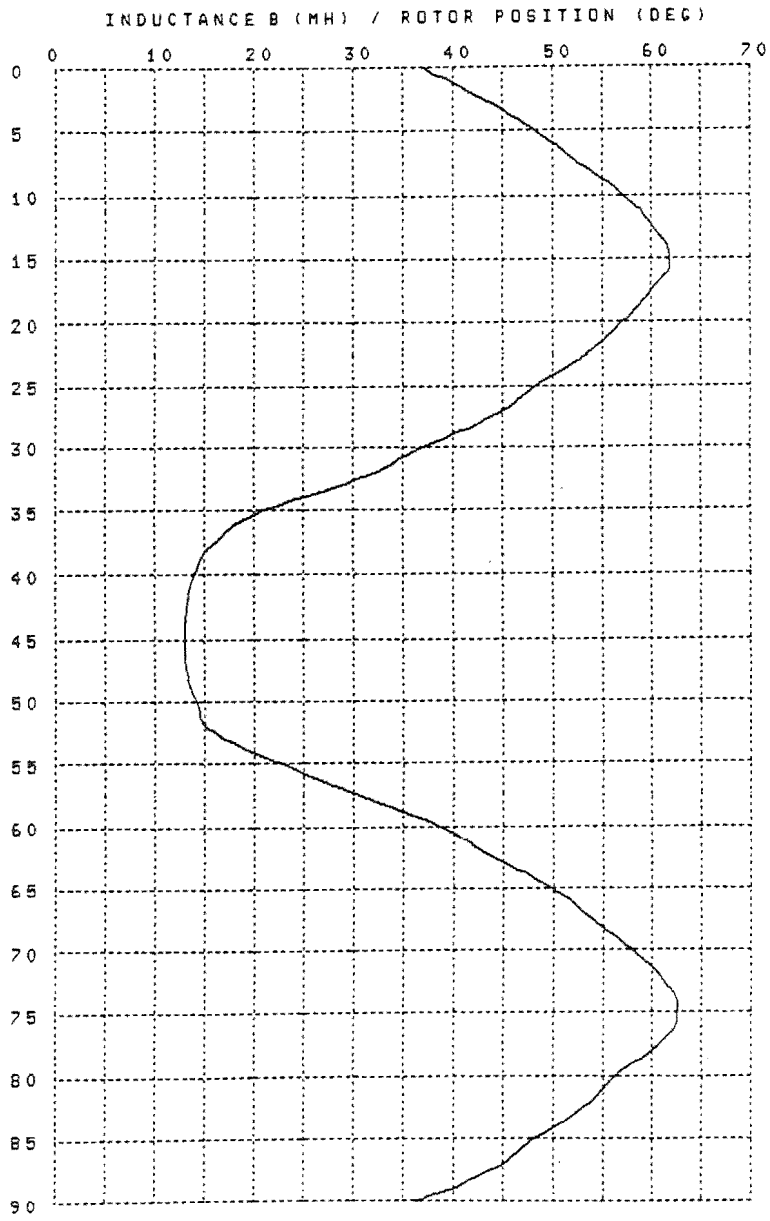
INDUCTANCE B (MH) / ROTOR POSITION (DEG)
0 10 20 30 40 50 60 70
0 5 10 15 20 25 30 35 40 45 50 55 60 65 70 75 80 85 90

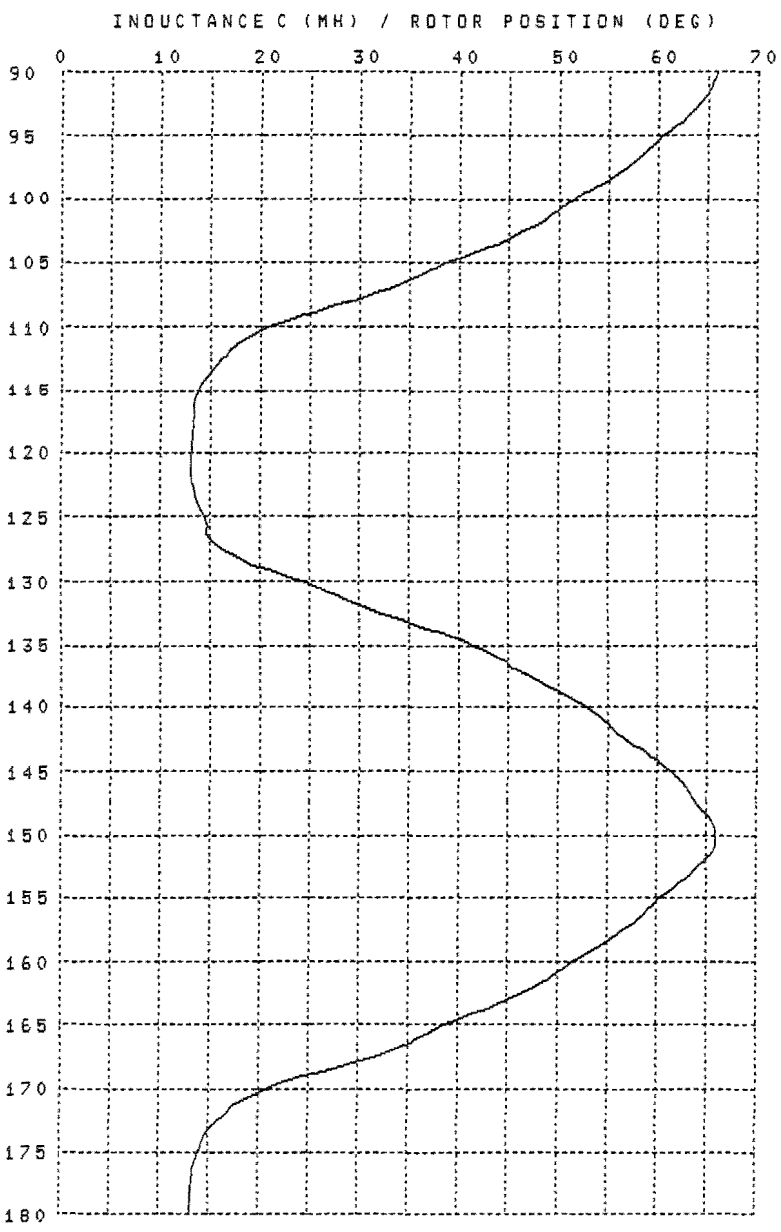
INDUCTANCE C (MH) / ROTOR POSITION (DEG)
0 10 20 30 40 50 60 70
90 95 100 105 110 115 120 125 130 135 140 145 150 155 160 165 170 175 180

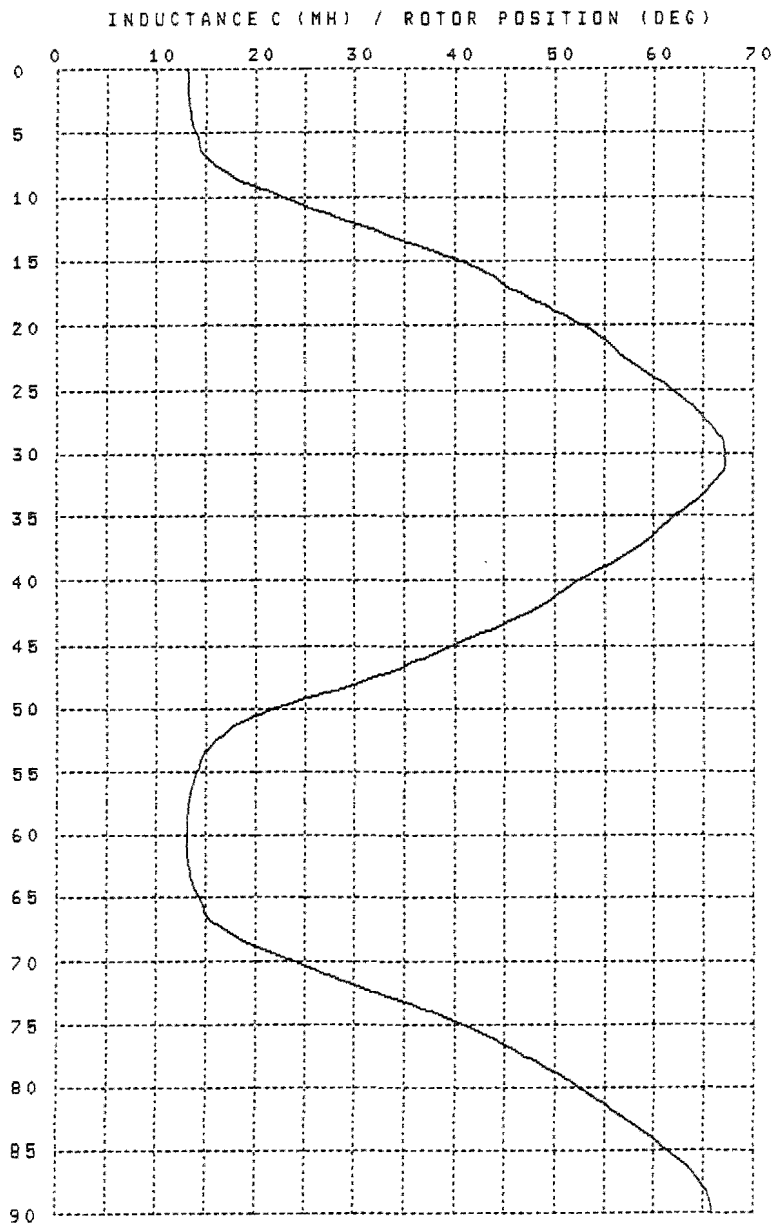
INDUCTANCE C (MH) / ROTOR POSITION (DEG)
0 10 20 30 40 50 60 70
0 5 10 15 20 25 30 35 40 45 50 55 60 65 70 75 80 85 90

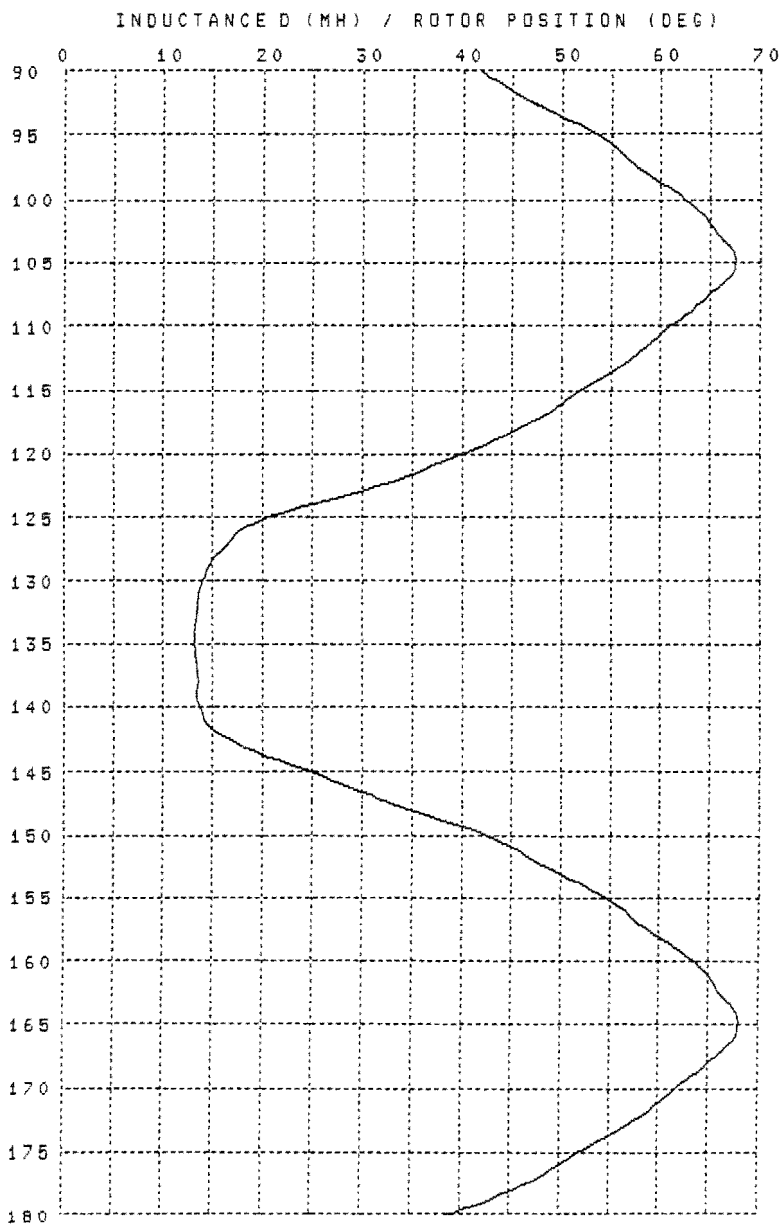
INDUCTANCE D (MH) / ROTOR POSITION (DEG)
0 10 20 30 40 50 60 70
90 95 100 105 110 115 120 125 130 135 140 145 150 155 160 165 170 175 180

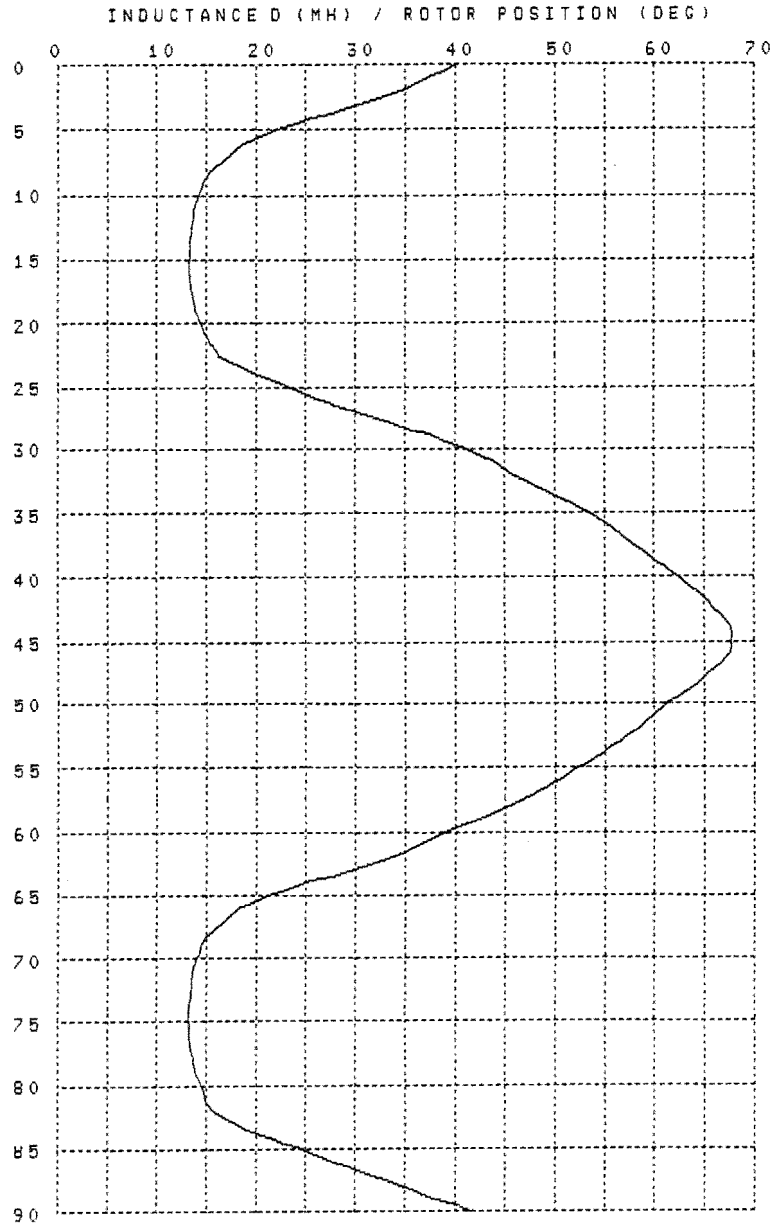
INDUCTANCE D (MH) / ROTOR POSITION (DEG)
0 10 20 30 40 50 60 70
0 5 10 15 20 25 30 35 40 45 50 55 60 65 70 75 80 85 90

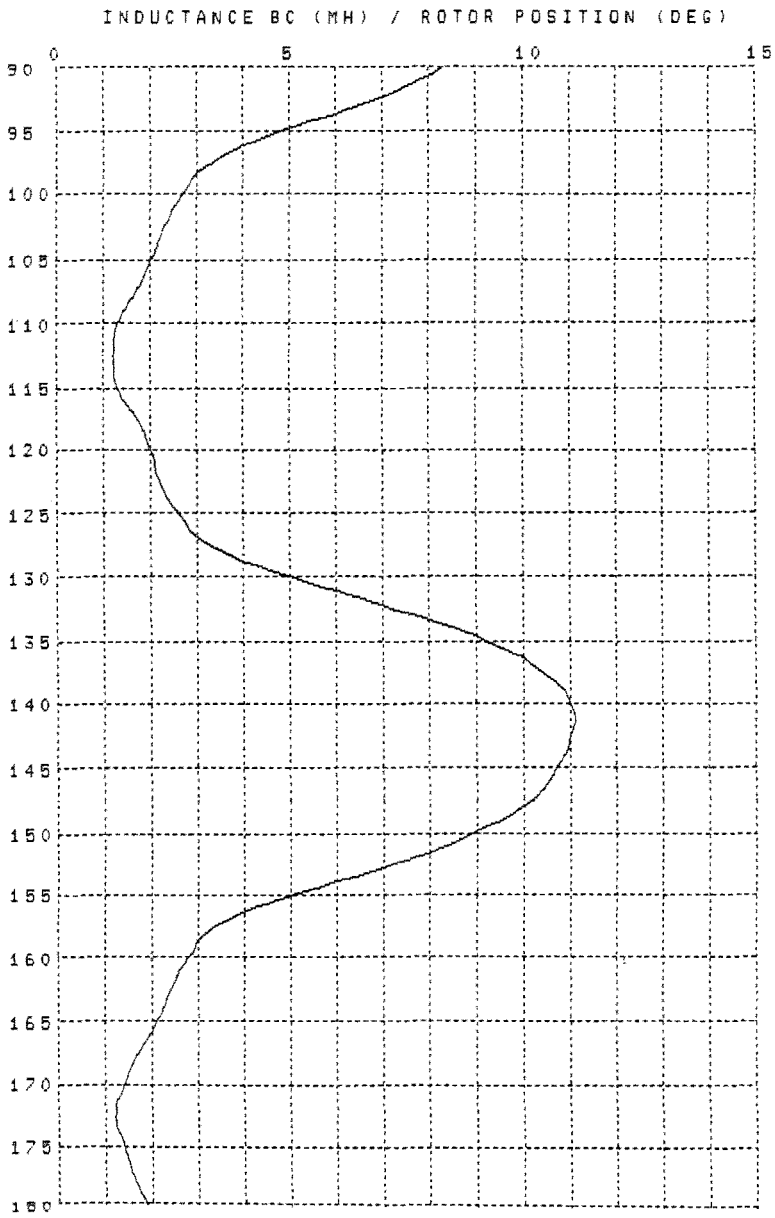
INDUCTANCE BC (MH) / ROTOR POSITION (DEG)
0
5
10
15
90
95
100
105
110
115
120
125
130
135
140
145
150
155
160
165
170
175
180

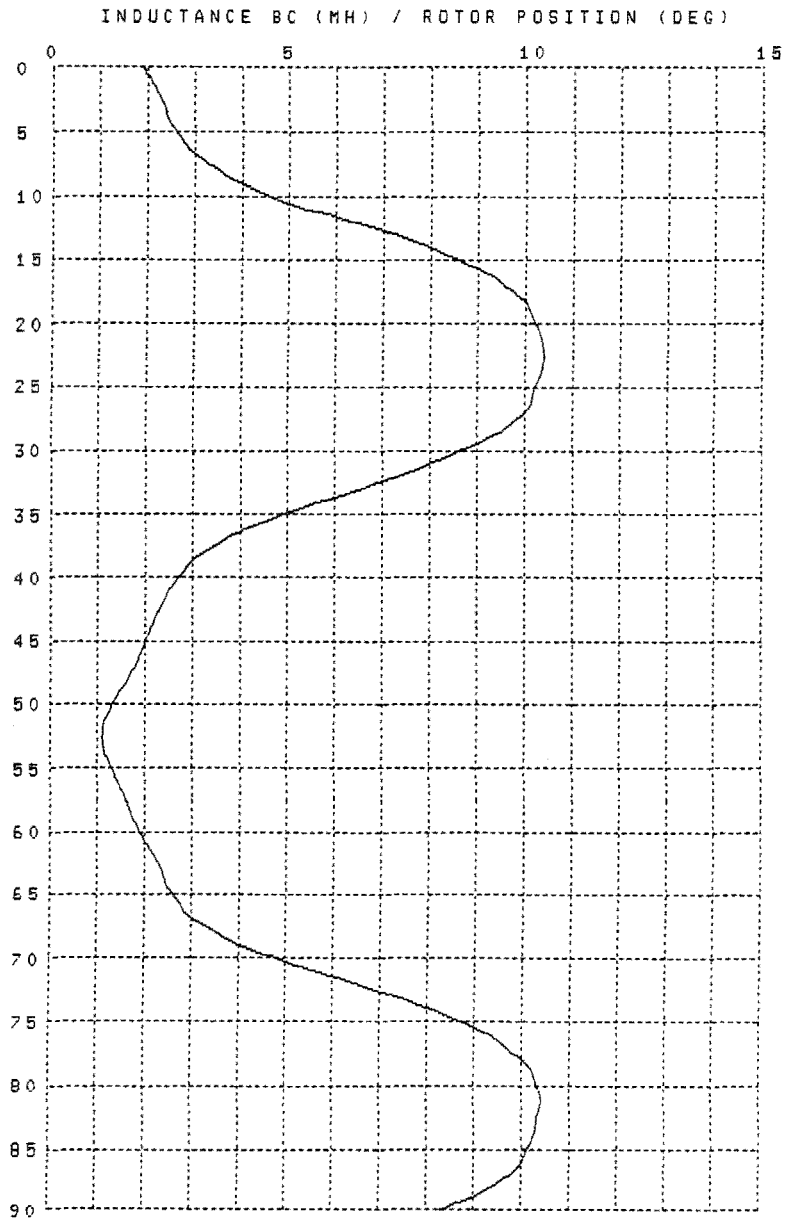
INDUCTANCE BC (MH) / ROTOR POSITION (DEG)
0
5
10
15
0
5
10
15
20
25
30
35
40
45
50
55
60
65
70
75
80
85
90

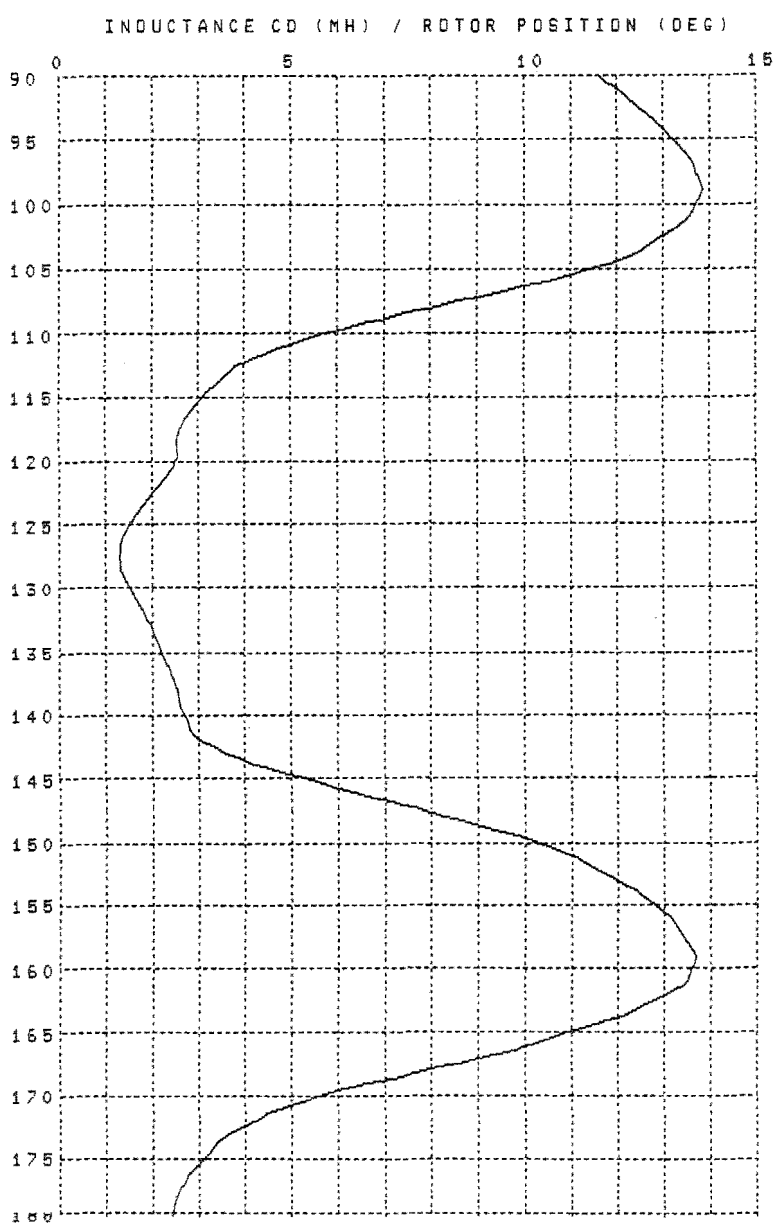
INDUCTANCE CD (MH) / ROTOR POSITION (DEG)
0
5
10
15
90
95
100
105
110
115
120
125
130
135
140
145
150
155
160
165
170
175

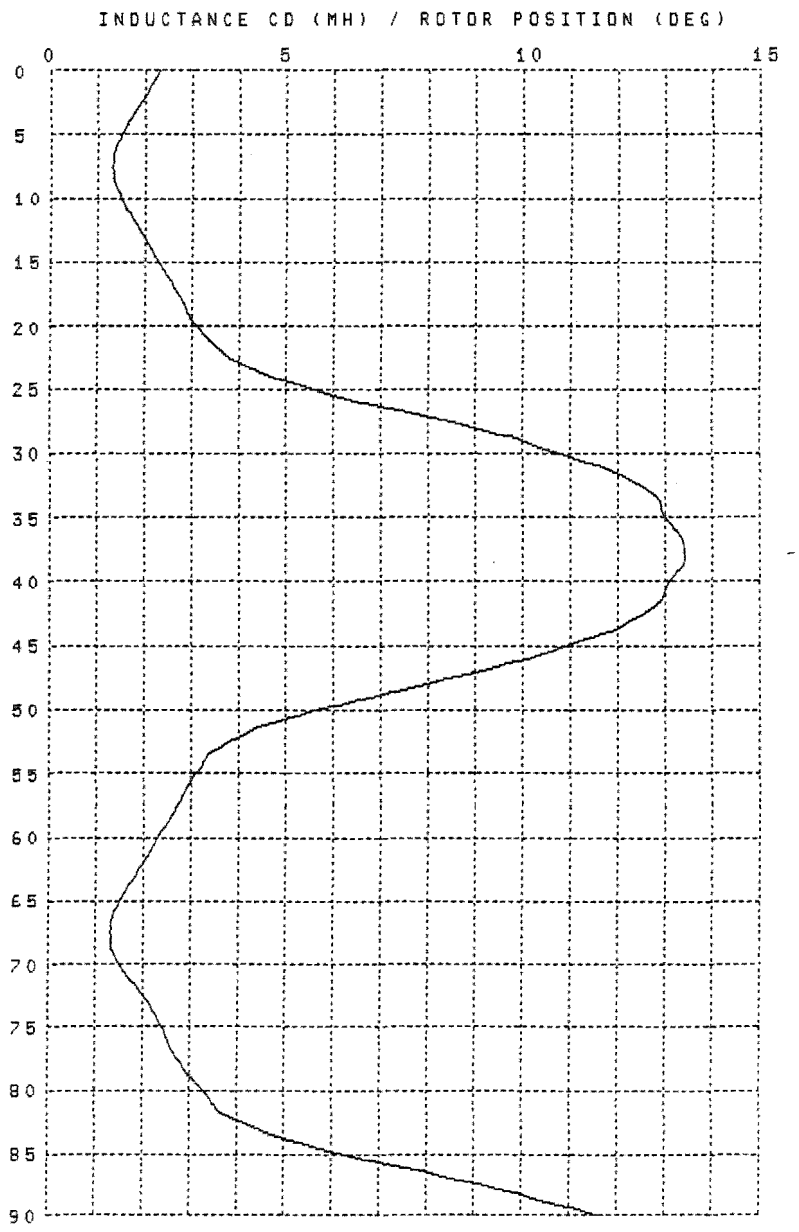
INDUCTANCE CD (MH) / ROTOR POSITION (DEG)
0
5
10
15
0
5
10
15
20
25
30
35
40
45
50
55
60
65
70
75
80
85
90

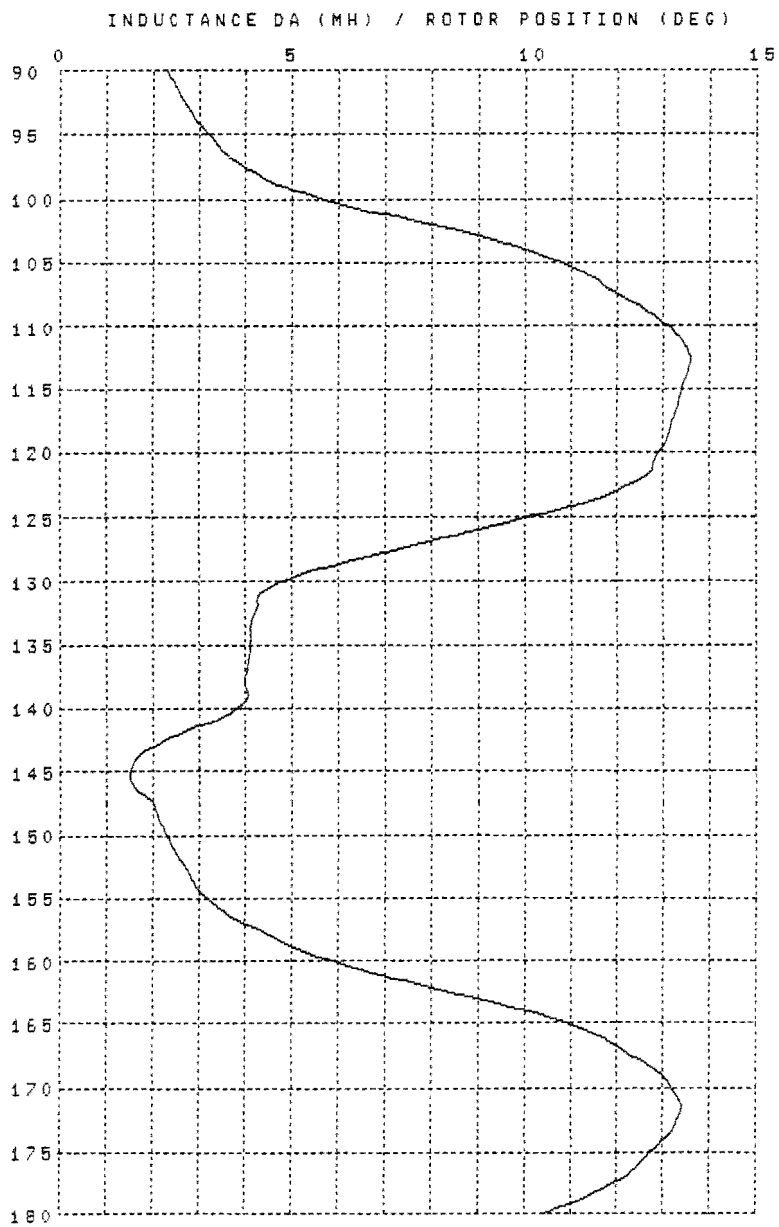
INDUCTANCE DA (MH) / ROTOR POSITION (DEG)
0
5
10
15
90
95
100
105
110
115
120
125
130
135
140
145
150
155
160
165
170
175
180

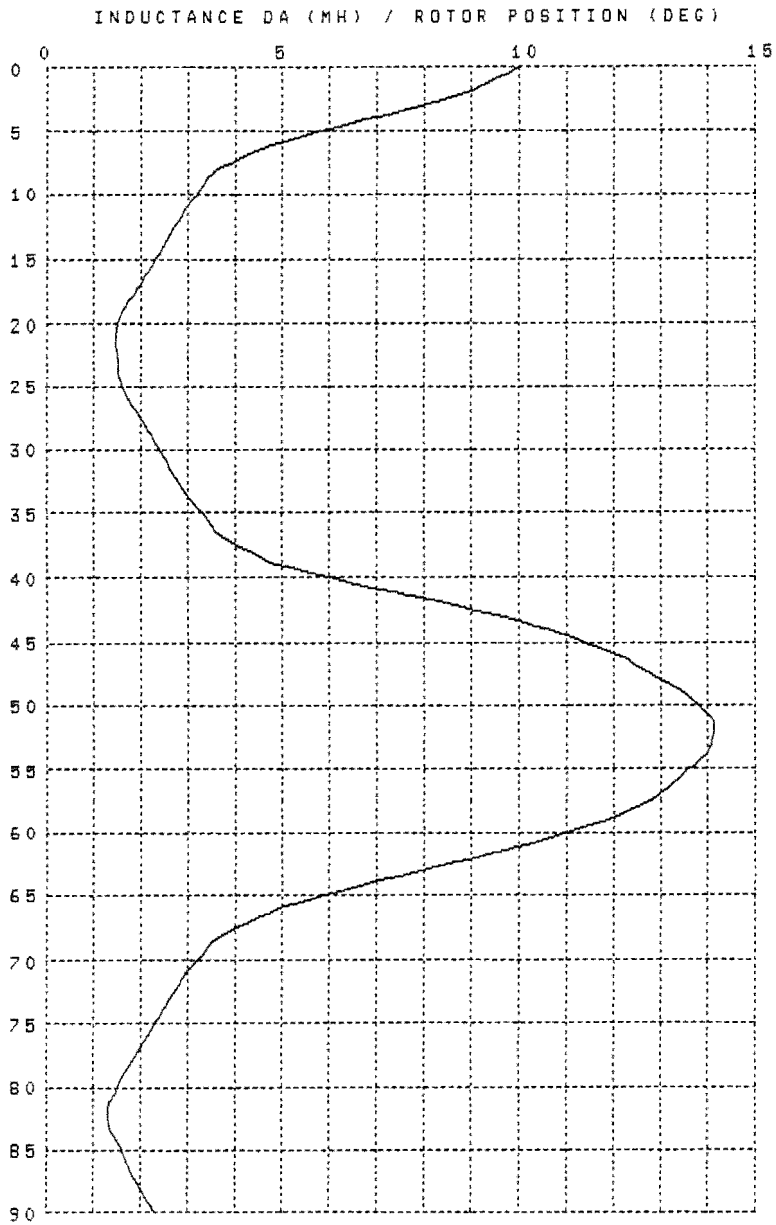
INDUCTANCE DA (MH) / ROTOR POSITION (DEG)
0
5
10
15
0
5
10
15
20
25
30
35
40
45
50
55
60
65
70
75
80
85
90

APPENDIX B.

```
C      ------------    PROGRAM VRM1    ------------
C
C      THIS PROGRAM USES THE FORTH ORDER RUNGE-KUTTA METHOD
C      IN EVALUATING THE ENERGISING AND THEN DE-ENERGISING CURRENTS.
C      THE CURRENT VALUES ARE THEN USED TO CALCULATE THE TORQUE.
C      OUTPUT TO SCREEN IS THE POSITION (RADS), THE PHASE CURRENT
C      (AMPS) AND TORQUE (NM). OUTPUT TO DISK IS THE INTERVAL NO.,
C      POSITION (RADS), PHASE CURRENT (AMPS) AND TORQUE (NM).
C
       PROGRAM VRM1
C
       REAL*8  LA,K1,K2,K3,K4,X,E,Y,Z,A,ER,F,H,XO,C,S
       COMMON VS, R
       DIMENSION Y(2)
       INTEGER*4 SPEED,G,M
C
       WRITE (6,15) 'NO. OF STEPS '
       READ (5,10) M
       WRITE (1,35) 'NO. OF STEPS ',M
       WRITE (6,15) 'SPEED '
       READ (5,10) SPEED
       WRITE (1,35) 'SPEED ',SPEED
       WRITE (6,15) 'SUPPLY VOLTAGE '
       READ (5,25) VS
       WRITE (1,40) 'SUPPLY VOLTAGE ',VS
       WRITE (6,15) 'CURRENT LIMIT '
       READ (5,25) CL
       WRITE (1,40) 'CURRENT LIMIT ',CL
       WRITE (6,15) 'SERIES RESISTANCE'
       READ (5,25) R
       WRITE (1,40) 'SERIES RESISTANCE',R
       WRITE (6,15) 'LEAD ANGLE (DEG) '
       READ (5,25) LA
       WRITE (1,40) 'LEAD ANGLE ',LA
C      WRITE (1,45)
  10   FORMAT (I4)
  15   FORMAT (A18)
  25   FORMAT (F6.1)
  35   FORMAT (A16, I4)
  40   FORMAT (A18, F6.1)
C 45   FORMAT (/,T3,'POSITION',T19,'CURRENT',T35,'TORQUE')
       DATA N,PI,K1,K2,K3,K4,X,E/16,3.141592653,6*0.0/
C
       H=PI/M/N
C      Set interval length.
       Y(1)=0.0
       Y(2)=0.0
       Z=0.0
       TQ=0.0
       TQS=0.0
       WK=0.0
       E=0.0
       K=0
       S=SPEED*PI/5.0
C      Lead angle phase sift.
```

```
      C=(LA-15.0)/30.0*PI
      WRITE (1,85) 0, 0.0, 0.0, 0.0
C
C     G=0 : energisation  G=1 : de-energisation
      DO 200 G=0,1
C
        DO 300 J=0,M/2-1,1
 800    CONTINUE
C
C         K=2 for double interval.
          DO 400 K=1,2
C
C           4th order Runge-Kutta routine.
            DO 500 I=0,N/K-1,1
            XO=E + PI*J/M + I*K*H
C
            A=Y(K)
            X=XO
            IF (G.EQ.0) CALL RISE (A, S, X, C, F)
            IF (G.EQ.1) CALL FALL (A, S, X, C, F)
            K1=H*K*F
C
            A=Y(K)+0.5*K1
            X=XO+0.5*K*H
            IF (G.EQ.0) CALL RISE (A, S, X, C, F)
            IF (G.EQ.1) CALL FALL (A, S, X, C, F)
            K2=H*K*F
C
            A=Y(K)+0.5*K2
            IF (G.EQ.0) CALL RISE (A, S, X, C, F)
            IF (G.EQ.1) CALL FALL (A, S, X, C, F)
            K3=H*K*F
C
            A=Y(K)+K3
            X=XO+H*K
            IF (G.EQ.0) CALL RISE (A, S, X, C, F)
            IF (G.EQ.1) CALL FALL (A, S, X, C, F)
            K4=H*K*F
C
            Y(K)=Y(K) + (K1 + 2.0*K2 + 2.0*K3 + K4)/6.0
C
 500        CONTINUE
C
 400      CONTINUE
C
C       Half interval error control.
        ER=ABS(Y(1)-Y(2))/7.5/H
C
        IF (ER .GT. 0.0001 .AND. N .LT. 33 .AND. Y(1) .LT. CL) THEN
        N=N*2
        H=H/2.0
C       Restore last current value and return.
        Y(1)=Z
        Y(2)=Z
        GOTO 800
```

```
C
        ELSEIF (ER .LT. 0.000005 .AND. N .GT. 3) THEN
        N=N/2
        H=H*2.0
C
        ENDIF
C
        IF (Y(1) .GT. 0.0 .AND. Y(1) .LT. CL) THEN
        YL=Y(1)
C
        ELSEIF (Y(1) .LE. 0.0) THEN
        YL=0.0
        F=0.0
C
        ELSE
        YL=CL
        F=0.0
C
        ENDIF
C
        TQ=0.081*COS(X-C)*YL*YL
C       Work value available.
C       WK=WK+TQ*PI/M
C       Sum torque over en and de-en steps.
        TQS=TQS+TQ
C
        WRITE (6,80) X, YL, TQ
        WRITE (1,85) (J + G*M/2 + 1), X, YL, TQ
 80     FORMAT ( 3(F10.4, 5X) )
 85     FORMAT ( I4, 5X, 3(F10.4, 5X) )
        Z=Y(1)
        Y(2)=Y(1)
C
 300    CONTINUE
      E=X
      Y(1)=YL
      Y(2)=YL
      Z=YL
 200  CONTINUE
C     evaluate mean torque
      WRITE (6,90) SPEED, TQS/M*2.0
 90   FORMAT (I5,1X,F10.7)
      END
C
C
C
      SUBROUTINE RISE (A, S, X, C, F)
      REAL*8  L,V,F,S,A,X,C
      COMMON VS, R
      V=VS-A*(R+S*0.027*COS(X-C))
      L=0.040 + 0.027*SIN(X-C)
      F=V/L/S
      RETURN
      END
C
```

```
C
C
      SUBROUTINE FALL (A, S, X, C, F)
      REAL*8  L,V,F,S,A,X,C
      COMMON VS, R
      V=-(VS+A*(R+S*0.027*COS(X-C)))
      L=0.040 + 0.027*SIN(X-C)
      F=V/L/S
      RETURN
      END
```

```
C     ----------------    PROGRAM VRM2    ----------------
C
C     VRM2 SIMULATES THE DRIVEN PHASE CURRENT WITH MUTUAL
C     EFFECTS INCLUDED. PERFORMED IN TWO PASSES WITH INITIAL
C     PASS CALCULATING THE MUTUAL FREE CURRENT. SECOND PASS
C     ADDS THE MUTUAL EFFECTS.
C
      PROGRAM VR2
C
      REAL*8  LA,K1,K2,K3,K4,X,E,Y,Z,A,ER,F,H,XO,C,CD,S,FR,YLR
     *       FF,YLF,FRV,YLRV,FFV,YLFV
      COMMON VS, S, X, C
      DIMENSION Y(2), FR(200), YLR(200), FF(200), YLF(200)
      INTEGER*4 SPEED,G,M
C
      WRITE (6,15) 'NO. OF STEPS '
      READ (5,10) M
      WRITE (1,35) 'NO. OF STEPS ',M
      WRITE (6,15) 'SPEED '
      READ (5,10) SPEED
      WRITE (1,35) 'SPEED ',SPEED
      WRITE (6,15) 'SUPPLY VOLTAGE '
      READ (5,25) VS
      WRITE (1,40) 'SUPPLY VOLTAGE ',VS
      WRITE (6,15) 'CURRENT LIMIT '
      READ (5,25) CL
      WRITE (1,40) 'CURRENT LIMIT ',CL
      WRITE (6,15) 'LEAD ANGLE (DEG) '
      READ (5,25) LA
      WRITE (1,40) 'LEAD ANGLE ',LA
      WRITE (6,15) 'MUTUAL TYPES '
      READ (5,30) KA, KB, KC, KD
      WRITE (1,45) KA, KB, KC, KD
      WRITE (1,50)
 10   FORMAT (I4)
 15   FORMAT (A18)
 25   FORMAT (F6.1)
 30   FORMAT ( 4(I2,1X) )
 35   FORMAT (A16, I4)
 40   FORMAT (A16, F6.1)
 45   FORMAT (1X,'KA=',I2,3X,'KB=',I2,3X,'KC=',I2,3X,'KD=',I2)
 50   FORMAT (/,T3,'POSITION',T19,'CURRENT',T35,'TORQUE')
C
      DATA N,PI,K1,K2,K3,K4,E/16,3.141592653,5*0.0/
C     Set interval length
      H=PI/M/N
      Y(1)=0.0
      Y(2)=0.0
      Z=0.0
      TQ=0.0
      TQS=0.0
      WK=0.0
      K=0
      S=SPEED*PI/5.0
C     Lead angle phase shift.
```

```
      C=(LA-15.0)/30.0*PI
C
C     first pass simulation with 0 coupling when MTL=0.
C     second pass simulation adds mutual terms to first
C     pass simulation.
      DO 100 MTL=0,1
C     G=0 : energisation  G=1 : de-energisation
      DO 200 G=0,1
C     phase shift for mutual inductance.
      CD=C - PI/4.0 + G*PI/2.0
C
        DO 300 J=0,M/2-1,1
C       Include mutual terms on 2nd pass (MTL =1)
        FRV=MTL*FR(J)
        YLRV=MTL*YLR(J)
        FFV=MTL*FF(J)
        YLFV=MTL*YLF(J)
 800    CONTINUE
C
C       K=2 for double interval.
        DO 400 K=1,2
C
C         4th order Runge-Kutta routine.
          DO 500 I=0,N/K-1,1
          XO=G*PI/2.0 + PI*J/M + I*K*H
          A=Y(K)
          X=XO
          IF (G.EQ.0) CALL RISE (KA, KB, A, CD, FFV, YLFV, F)
          IF (G.EQ.1) CALL FALL (KC, KD, A, CD, FRV, YLRV, F)
          K1=H*K*F
C
          A=Y(K)+0.5*K1
          X=XO+0.5*K*H
          IF (G.EQ.0) CALL RISE (KA, KB, A, CD, FFV, YLFV, F)
          IF (G.EQ.1) CALL FALL (KC, KD, A, CD, FRV, YLRV, F)
          K2=H*K*F
C
          A=Y(K)+0.5*K2
          IF (G.EQ.0) CALL RISE (KA, KB, A, CD, FFV, YLFV, F)
          IF (G.EQ.1) CALL FALL (KC, KD, A, CD, FRV, YLRV, F)
          K3=H*K*F
C
          A=Y(K)+K3
          X=XO+H*K
          IF (G.EQ.0) CALL RISE (KA, KB, A, CD, FFV, YLFV, F)
          IF (G.EQ.1) CALL FALL (KC, KD, A, CD, FRV, YLRV, F)
          K4=H*K*F
          Y(K)=Y(K) + (K1 + 2.0*K2 + 2.0*K3 + K4)/6.0
 500      CONTINUE
C
 400    CONTINUE
C
C       Half interval error control.
        ER=ABS(Y(1)-Y(2))/7.5/H
C
```

```
        IF (ER .GT. 0.00005 .AND. N .LT. 33) THEN
        N=N*2
        H=H/2.0
        Y(1)=Z
        Y(2)=Z
        GOTO 800
C
        ELSEIF (ER .LT. 0.000001 .AND. N .GT. 3) THEN
        N=N/2
        H=H*2.0
C
        ENDIF
C
        IF (Y(1) .GT. 0.0 .AND. Y(1) .LT. CL) THEN
        YL=Y(1)
C
        ELSEIF (Y(1) .LE. 0.0) THEN
        YL=0.0
C
        ELSE
        YL=CL
C
        ENDIF
C
C       Store first pass energisation currents and gradients.
        IF (MTL .EQ. 0 .AND. G .EQ. 0) THEN
        FR(J+1)=F
        YLR(J+1)=YL
C
C       Store first pass de-energisation currents and grad's.
        ELSEIF (MTL .EQ. 0 .AND. G .EQ. 1) THEN
        FF(J+1)=F
        YLF(J+1)=YL
C
        ENDIF
C
C       Calculate torque.
        TQ=0.081*COS(X-C)*YL*YL
        WRITE (6,80) X, YL, TQ, N
        WRITE (1,85) X, YL, TQ
 80     FORMAT ( 3(F10.4, 5X), I3 )
 85     FORMAT ( 3(F10.4, 5X) )
        Z=Y(1)
        Y(2)=Y(1)
 300    CONTINUE
C
      Y(1)=YL
      Y(2)=YL
      Z=YL
 200  CONTINUE
 100  CONTINUE
      END
C
C
C
```

```
      SUBROUTINE RISE (KA, KB, A, CD, FFV, YLFV, F)
      REAL*8  L,V,F,FFV,YLFV,S,A,X,C,CD
      COMMON VS, S, X, C
      V=VS - A*( 3.0 + S*0.027*COS(X-C) )
     *     +KA*FFV*S*( 0.012 + 0.010*SIN(X-CD) )
     *     +KB*YLFV*0.010*S*COS(X-CD)
      L=0.040 + 0.027*SIN(X-C)
      F=V/L/S
      RETURN
      END
C
C
C
      SUBROUTINE FALL (KC, KD, A, CD, FRV, YLRV, F)
      REAL*8  L,V,F,FRV,YLRV,S,A,X,C,CD
      COMMON VS, S, X, C
      V=-( VS + A*( 3.0 + S*0.027*COS(X-C) ) )
     *  +KC*FRV*S*( 0.012 + 0.010*SIN(X-CD) )
     *  +KD*YLRV*0.010*S*COS(X-CD)
      L=0.040 + 0.027*SIN(X-C)
      F=V/L/S
      RETURN
      END
```

```
C      ----------------   PROGRAM VRM4   ----------------
C
C      VRM4 SIMULATES THE MONITORING PHASE CURRENT WAVEFORM.
C      THE DRIVEN PHASE CURRENT IS SIMULATED OVER ONE STEP
C      THEN DE-ENERGISATION IS ENFORCED. THE MUTUAL EFFETS
C      BETWEEN MONITORING AND DE-ENERGISING FLUXES ARE
C      INCLUDED IN THE ANALYSIS.
C
       REAL*8  LA,K1,K2,K3,K4,X,Y,YL,Z,A,ER,FD,FM,H,X0,C,S
       REAL*8  HD,HM,B,BC,XT,YLT
       DIMENSION  Y(2)
       INTEGER*4  SPEED, G, M
C
       WRITE (6,15) 'NO. OF STEPS '
       READ (5,10) M
       WRITE (6,15) 'SPEED '
       READ (5,10) SPEED
       WRITE (6,15) 'SUPPLY VOLTAGE '
       READ (5,25) VS
       WRITE (6,15) 'CURRENT LIMIT '
       READ (5,25) CL
       WRITE (6,15) 'LEAD ANGLE (DEG) '
       READ (5,25) LA
C      FD TYPE is -1, 0 or 1. It expresses the polarity of flux
C      leakage gradient.
       WRITE (6,15) 'FD TYPE '
       READ (5,10) KFD
C      YL TYPE is -1, 0 or 1. It expresses the polarity of flux
C      leakage.
       WRITE (6,15) 'YL TYPE '
       READ (5,10) KYL
       WRITE (1,30) 'VS=', VS, 'CL=', CL, 'LA=', LA
       WRITE (1,40) 'FD TYPE = ', KFD, 'YL TYPE = ', KYL
 10    FORMAT (I4)
 15    FORMAT (A18)
 25    FORMAT (F6.1)
 30    FORMAT (A4, F6.1, 1X, A4, F6.1, 1X, A4, F6.1)
 40    FORMAT (A10,I4, 5X, A10, I4)
C
       DATA NDT,NM,PI,K1,K2,K3,K4,X,FD,FM/2*16,
      * 3.141592653,7*0.0/
       Z=0.0
       K=0
       S=SPEED*PI/5.0
C      set interval for drive current evaluation.
       HD=PI/M
C      set interval for monitoring current evaluation.
       HM=0.00006*S
C      set phase angles between self and mutual inductances.
       B=(LA-30.0)/30.0*PI
       C=(LA-15.0)/30.0*PI
       BC=(LA-22.5)/30.0*PI
       ML=M/2-1
       WRITE (6,35) 'SPEED =', SPEED, 'LEAD ANGLE =', LA
 35    FORMAT (/, A18, 1X, I5, 5X, A12, 1X, F5.2)
```

```
C
C       G=0 : energisation  G=1 : de-energisation.
        DO 100 G=0,1
C
C       next drive current evaluation point.
        H=HD - G*HM
          DO 200 J=0,ML
C         set interval for energisation then de-energisation.
          ND=NDT
          CALL DRIVE (G, X, H, S, C, ND, CL, VS, FD, YL)
          NDT=ND
          IF (G .EQ. 0) GOTO 200
C
  500       CONTINUE
C           DO 300 K=1,2
            K=1
            ND=8
C           scale interval down for NM steps.
C           divide by 2 for 4th order Runge-Kutta half interval
            H=HM*K/NM/2.0
C
              DO 400 I=0,NM/K-1,1
              A=Y(K)
              CALL MON (VS, A, S, X, B, BC, YL, FD, KFD, KYL, FM)
              K1=HM/NM*K*FM
C
C             second half interval starts here.
              CALL DRIVE (G, X, H, S, C, ND, CL, VS, FD, YL)
              A=Y(K)+0.5*K1
              CALL MON (VS, A, S, X, B, BC, YL, FD, KFD, KYL, FM)
              K2=HM/NM*K*FM
C
              A=Y(K)+0.5*K2
              CALL MON (VS, A, S, X, B, BC, YL, FD, KFD, KYL, FM)
              K3=HM/NM*K*FM
C
              CALL DRIVE (G, X, H, S, C, ND, CL, VS, FD, YL)
              A=Y(K)+K3
              CALL MON (VS, A, S, X, B, BC, YL, FD, KFD, KYL, FM)
              K4=HM/NM*K*FM
C
              Y(K)=Y(K) + (K1 + 2.0*K2 + 2.0*K3 + K4)/6.0
C
  400         CONTINUE
C 300       CONTINUE
C
C         ER=ABS( Y(1) - Y(2) )/7.5/HM*NM
C
C         IF (ER .GT. 0.001 .AND. NM .LT. 33) THEN
C         Y(1)=0.0
C         Y(2)=0.0
C         NM=NM*2
C         GOTO 500
C
C         ELSEIF (ER .LT. 0.00005 .AND. NM .GT. 3) THEN
```

```
C          NM=NM/2
C
C          ENDIF
C
           Z=Y(1)
           Y(1)=0.0
C          Y(2)=0.0
C
           IF (G .EQ. 1) THEN
           WRITE (1,65) (G*M/2 + J + 1), X, YL, Z
  65       FORMAT ( I4, 5X, 2(F10.6, 5X), F10.7 )
           WRITE (6,60) X, YL, FD, Z
  60       FORMAT ( 3(F10.6, 5X), F10.7)
           ENDIF
C
 200       CONTINUE
C
 100     CONTINUE
       END
C
C      ************************************************************
C
       SUBROUTINE DRIVE (G, X, H, S, C, ND, CL, VS, FD, YL)
       DIMENSION Y(2)
       INTEGER G
       REAL*8  K1, K2, K3, K4, X, Y, YL, H
       REAL*8  A, S, XD, C, FD, ER, HD, Z
 600   CONTINUE
       HD=H/ND
       DO 700 K=1,2
C
         DO 800 I=0,ND/K-1
         XD=X + I*K*HD
         A=Y(K)
         IF (G.EQ.0) CALL RISE (A, XD, S, C, VS, FD)
         IF (G.EQ.1) CALL FALL (A, XD, S, C, VS, FD)
         K1=HD*K*FD
C
         A=Y(K)+0.5*K1
         XD=X + (I + 0.5)*K*HD
         IF (G.EQ.0) CALL RISE (A, XD, S, C, VS, FD)
         IF (G.EQ.1) CALL FALL (A, XD, S, C, VS, FD)
         K2=HD*K*FD
C
         A=Y(K)+0.5*K2
         IF (G.EQ.0) CALL RISE (A, XD, S, C, VS, FD)
         IF (G.EQ.1) CALL FALL (A, XD, S, C, VS, FD)
         K3=HD*K*FD
C
         A=Y(K)+K3
         XD=X + (I + 1.0)*K*HD
         IF (G.EQ.0) CALL RISE (A, XD, S, C, VS, FD)
         IF (G.EQ.1) CALL FALL (A, XD, S, C, VS, FD)
         K4=HD*K*FD
C
```

```
        Y(K)=Y(K) + (K1 + 2.0*K2 + 2.0*K3 + K4)/6.0
C
 800    CONTINUE
 700  CONTINUE
C
      ER=ABS( Y(1) - Y(2) )/7.5/HD
C
      IF (ER .GT. 1.0E-8 .AND. ND .LT. 33) THEN
      ND=ND*2
      Y(1)=Z
      Y(2)=Z
      GOTO 600
C
      ELSEIF (ER .LT. 5.0E-10 .AND. ND .GT. 3) THEN
      ND=ND/2
C
      ENDIF
C
      IF (Y(1) .GT. 0.0 .AND. Y(1) .LT. CL) THEN
      YL=Y(1)
      Z=Y(1)
C
      ELSEIF (Y(1) .LE. 0.0) THEN
      YL=0.0
      FD=0.0
      Z=Y(1)
C
      ELSEIF (G .EQ. 1 .AND. Y(1) .GE. CL) THEN
      Z=CL
C
      ELSE
      YL=CL
      FD=0.0
      Z=Y(1)
C
      ENDIF
C
      Y(2)=Y(1)
      X=XD
C
      RETURN
      END
C
C     ************************************************************
C
      SUBROUTINE RISE (A, XD, S, C, VS, FD)
      REAL*8  L, V, A, XD, S, C, FD
      V=VS - A*( 3.0 + S*0.027*COS(XD-C) )
      L=0.040 + 0.027*SIN(XD-C)
      FD=V/L/S
      RETURN
      END
C
C     ************************************************************
C
```

```
      SUBROUTINE FALL (A, XD, S, C, VS, FD)
      REAL*8  L, V, A, XD, S, C, FD
      V=-( VS + A*( 3.0 + S*0.027*COS(XD-C) ) )
      L=0.040 + 0.027*SIN(XD-C)
      FD=V/L/S
      RETURN
      END
C
C     ************************************************************
C
      SUBROUTINE MON (VS, A, S, X, B, BC, YL, FD, KFD, KYL, FM)
      REAL*8  L, V, A, X, S, B, BC, YL, FD, FM
      V=VS - A*( 888.0 + S*0.025*COS(X-B) )
     * + KFD*FD*S*( 0.005 + 0.004*SIN(X-BC) )
     * + KYL*YL*0.004*S*COS(X-BC)
      L=0.035 + 0.025*SIN(X-B)
      FM=V/L/S
      RETURN
      END
```

APPENDIX C.

```
SET NO DOUBLE
10    REM  ------------------    PROGRAM DECODE    ------------------------
20    REM
30    REM  PROGRAM TO DECODE ENCODER OUTPUTS FROM 15 DEGREE EQUISPACED
40    REM  SENSORS.
50    REM    MOTOR4 GENERATES THE 4-BIT PATTERN REQUIRED TO SEQUENTIALLY
60    REM  SELECT EACH OF THE 4 PHASES FOR MOTOR DRIVING.THE OUTPUT BITPAT

70    REM  ALSO INCLUDES AN ERROR BIT WHICH INDICATES ERRONEOUS INPUT
80    REM  FROM THE OPTICAL ENCODER TO FACILITATE CORRECT COUPLING.
90    REM  3 FURTHER BITS FORM A  BCD  POINTER WHICH POINTS TO THE
100   REM  1 OF 8 CORRECT 4-BIT PATTERNS OUTPUT BY THE OPTICAL ENCODER.
110   REM  THE OTHER 8 4-BIT PATTERNS POSSIBLE FROM THE ENCODER ARE
120   REM  ERRONEOUS AND FORCE THE ERROR BIT HIGH.THE 4-BIT PATTERN
130   REM  USED TO SELECT PHASES IS IN THE LOW NIBBLE AND CALLED LNIB.
140   REM  THE ERROR AND POINTER BITS FORM THE HIGH NIBBLE CALLED HNIB.
150   REM  LNIB AND HNIB ARE ADDED TO FORM A BYTE WHICH IS STORED IN
160   REM  "TEMP" FOR LOADING INTO A 2732 4K EPROM.MANUAL PHASE SELECTION
170   REM  "LOCK" IS PROVIDED WHICH OVERRIDES THE ENCODER.A "COAST" INPUT
180   REM  IS PROVIDED TO SWITCH ALL PHASES OFF AND OVERRIDES ALL ELSE.
190   REM  THE LEAD ANGLE CAN BE ALTERED IN 8 STEPS CORRESPONDING TO
200   REM  INCREMENTS BETWEEN ADJACENT ENCODER OUTPUT STATES BY ROTATING
210   REM  THE 8 LNIB BITPATS WITH RESPECT TO THE 8 PERMISSABLE ENCODER
220   REM  OUTPUTS.
230   REM
240   REM  LNIB FROM D3 TO D0 , ERROR BIT D4 , POINTER FROM D5 TO D7
250   REM  ENCODER INPUT A3 TO A0 , SWITCHING ANGLE SELECT A4 TO A7
260   REM  PHASE LOCKING A8 TO A11 , COAST A12.
270   REM
280   OPEN 'TEMP' FOR OUTPUT AS FILE #1
290   PRINT #1,'MOTOR4 OUTPUT 25-1-86'
300   PRINT #1,4%
310   COUNT%=0%
320   REM
330   REM    SET UP BIT PATTERNS.
340   REM
350   DIM L(7)
360   L(0)=14%\L(1)=14%\L(2)=13%\L(3)=13%
370   L(4)=11%\L(5)=11%\L(6)=7%\L(7)=7%
380   REM
390   REM    SET UP BINARY ADDRESSES.
400   REM
410   FOR COAST%=0% TO 1%
420   FOR LOCK4%=0% TO 1%
430   FOR LOCK3%=0% TO 1%
440   FOR LOCK2%=0% TO 1%
450   FOR LOCK1%=0% TO 1%
460   FOR INJECT%=0% TO 7%
470   FOR ENCODE%=0% TO 15%
480   LNIB%=15%
490   POINTER%=0%
500   HNIB%=128%
510   REM
520   REM    LOGICAL EXPRESSION IN TERMS OF ADDRESSES.
530   REM
540   IF ENCODE%=3% THEN POINTER%=3%\HNIB%=48%\ GOTO 620
```

```
550  IF ENCODE%=6% THEN POINTER%=5%\HNIB%=80%\ GOTO 620
560  IF ENCODE%=7% THEN POINTER%=4%\HNIB%=64%\ GOTO 620
570  IF ENCODE%=9% THEN POINTER%=1%\HNIB%=16%\ GOTO 620
580  IF ENCODE%=11% THEN POINTER%=2%\HNIB%=32%\ GOTO 620
590  IF ENCODE%=12% THEN POINTER%=7%\HNIB%=112%\ GOTO 620
600  IF ENCODE%=13% THEN POINTER%=0%\HNIB%=0%\ GOTO 620
610  IF ENCODE%=14% THEN POINTER%=6%\HNIB%=96% ELSE 650
620  LET SUM%=POINTER%+INJECT%
630  IF SUM%>7% THEN SUM%=SUM%-8%
640  LNIB%=L(SUM%)
650  IF COUNT%>255% THEN LNIB%=15%
660  IF LOCK1%=1% THEN LNIB%=14%
670  IF LOCK2%=1% THEN LNIB%=LNIB%-2%
680  IF LOCK3%=1% THEN LNIB%=LNIB%-4%
690  IF LOCK4%=1% THEN LNIB%=LNIB%-8%
700  IF COAST%=1% THEN LNIB%=15%
710  DATA%=HNIB%+LNIB%
720  PRINT #1,DATA%
730  COUNT%=COUNT%+1%
740  NEXT ENCODE%
750  NEXT INJECT%
760  NEXT LOCK1%
770  NEXT LOCK2%
780  NEXT LOCK3%
790  NEXT LOCK4%
800  NEXT COAST%
810  CLOSE #1
820  END
```

```
SET NO DOUBLE
10   REM  ------------  PROGRAM SHIFT  ------------
20   REM
30   REM   THIS PROGRAM GENERATES THE DATA FOR THE CONTROL OF
40   REM   THE Q2 MOSFETS OF THE CHOPPER DRIVES FROM THE FOUR
50   REM   LEAST SIGNIFICANT BITS. THE NEXT TWO BITS REPRESENT
60   REM   THE OUTPUTS TO THE Q2 IN BINARY FORM.
70   REM
80   OPEN "SHIFT" FOR OUTPUT AS FILE #1
90   PRINT #1,"OUTPUT FROM SHIFT 7/3/86"
100  PRINT #1,4
110  REM
120  REM   SET UP BIT PATTERNS.
130  REM
140  A(0)=14\A(1)=29\A(2)=43\A(3)=55\A(4)=14
150  REM
160  REM   SET UP BINARY ADDRESSES.
170  REM
180  FOR A6=0 TO 1
190  FOR A5=0 TO 1
200  FOR A4=0 TO 1
210  FOR A3=0 TO 1
220  FOR A2=0 TO 1
230  FOR A1=0 TO 1
240  FOR A0=0 TO 1
250  REM
260  REM   LOGICAL EXPRESSION IN TERMS OF ADDRESSES.
270  REM
280  A=A(4*A6)*((1-A1)*(1-A0)*(1-A2)+A2)*(1-A3)*(1-A4)*(1-A5)
290  B=A(1+2*A6)*((1-A1)*A0*(1-A3)+A3)*(1-A2)*(1-A4)*(1-A5)
300  C=A(2)*(A1*(1-A0)*(1-A4)+A4)*(1-A2)*(1-A3)*(1-A5)
310  D=A(3-2*A6)*(A1*A0*(1-A5)+A5)*(1-A2)*(1-A3)*(1-A4)
320  SUM=A+B+C+D
330  IF SUM=0 THEN BYTE=(15+16*(2*A1-4*A1*A6-2*A0*A6+3*A6+A0)) ELSE BYTE=S
UM
340  PRINT #1,BYTE
350  NEXT A0
360  NEXT A1
370  NEXT A2
380  NEXT A3
390  NEXT A4
400  NEXT A5
410  NEXT A6
420  FOR I=1 TO 992
430  FOR J=0 TO 3
440  PRINT #1,15+16*J
450  NEXT J
460  NEXT I
470  CLOSE #1
480  END
```

```
SET NO DOUBLE
10    REM    ------------    PROGRAM CHOP    ------------
20    REM
30    REM    THIS PROGRAM GENERATES THE DATA FOR THE SWITCHING
40    REM    OF THE Q1 AND Q3 MOSFETS FOR BOTH DRIVING AND
50    REM    POSITION MONITORING. THE FOUR LEAST SIGNIFICANT
60    REM    BITS CONTROL THE Q1 AND THE FOUR MSB CONTROL THE
70    REM    Q3.
80    REM
90    OPEN "CHOP" FOR OUTPUT AS FILE #1
100   PRINT #1,"OUTPUT FROM CHOP FOR DRIVE AND MONITORING"
110   PRINT #1,4
120   REM
130   REM    SET UP BIT PATTERNS.
140   REM
150   DIM A(6)\ DIM B(6)\ DIM HNIB(6)\ DIM L(6)
160   FOR I=0 TO 5
170   A(I)=0\B(I)=0\HNIB(I)=240
180   NEXT I
190   L(0)=208\L(1)=176\L(2)=112\L(3)=224\L(4)=208\L(5)=176
200   M(0)=2\M(1)=4\M(2)=8\M(3)=1\M(4)=2\M(5)=4
210   D(0)=1\D(1)=2\D(2)=4\D(3)=8
220   REM
230   REM    SET UP BINARY ADDRESSES.
240   REM
250   FOR A7=0 TO 1
260   FOR A6=0 TO 1
270   FOR A5=0 TO 1
280   FOR A4=0 TO 1
290   REM
300   REM    SET UP HIGH NIBBLE (4 MSB) FOR Q3 CONTROL.
310   REM
320   HNIB(0)=L(1-A4+A5)\HNIB(1)=L(2-A4+A5)
330   HNIB(2)=L(3-A4+A5)\HNIB(3)=L(4-A4+A5)
340   REM
350   REM    SET UP POINTER FOR SHIFT LEFT / SHIFT RIGHT
360   REM
370   A(0)=M(1-A4+A5)\A(1)=M(2-A4+A5)
380   A(2)=M(3-A4+A5)\A(3)=M(4-A4+A5)
390   REM
400   REM    COMPLETE ADDRESSING.
410   REM
420   FOR A3=0 TO 1
430   FOR A2=0 TO 1
440   FOR I=0 TO 3
450   REM
460   REM    LOGICAL EXPRESSION IN TERMS OF ADDRESSES.
470   REM
480   BYTE=(A3*A6+A7*(1-A6))*(HNIB(I)+A(I))+A2*D(I)
490   BYTE=BYTE+(A6*(1-A3)+(1-A6)*(1-A7))*240
500   PRINT #1,BYTE
510   NEXT I
520   NEXT A2
530   NEXT A3
540   NEXT A4
550   NEXT A5
```

```
560    NEXT A6
570    NEXT A7
580    FOR I=1 TO 16
590    FOR J=0 TO 1
600    FOR K=0 TO 31
610    FOR L=1 TO 4
620    PRINT #1,(L(L)+M(L)-240)*J+240
630    NEXT L
640    NEXT K
650    NEXT J
660    NEXT I
670    CLOSE #1
680    END
```

APPENDIX D.

```
SET NO DOUBLE
1       REM  ------------  PROGRAM GRAPH4B  -----------------
2       REM
3       REM  GRAPH4B PLOTS CURVES ON A CARTESIAN PLANE OF Y-AXIS
4       REM  0 TO 70 AND X-AXIS 90 TO 180.THE PLOT IS DISTRIBUTED
5       REM  OVER 3 SCREENS (THE X-AXIS BEING VERTICLE) TO INCREASE
6       REM  RESOLUTION.
7       REM
10      PRINT "WHICH DATA TO BE PLOTTED"
20      INPUT DATA$
30      PRINT "ENTER N TO BLOCK PRINT-OUT"
40      INPUT OUT$
50      OPEN DATA$ FOR INPUT AS FILE #1
60      DIM X(17)\ DIM Y(17)
70      CLEAR
80      SET VIEWPORT 0,1,0,.625
82      REM
84      REM ******* FIRST SCREEN *******
86      REM
90      SET WINDOW -72,7,147.5,182.5
100     SET LINE STYLE 4
110     FOR I=180 TO 150 STEP -5
120     PLOT (-70,I),(0,I)
130     SET POSITION (7,I-2)
140     SET TEXT ANGLE 4
150     GRAPHIC PRINT I
160     SET TEXT ANGLE 0
170     NEXT I
180     FOR I=0 TO 70 STEP 5
190     PLOT (-I,180),(-I,147.5)
200     NEXT I
210     FOR K=13 TO 0 STEP -1
220     INPUT #1,X(K)\ INPUT #1,B\Y(K)=-B
230     NEXT K
240     SET LINE STYLE 1
250     PLOT CURVE (Y(),X(),14,0)
260     IF OUT$="N" GOTO 280
270     PRINTSCREEN
280     SET LINE STYLE 4
290     CLEAR
292     REM
294     REM ******* SECOND SCREEN *******
296     REM
300     SET WINDOW -72,7,112.5,147.5
310     FOR I=145 TO 115 STEP -5
320     PLOT (-70,I),(0,I)
330     SET POSITION (7,I-2)
340     SET TEXT ANGLE 4
350     GRAPHIC PRINT I
360     SET TEXT ANGLE 0
370     NEXT I
380     FOR I=0 TO 70 STEP 5
390     PLOT (-I,147.5),(-I,112.5)
400     NEXT I
410     X(14)=X(0)\Y(14)=Y(0)
420     FOR K=13 TO 0 STEP -1
```

```
430     INPUT #1,X(K)\ INPUT #1,B\Y(K)=-B
440     NEXT K
450     SET LINE STYLE 1
460     PLOT CURVE (Y(),X(),15,0)
470     IF OUT$="N" GOTO 490
480     PRINTSCREEN
490     SET LINE STYLE 4
500     CLEAR
502     REM
504     REM ******* THIRD SCREEN *******
506     REM
510     SET WINDOW -72,7,77.5,112.5
520     FOR I=110 TO 90 STEP -5
530     PLOT (-70,I),(0,I)
540     SET POSITION (7,I-2)
550     SET TEXT ANGLE 4
560     GRAPHIC PRINT I
570     SET TEXT ANGLE 0
580     NEXT I
590     FOR I=0 TO 70 STEP 5
600     PLOT (-I,112.5),(-I,90)
610     NEXT I
620     SET TEXT ANGLE 4
630     FOR I=0 TO 70 STEP 10
640     SET POSITION (-I+2.4,86.75)
650     GRAPHIC PRINT I
660     NEXT I
670     SET TEXT ANGLE 0
680     X(9)=X(0)\Y(9)=Y(0)
690     FOR K=8 TO 0 STEP -1
700     INPUT #1,X(K)\ INPUT #1,B\Y(K)=-B
710     NEXT K
720     SET LINE STYLE 1
730     PLOT CURVE (Y(),X(),10,0)
740     SET POSITION (-5,84)
750     SET TEXT ANGLE 4
760     GRAPHIC PRINT "INDUCTANCE"
770     SET POSITION (-21.5,84)
780     GRAPHIC PRINT DATA$
790     SET POSITION (-24,84)
800     GRAPHIC PRINT "(MH) / ROTOR POSITION (DEG)"
810     SET TEXT ANGLE 0
820     IF OUT$="N" GOTO 840
830     PRINTSCREEN
840     END
```

```
SET NO DOUBLE
1       REM  -------------  PROGRAM GRAPH5B  -----------------
2       REM
3       REM  GRAPH5B PLOTS CURVES ON A CARTESIAN PLANE OF Y-AXIS
4       REM  0 TO 80 AND X-AXIS 90 TO 180.THE PLOT IS DISTRIBUTED
5       REM  OVER 3 SCREENS (THE X-AXIS BEING VERTICLE) TO INCREASE
6       REM  RESOLUTION.
7       REM
10      PRINT "WHICH DATA TO BE PLOTTED"
20      INPUT DATA$\ INPUT SEC$\ INPUT THIRD$\ INPUT FTH$
30      PRINT "ENTER N TO BLOCK PRINT-OUT"
40      INPUT OUT$
50      OPEN DATA$ FOR INPUT AS FILE #1\ OPEN SEC$ FOR INPUT AS FILE #2
55      OPEN THIRD$ FOR INPUT AS FILE #3\ OPEN FTH$ FOR INPUT AS FILE #4
60      DIM X(17)\ DIM Y1(17)\ DIM Y2(17)\ DIM Y3(17)\ DIM Y4(17)
70      CLEAR
80      SET VIEWPORT 0,1,0,.625
82      REM
84      REM ******* FIRST SCREEN *******
86      REM
90      SET WINDOW -82,8,147.5,182.5
100     SET LINE STYLE 4
110     FOR I=180 TO 150 STEP -5
120     PLOT (-80,I),(0,I)
130     SET POSITION (8,I-2)
140     SET TEXT ANGLE 4
150     GRAPHIC PRINT I
160     SET TEXT ANGLE 0
170     NEXT I
180     FOR I=0 TO 80 STEP 5
190     PLOT (-I,180),(-I,147.5)
200     NEXT I
210     FOR K=13 TO 0 STEP -1
220     INPUT #1,X(K)\ INPUT #1,B\Y1(K)=-B
223     INPUT #2,X(K)\ INPUT #2,B\Y2(K)=-B
225     INPUT #3,X(K)\ INPUT #3,B\Y3(K)=-B
227     INPUT #4,X(K)\ INPUT #4,B\Y4(K)=-B
230     NEXT K
240     SET LINE STYLE 1
250     PLOT CURVE (Y1(),X(),14,0)
253     PLOT CURVE (Y2(),X(),14,0)
255     PLOT CURVE (Y3(),X(),14,0)
257     PLOT CURVE (Y4(),X(),14,0)
260     IF OUT$="N" GOTO 280
270     PRINTSCREEN
280     SET LINE STYLE 4
290     CLEAR
292     REM
294     REM ******* SECOND SCREEN *******
296     REM
300     SET WINDOW -82,8,112.5,147.5
310     FOR I=145 TO 115 STEP -5
320     PLOT (-80,I),(0,I)
330     SET POSITION (8,I-2)
340     SET TEXT ANGLE 4
350     GRAPHIC PRINT I
```

```
360     SET TEXT ANGLE 0
370     NEXT I
380     FOR I=0 TO 80 STEP 5
390     PLOT (-I,147.5),(-I,112.5)
400     NEXT I
410     X(14)=X(0)\Y1(14)=Y1(0)\Y2(14)=Y2(0)\Y3(14)=Y3(0)\Y4(14)=Y4(0)
420     FOR K=13 TO 0 STEP -1
430     INPUT #1,X(K)\ INPUT #1,B\Y1(K)=-B
433     INPUT #2,X(K)\ INPUT #2,B\Y2(K)=-B
435     INPUT #3,X(K)\ INPUT #3,B\Y3(K)=-B
437     INPUT #4,X(K)\ INPUT #4,B\Y4(K)=-B
440     NEXT K
450     SET LINE STYLE 1
460     PLOT CURVE (Y1(),X(),15,0)
463     PLOT CURVE (Y2(),X(),15,0)
465     PLOT CURVE (Y3(),X(),15,0)
467     PLOT CURVE (Y4(),X(),15,0)
470     IF OUT$="N" GOTO 490
480     PRINTSCREEN
490     SET LINE STYLE 4
500     CLEAR
502     REM
504     REM ******* THIRD SCREEN *******
506     REM
510     SET WINDOW -82,8,77.5,112.5
520     FOR I=110 TO 90 STEP -5
530     PLOT (-80,I),(0,I)
540     SET POSITION (8,I-2)
550     SET TEXT ANGLE 4
560     GRAPHIC PRINT I
570     SET TEXT ANGLE 0
580     NEXT I
590     FOR I=0 TO 80 STEP 5
600     PLOT (-I,112.5),(-I,90)
610     NEXT I
620     SET TEXT ANGLE 4
625     SET POSITION (.8,86.75)
627     GRAPHIC PRINT "0"
630     FOR I=10 TO 80 STEP 10
640     SET POSITION (-I+3.2,86.75)
650     GRAPHIC PRINT I
660     NEXT I
670     SET TEXT ANGLE 0
680     X(9)=X(0)\Y1(9)=Y1(0)\Y2(9)=Y2(0)\Y3(9)=Y3(0)\Y4(9)=Y4(0)
690     FOR K=8 TO 0 STEP -1
700     INPUT #1,X(K)\ INPUT #1,B\Y1(K)=-B
703     INPUT #2,X(K)\ INPUT #2,B\Y2(K)=-B
705     INPUT #3,X(K)\ INPUT #3,B\Y3(K)=-B
707     INPUT #4,X(K)\ INPUT #4,B\Y4(K)=-B
710     NEXT K
720     SET LINE STYLE 1
730     PLOT CURVE (Y1(),X(),10,0)
733     PLOT CURVE (Y2(),X(),10,0)
735     PLOT CURVE (Y3(),X(),10,0)
737     PLOT CURVE (Y4(),X(),10,0)
740     SET POSITION (-5,84)
750     SET TEXT ANGLE 4
```

```
760     GRAPHIC PRINT "INDUCTANCE"
770     SET POSITION (-24.5,84)
780     GRAPHIC PRINT DATA$
790     SET POSITION (-27,84)
800     GRAPHIC PRINT "(MH) / ROTOR POSITION (DEG)"
810     SET TEXT ANGLE 0
820     IF OUT$="N" GOTO 840
830     PRINTSCREEN
840     END
```